

INFORMATION TO USERS

This manuscript has been reproduced from the microfilm master. UMI films the text directly from the original or copy submitted. Thus, some thesis and dissertation copies are in typewriter face, while others may be from any type of computer printer.

The quality of this reproduction is dependent upon the quality of the copy submitted. Broken or indistinct print, colored or poor quality illustrations and photographs, print bleedthrough, substandard margins, and improper alignment can adversely affect reproduction.

In the unlikely event that the author did not send UMI a complete manuscript and there are missing pages, these will be noted. Also, if unauthorized copyright material had to be removed, a note will indicate the deletion.

Oversize materials (e.g., maps, drawings, charts) are reproduced by sectioning the original, beginning at the upper left-hand corner and continuing from left to right in equal sections with small overlaps.

Photographs included in the original manuscript have been reproduced xerographically in this copy. Higher quality 6" x 9" black and white photographic prints are available for any photographs or illustrations appearing in this copy for an additional charge. Contact UMI directly to order.

**ProQuest Information and Learning
300 North Zeeb Road, Ann Arbor, MI 48106-1346 USA
800-521-0600**

UMI[®]

Prevention of Coronary Restenosis
Using a Radioactive Stent: Radiobiological Studies

by

Olivier F. Bertrand, MD

Department of Medicine
Division of Experimental Medicine
McGill University, Montreal

A thesis submitted to the
Faculty of Graduate Studies and Research
in partial fulfillment of the requirements for the degree of
Doctor of Philosophy

© Olivier F. Bertrand, 1999



**National Library
of Canada**

**Acquisitions and
Bibliographic Services**

**395 Wellington Street
Ottawa ON K1A 0N4
Canada**

**Bibliothèque nationale
du Canada**

**Acquisitions et
services bibliographiques**

**395, rue Wellington
Ottawa ON K1A 0N4
Canada**

Your file Votre référence

Our file Notre référence

The author has granted a non-exclusive licence allowing the National Library of Canada to reproduce, loan, distribute or sell copies of this thesis in microform, paper or electronic formats.

The author retains ownership of the copyright in this thesis. Neither the thesis nor substantial extracts from it may be printed or otherwise reproduced without the author's permission.

L'auteur a accordé une licence non exclusive permettant à la Bibliothèque nationale du Canada de reproduire, prêter, distribuer ou vendre des copies de cette thèse sous la forme de microfiche/film, de reproduction sur papier ou sur format électronique.

L'auteur conserve la propriété du droit d'auteur qui protège cette thèse. Ni la thèse ni des extraits substantiels de celle-ci ne doivent être imprimés ou autrement reproduits sans son autorisation.

0-612-64515-0

Canada

The best interest of the patient is the only interest to be considered

Dr. W.J. Mayo

PREFACE

This thesis is submitted to the McGill Faculty of Graduate Studies and Research which gives candidates the choice of two options in the submission of their thesis. Option A is the conventional format known to all universities while option B is in the form of published or publishable papers. This work is submitted in the form of option B according to the thesis guidelines of the Faculty of Graduate Studies and Research:

Candidates have the option of including, as part of the thesis, the text of one or more papers submitted or to be submitted for publication, or the clearly-duplicated text of one or more published papers. These texts must be bound as an integral part of the thesis.

If this option is chosen, connecting texts that provide logical bridges between the different papers are mandatory. The thesis must be written in such a way that it is more than a mere collection of manuscripts; in other words, results of a series of papers must be integrated.

The thesis must still conform to all other requirements of the "Guidelines for Thesis Preparation". The thesis must include: A Table of Contents, an abstract in English and French, an introduction which clearly states the rationale and objectives of the study, a review of the literature, a final conclusion and summary, and a thorough bibliography or reference list.

Additional material must be provided where appropriate (e.g. in appendices) and in sufficient detail to allow a clear and precise judgement to be made of the importance and originality of the research reported in the thesis.

In the case of manuscripts co-authored by the candidate and others, the candidate is required to make an explicit statement in the thesis as to who contributed to such work and to what extent. Supervisors must attest to the accuracy of such statements at the doctoral oral defense. Since the task of the

examiners is made more difficult in these cases, it is in the candidate's interest to make perfectly clear the responsibilities of all authors of the co-authored papers.

This thesis includes 8 chapters, which are all submitted or published manuscripts. Chapter I is a general introduction to the problem of restenosis after percutaneous coronary interventions. Current understanding of its pathophysiology as well as different approaches to prevent or treat it are presented. A shortened version of this manuscript has been published as a book chapter. Co-authors are Dr. D. Meerkin, Dr. JC. Tardif and Dr. R. Bonan who reviewed and edited the manuscript and discussed the results of previous publications.

Chapter II reviews the use of ionizing radiation to prevent restenosis. Pr. S. Lehnert helped in writing the discussion and explaining radiobiological concepts, Dr. L. Bilodeau, Dr. JF.Tanguay, Dr. G. Côté and Dr. M.G. Bourassa extensively reviewed the manuscript and helped to collect the relevant information. Dr. R. Mongrain and Mr. J. Laurier helped with the physics and the radiation protection notions developed in the manuscript.

Chapter III reviews the biocompatibility aspects and efficacy of different stent designs to counteract restenosis. Pr. R. Sipehia helped with the polymer biocompatibility and degradation aspects. Dr. R. Mongrain helped with the engineering aspects of stent development and biocompatibility. Dr. J. Rodés, Dr. JC. Tardif, Dr. L. Bilodeau, Dr. G. Côté and Dr. M.G. Bourassa discussed results in the different animal models as well as the current limitations of the different stent designs. All co-authors extensively reviewed and edited the drafted manuscript.

Chapter IV reviews potential side effects of radiation therapy as it applies to restenosis prevention. Co-authors were Pr. S. Lehnert who discussed radiobiological concepts, Dr. R. Mongrain who discussed inhomogeneities in radiation delivery including the different modes of delivery and Dr. M.G. Bourassa who reviewed and edited several drafts of the manuscript.

Chapter V describes the potential target volumes and critical cells exposed to ionizing radiation. Mr. J. Brunette and Dr. R. Mongrain helped with the program and the technique used to measure vessel layer areas and to extrapolate vascular cell densities. Dr. T.K. Leung harvested coronary arteries, processed all arterial segments and reviewed the respective morphologic characteristics. Pr. S. Lehnert reviewed the protocol and analyzed the results. All co-authors reviewed and edited the manuscript.

Chapter VI analyzes the *in vitro* responses of human and porcine vascular cell lines exposed to high dose-rate γ irradiation. Co-investigators were Dr. R. Mongrain who wrote a program to analyze cell survival, Dr. E. Thorin who assisted with cell isolation and culture and Pr. S. Lehnert who discussed the different protocols and analyzed cell survival parameters. All co-authors reviewed and edited the different drafts of the manuscript.

Chapter VII describes the experimental setup and the dosimetric aspects of the bioassay to measure the effects of low energy β -emitters on vascular cells in culture. Dr. R. Mongrain designed the alcove chambers to isolate petri dishes and performed all dosimetric calculations. Dr. P. Yuen calibrated and provided special dosimeters for our experiments. He also verified all dosimetric calculations. Pr. S. Lehnert participated in the protocol elaboration and reviewed and edited the manuscript.

Chapter VIII measured the dose-rate effect of vascular smooth muscle cells when exposed *in vitro* to an original isotope complex ($^{45}\text{Ca-DTPA}$). Co-investigators were Dr. R. Mongrain who assisted with the experiments and performed the dosimetry of the β irradiation, Dr. E. Thorin helped with cell isolation and cultures. Pr. S. Lehnert discussed the protocol and performed cell survival analysis. All co-authors reviewed and edited the manuscript.

Acknowledgements

It is generally considered a difficult task to acknowledge the different people who have from near or far contributed to the completion of a thesis. During the course of my Ph.D., I have always thought of this section as a unique opportunity to pay tribute to people who have chosen to help me to different degrees during my training in medicine and the period of this Ph.D. thesis.

It is only justice to thank first my parents for their continuing support and especially my father, a psychiatrist, who inspired me to become a medical doctor. Despite having chosen to work for some time with cell culture and basic sciences, I do not forget that my primary task is to treat patients. I bear tremendous respect for what he taught me, to pay as much attention to the psychological aspects of the relationship with patients, as to analyze symptoms and signs of a disease.

I have great admiration for the teachers who participated in my medical education and introduced me to research. Pr. P. Franchimont, Pr. H. Van Cauwenberge and Pr. P. Lefèbvre taught me internal medicine. At that time, their ability to communicate and their great knowledge, made me interested in all the different aspects of medicine. Pr. G. Moonen accepted me as a research student in his laboratory, gave me my first chance to work in basic sciences and introduced me to cell culture techniques. Years later, I still benefit from his example and I always remember the importance of asking to myself the “so what?” before initiating a series of experiments. Pr. A. Maseri accepted me in the Cardiovascular Research Unit at Hammersmith Hospital (London, UK) for an elective period. Since that time, I cannot consider practicing medicine without doing research. I will always remember his extraordinary faculty to refuse dogmas in medicine as established facts and always formulate new hypotheses. Pr. H. Kulbertus accepted me in the cardiology program and Dr. V. Legrand introduced me to coronary angioplasty techniques. As a clinician and cardiologist, I owe deep gratitude to the several doctors who

inspired me and I want to mention Dr. JM. Andrien, Dr. J. Boland, Dr. JC. Demoulin and Dr. D. Soyeur.

After a short period at the Montreal Heart Institute, working with Dr. M. Juneau in the coronary care unit, I decided that I would return some day for a full fellowship. Five years later, acting as Chief of Medicine, it was once again Dr. M. Juneau who accepted me for an interventional cardiology fellowship. Moreover, he did everything possible to make our life in Montreal a bit easier when it became clear that two years would not be enough to achieve the tasks of completing, my wife and I, our respective theses. He also introduced me to the interventional cardiology staff at the Montreal Heart Institute and especially to Dr. L. Bilodeau, Dr. G. Côté, and Dr. JF. Tanguay. These individuals supported me since the first day that this Ph.D. idea came to my mind. I have tremendous respect and admiration for Pr. M.G. Bourassa who accepted to become a mentor and a guide for me throughout my stay in Montreal. I do hope he will continue to provide me with his precious advice for the next coming years.

I was particularly well integrated in the cardiac catheterization laboratory, and this was due to the extraordinary friendship and expertise of all cardiologists, nurses and technicians. It is with them that I really became an interventional cardiologist. I had also the opportunity to work with cardiologists who pioneered the use of catheter-based brachytherapy in Canada, Dr. R. Bonan and Dr. M. Joyal, who shared many of their interesting results with me. Dr. D. Meerkin and I were in a similar position although coming from two different worlds. From time to time, I have become addicted to the impromptu discussions in which we shared a common interest for the use of radiation therapy in cardiology, but also tried to speculate on potential limitations. I wish you success, David, and I do hope we will continue to work together. Dr. JC Tardif has also become an important person during my fellowship and my Ph.D. Because of his deep interest in antioxidants, he is probably one of the most skeptical cardiologists about the possible use of ionizing radiation as a new form of therapy in coronary artery disease. It has always been challenging to discuss the potential mechanisms of action of these respective therapies. After all, it is quite possible that both will find their application in cardiology in the future.

At the Montreal Heart Institute Research Center, two basic scientists kindly provided me with important advice. Dr. M. Sirois introduced me to the technique of isolating smooth muscle cells and fibroblasts from pig aortas. Dr. E. Thorin welcomed me in his laboratory for all the experiments that were done at the Montreal Heart Institute. His expertise in cell culture and endothelial cell physiology has been very important for my work. He also provided much needed support when on a few occasions, we had to discard contaminated cells. At that time, I was convinced I was the only one in the world to whom this happened....

During the course of this thesis, I spent much time with computers in the Department of Biomedical Engineering at the Montreal Heart Institute. I wish to express my sincere gratitude to Mr. J. Laurier who generously spent time (and more time) analyzing survival data and verifying statistical results. At the medical library, Mrs. M.A. Normand was very helpful in locating and collecting numerous articles, which were essential to my work.

This Ph.D. thesis would not have been possible without the close collaboration of Dr. R. Mongrain. From the very beginning, he has provided much of his time once he became convinced that this project was not another crazy idea from a cardiologist! For the last four years, he has always been besides me for all aspects of the project and his knowledge and expertise remain absolutely necessary for the ultimate completion of the project. I am also proud to say that I have found a new friend!

Pr. S. Lehnert has given me the enormous privilege to work under her supervision to complete this Ph.D. thesis. I am sure she had never thought to have one day, an interventional cardiologist doing a Ph.D. thesis in radiation biology with the declared goal of irradiating human blood vessels.... I strongly believe that this work is only preliminary and that many aspects remain to be investigated. I do hope that we will continue to collaborate in the future and I want to thank her once again for having shared with me all the notions of radiobiology necessary to advance in

this new field. It is also my pleasure to thank the technicians in her laboratory, Mr. D. Chow and Mr. P. Kauler, whose contributions were key factors in the completion of some experiments.

I want to deeply thank my wife, M. Jadin. Once my father said: C'est la femme qui fait l'homme. This is absolutely true for me. Without Michèle, no Montreal, no fellowship, no thesis, no love, no passion and no family. She also gave me two wonderful daughters and a delightful son. This also reminds me that work is not the most important thing in a man's life.

Importantly, I want to thank the several people, organizations and industries who financially made this ongoing project feasible to varying degrees, Mr. E. Berg, R. Doré, D. Falque, R. Flanagan, M. Jaspers, P. Lefèbvre, G. Loix, C. Menessiez, JC. Sermeus, F. Villijn, la Fondation Horlait-Dapsens, le Fonds de la Recherche en Santé du Québec, le Fonds de la Recherche de l'Institut de Cardiologie de Montréal, Medtronic Inc. and Draximage Inc. I apologize to those I may have forgotten. Finally, I want to thank all members of the jury and especially, Pr. R. Schwartz from the Mayo Clinic who agreed to serve as external reviewer. This thesis involved the work of several people but mistakes are mine.

ABSTRACT

Radiation therapy is currently under investigation as a therapeutic option for the prevention and the treatment of restenosis following percutaneous coronary interventions. Restenosis after vessel injury is associated with a transient state of cell proliferation and bears many similarities with wound healing. It is known that ionizing radiation can delay or impair wound healing. One proposed approach uses the deployment of a radioactive stent and continuous low dose-rate treatment. Our experimental studies have been conducted to better evaluate the radiobiology of vascular cells and as a preamble to the design of an original radioactive stent based on a ^{45}Ca -DTPA polymer-coated stent.

We performed morphometric analysis of human coronary segments with restenosis. Most of vessel area was occupied by atherosclerotic plaque and neointima accounted for a limited part. Adventitial and medial thicknesses were significantly thinner than the atherosclerotic plaque and neointima. The medial layer was the most cellular. Our results indicated that target volumes for endovascular catheter-based brachytherapy or radioactive stents remain small. After delivery of doses such as proposed in the current experience, only a few thousand cells would remain clonogenic. Depending of the residual growth stimulus, this would create a permanent impairment or a significant delay in the healing and the restenosis process.

We compared in vitro responses of human and pig fibroblasts, smooth muscle cells and endothelial cells exposed to high dose-rate γ irradiation. Using clonogenic assays, growth inhibition and filter elution techniques, we found that human and pig cells have similar radiation responses. Our results suggest that vascular cell lines cover a broad range of radiosensitivities without specific differences between cell types.

We developed an experimental set-up to evaluate the in vitro effects of low energy β -emitters on vascular cells. The complex is the ^{45}Ca -diethylenetriaminepentaacetate (^{45}Ca -DTPA)

with a maximal energy of 255 KeV. There was a good correlation between calculated doses and doses measured by dosimeters placed at the bottom of petri dishes. However, it seems that doses administered to cell monolayers would be better evaluated by the dose calculated by the Medical Internal Radiation Dose (MIRD) instead of half the calculated dose, as previously suggested.

We evaluated the dose-rate effect of vascular smooth muscle cells exposed to low dose-rate irradiation with the ^{45}Ca -DTPA complex. Clonogenic survival and growth inhibition were compared with results obtained at high dose-rate with a ^{60}Co source. It was demonstrated that in vitro smooth muscle cells exhibit a significant dose-rate effect, indicating that this should be considered in the design of a radioactive stent.

In conclusion, a chelated complex of ^{45}Ca -DTPA appears suitable for incorporation into a polymer matrix to be coated onto a stent. Using diffusion-based release from the coated stent, surrounding tissues might be irradiated with a continuous low-dose rate administration. Our results suggest that irradiation with a dose-rate of 0.675 Gy/h allows complete sub-lethal damage repair, which might be important to determine an optimal therapeutic ratio. With this proposed approach and the isotopic complex, a limited tissue volume will be irradiated. Continuing challenges will be to determine the initial activity required to deliver a therapeutic dose to the presumed target tissue. The total dose and dose-rate calculations will need to take into account local blood flow dynamics, the release kinetics from the polymer matrix and the biological half-life of the radioisotope in the vascular wall.

RESUME

La radiothérapie est actuellement évaluée comme une nouvelle possibilité de prévention ou de traitement de la resténose coronarienne après une intervention percutanée. La resténose après une blessure du vaisseau est associée à une prolifération cellulaire transitoire qui ressemble beaucoup à un processus cicatriciel. On sait que les radiations ionisantes retardent ou suppriment la cicatrisation. Une approche possible utilise la mise en place d'un stent radioactif et un traitement à un faible débit de dose continu. Nos études expérimentales ont été conduites dans le but de mieux comprendre la radiobiologie des cellules vasculaires et de développer un nouveau concept de stent radioactif basé sur une endoprothèse recouverte d'une matrice polymérique incorporant du $^{45}\text{Ca-DTPA}$.

Nous avons fait une analyse histomorphométrique de segments d'artères coronaires humaines restenosées. Nous avons trouvé que la plaque athérosclérotique occupait la majeure portion du vaisseau et que la neointima ne représentait qu'une surface relative limitée. La média était la couche la plus cellulaire. Nos résultats indiquent que les volumes cibles pour la brachythérapie par cathéter or par stent radioactif restent limités. Après livraison de doses telles qu'utilisées dans l'expérience clinique actuelle, seulement quelques milliers de cellules conserveront un potentiel intact de prolifération. Selon le stimulus de croissance résiduel, cela pourrait engendrer une abolition permanente de la resténose ou un long délai de récidence.

Nous avons comparé les réponses in vitro de fibroblastes, de cellules musculaires lisses et de cellules endothéliales humaines et porcines, exposées à une irradiation γ à haut débit de dose. En évaluant les survies clonogéniques, le retard de croissance et la technique d'élution par filtre, nous avons trouvé que les cellules humaines et porcines présentent des réponses similaires à la radiation. Nos résultats suggèrent que les radiosensibilités des cellules vasculaires couvrent un large éventail sans qu'il n'existe de différence systématique entre les différents types cellulaires.

Nous avons développé un modèle expérimental pour évaluer les effets in vitro d'isotopes β de faible énergies. Le complexe de $^{45}\text{Ca-DTPA}$ a une énergie maximale de 255 KeV. On observait une bonne corrélation entre les doses calculées et les doses mesurées par les dosimètres placés au fond des boîtes. Cependant, il semble que les doses administrées à des monocouches de cellules sont mieux appréciées par le calcul des doses selon MIRD (Medical Internal Radiation Dose) plutôt qu'en divisant cette valeur par deux, comme il a été suggéré préalablement dans la littérature.

Nous avons évalué l'effet du débit de dose sur des cellules musculaires lisses en les exposant à une irradiation à faible débit de dose avec le complexe de $^{45}\text{Ca-DTPA}$. Le taux de survie clonogénique et le retard de croissance ont été comparés avec les résultats obtenus à haut débit de dose avec une source de ^{60}Co . Nous avons montré que les cellules musculaires lisses présentaient un effet du débit de dose significatif qui devait être pris en considération dans le design d'un stent radioactif.

En conclusion, l'incorporation de $^{45}\text{Ca-DTPA}$ dans une matrice polymérique appliquée sur un stent apparaît faisable. En utilisant une libération progressive basée sur les principes de diffusion, les tissus avoisinants peuvent être irradiés avec une irradiation continue à faible débit de dose. Nos résultats suggèrent qu'une irradiation continue avec un débit de dose de 0,675 Gy/h permet une réparation complète des lésions sub-léthales, ce qui peut être important dans la détermination d'un rapport thérapeutique optimal. Avec cette approche et ce complexe isotopique, un volume tissulaire limité sera irradié. Les questions non résolues concernent le niveau d'activité initial requis pour délivrer une dose thérapeutique au tissu cible présumé. La dose totale et le débit de dose seront déterminés en considérant la mécanique sanguine locale, la cinétique de libération de l'isotope depuis la matrice polymérique et la demi-vie biologique du complexe radioactif dans la paroi artérielle.

Publications Arising from Work of the Thesis

1. **New Understandings and Trends in the Prevention of Coronary Restenosis.** O.F. Bertrand, D. Meerkin, J.C. Tardif, R. Bonan in *Management of Complex Cardiovascular Problems. The Consultant's Approach.* T Nguyen, D Hu, S Saito, LY Leng, V Dave eds. Futura Publishing Corporation (published in September 1999).
2. **Intravascular Radiation Therapy in Atherosclerotic Disease. Promises and Premises.** O.F. Bertrand, R. Mongrain, S. Lehnert, L. Bilodeau, JF. Tanguay, J Laurier, G. Côté, M.G. Bourassa. *Eur Heart J* 1997;18:1385-95.
3. **Biocompatibility Aspects of New Stent Technology.** O.F. Bertrand, R. Sipehia, R. Mongrain, J. Rodés, J.C. Tardif, L. Bilodeau, G. Côté, M.G. Bourassa. *J Am Coll Cardiol* 1998;32:562-71.
4. **Early and Late Results of Radiation therapy for Prevention of Restenosis. A Critical Appraisal.** O.F. Bertrand, S. Lehnert, R. Mongrain, M.G. Bourassa. *HEART* 1999;82:658-662.
5. **Histo-morphologic Aspects of Coronary Restenosis after Balloon Angioplasty in Humans. Relevance for Radiation therapy.** O.F. Bertrand, J. Brunette, TK Leung, R. Mongrain, S. Lehnert. *Cardiovasc Pathol* 1999 (submitted).
6. **In Vitro Response of Human and Porcine Vascular Cells Exposed to High Dose-rate γ Irradiation.** O.F. Bertrand, R. Mongrain, E. Thorin, S. Lehnert. *Int J Rad Biol* 1999 (accepted).

7. **Dosimetric Considerations to Study *in vitro* the Effects of Low Energy β -Emitters.** O.F. Bertrand, R. Mongrain, P.S. Yuen, S. Lehnert. Cardiovasc Rad Med 1999 (submitted).

8. **Effects of Low Dose-rate β irradiation on Vascular Smooth Muscle Cells. Comparison with High Dose-rate Exposure.** O.F. Bertrand, R. Mongrain, E. Thorin, S. Lehnert. Cardiovasc Radiat Med 1999;1:125-30.

TABLE OF CONTENTS

PREFACE	3
ACKNOWLEDGEMENTS	6
ABSTRACT	10
RESUME	12
PUBLICATIONS ARISING FROM WORK OF THE THESIS	14
TABLE OF CONTENTS	16
LIST OF FIGURES	19
LIST OF TABLES	20
INTRODUCTION	21
CHAPTER I: NEW UNDERSTANDINGS AND TRENDS IN THE PREVENTION OF CORONARY RESTENOSIS	23
INTRODUCTION	24
NEW UNDERSTANDINGS IN RESTENOSIS PATHOPHYSIOLOGY	24
NOVEL THERAPIES AND TREATMENT CHALLENGES IN RESTENOSIS PREVENTION	31
<i>Stents</i>	31
<i>Radiation</i>	33
<i>Pharmacological compounds and antioxidants</i>	36
<i>Gene Therapy</i>	37
CONCLUSION	38
REFERENCES	39
CHAPTER II: INTRAVASCULAR RADIATION THERAPY IN ATHEROSCLEROTIC DISEASE: PROMISES AND PREMISES	47
INTRODUCTION	48
EXTERNAL IRRADIATION	50
ENDOVASCULAR HIGH-DOSE RATE IRRADIATION THERAPY	51
RADIOACTIVE STENTS	53
HUMAN EXPERIENCE WITH ENDOVASCULAR RADIATION	55
SUMMARY OF THE UNRESOLVED ISSUES	56
<i>Mechanisms of action</i>	56
<i>Gamma or beta irradiation</i>	58
<i>Administered doses</i>	60
<i>High dose-rate vs low dose-rate</i>	60
<i>Delayed effects</i>	61
CONCLUSION	62
REFERENCES	63
APPENDIX: RADIATION GLOSSARY	71

CHAPTER III: BIOCOMPATIBILITY ASPECTS OF NEW STENT TECHNOLOGY.....	73
ABSTRACT	74
INTRODUCTION	75
CORONARY STENTS: MATERIAL AND DESIGN	75
POLYMER COATINGS	78
<i>Non biodegradable synthetic polymers</i>	78
<i>Biodegradable synthetic polymers</i>	80
<i>Natural coated and covered stents</i>	80
HEPARIN-COATED STENTS	81
DRUG-ELUTING STENTS	83
POLYMERIC STENTS	84
ENDOTHELIAL CELL SEEDING	86
RADIOACTIVE STENTS	86
DISCUSSION	87
CONCLUSION	89
REFERENCES.....	90
CHAPTER IV: EARLY AND LATE EFFECTS OF RADIATION THERAPY FOR PREVENTION OF CORONARY RESTENOSIS: A CRITICAL APPRAISAL.....	99
INTRODUCTION	100
CELLULAR EFFECTS OF RADIATION THERAPY	101
GENE REGULATION AFTER RADIATION THERAPY	104
REFERENCES.....	108
CHAPTER V: HISTO-MORPHOLOGIC ASPECTS OF CORONARY RESTENOSIS AFTER BALLOON ANGIOPLASTY IN HUMANS: RELEVANCE FOR RADIATION THERAPY	113
ABSTRACT	114
INTRODUCTION	115
MATERIALS AND METHODS.....	116
<i>Pathology</i>	116
<i>Image and morphometric analysis</i>	116
<i>Data analysis</i>	117
RESULTS	117
DISCUSSION	119
REFERENCES.....	126
CHAPTER VI: IN VITRO RESPONSE OF HUMAN AND PORCINE VASCULAR CELLS EXPOSED TO HIGH DOSE-RATE γ IRRADIATION	130
ABSTRACT	131
INTRODUCTION	132
MATERIALS AND METHODS.....	133
<i>Cell lines</i>	133
<i>Radiation procedure</i>	134
<i>Survival</i>	134
<i>Growth inhibition and delay</i>	134
<i>Alkaline filter elution</i>	135
<i>Statistical analysis</i>	136
RESULTS	136
<i>Clonogenic survival</i>	136
<i>Growth inhibition and growth delay</i>	136
<i>DNA single strand breaks</i>	137
DISCUSSION	137

REFERENCES.....	142
-----------------	-----

**CHAPTER VII: DOSIMETRIC CONSIDERATIONS TO STUDY *IN VITRO*
THE EFFECTS OF LOW ENERGY β EMITTERS ON VASCULAR CELLS 147**

ABSTRACT.....	148
INTRODUCTION.....	149
MATERIAL AND METHODS	150
<i>Prototype</i>	150
<i>Radiation protocol</i>	150
<i>Cells</i>	150
<i>Dosimetry calculations</i>	151
<i>Dosimetry measurements</i>	152
RESULTS.....	153
<i>Dose-rate calculations</i>	153
<i>Dose-rate measurements</i>	153
<i>Effects of chelation</i>	154
DISCUSSION.....	154

**CHAPTER VIII: EFFECTS OF LOW DOSE-RATE β -IRRADIATION
ON SMOOTH MUSCLE CELLS: COMPARISON WITH HIGH DOSE-RATE EXPOSURE..... 159**

ABSTRACT.....	160
INTRODUCTION.....	161
MATERIALS AND METHODS.....	161
<i>Cell lines</i>	161
<i>Radiation Procedure for HDR</i>	162
<i>Radiation Procedure for LDR</i>	162
<i>Survival</i>	162
<i>Growth delay</i>	163
<i>Data analysis</i>	163
RESULTS.....	163
<i>Clonogenic survival</i>	163
<i>Growth delay</i>	164
DISCUSSION.....	164
REFERENCES.....	168

GENERAL CONCLUSION 170

CONTRIBUTION TO ORIGINAL RESEARCH 172

LIST OF FIGURES

Chapter 1

1. Restenosis pathways

Chapter 4

1. Similar pathways after vessel injury and radiation therapy
2. Hypothetical pathways after radiation therapy for restenosis prevention

Chapter 5

1. Representative specimens of the 7 coronary arteries analyzed
2. Relative vessel areas
3. Vessel layer thickness and relative distances
4. Representative specimen of a human coronary lesion obtained a few hours after balloon angioplasty
5. Restenosis pathophysiology after catheter-based intervention and stent implantation
6. Hypothetical target volumes for endovascular catheter-based brachytherapy and radioactive stent.
7. Neointima cell densities as a function of time.

Chapter 6

1. Clonogenic survival of human vascular cells
2. Clonogenic survival of pig vascular cells
3. Growth arrest effect of radiation on human cell population
4. Growth delay after irradiation of human cells
5. Representative experiment with filter elution of human fibroblasts
6. Comparison between relative elution of human and pig smooth muscle cells
7. Hypothetical pathways of growth and restenosis formation with and after irradiation

Chapter 7

1. Prototype of β -irradiation chambers used for experiments
2. Example of a GR200F TLD embedded in plastic pouch
3. Relationship between activities and doses at low dose-rate
4. Relationship between activities and doses at high dose-rate

Chapter 8

1. Clonogenic survival of smooth muscle cells at high and low dose-rates
2. Growth delay of smooth muscle cells after high and low dose-rate exposure.

LIST OF TABLES

Chapter 1

- I. Intravascular ultrasound after catheter-based coronary intervention.

Chapter 2

- I. External radiation
- II. Histological results after external irradiation
- III. Endovascular radiation
- IV. Histological results after endovascular irradiation
- V. Radioactive stent
- VI. Histological results after radioactive stent implantation
- VII. Human experience

Chapter 3

- I. Polymer used as stent coatings
- II. Heparin-coated stents
- III. Drug-eluting stents
- IV. Polymeric stents

Chapter 5

- I. Clinical characteristics
- II. Relative vessel layer areas
- III. Vessel layer densities
- IV. Vessel layer thickness and relative distances
- V. Calculated target volumes

Chapter 6

- I. Survival parameters

Introduction

There are presently two ways to deliver intravascular radiation therapy to prevent restenosis. Endovascular radiation can be applied using a catheter-based system or alternatively with a radioactive implant, such as a stent. The first relies on high activity γ or β emitting sources such as ribbons, seeds, liquid or gas to deliver a single dose of radiation locally through an endoluminal catheter within a limited period of time. The second approach uses the deployment of a radioactive stent with resultant longer exposure time and continuous low dose-rate treatment.

Other investigators have designed radioactive stents using either particle bombardment of the metallic structure or ion-implantation of ^{32}P on the stent surface. In these cases, the duration of exposure is exclusively regulated by the initial radioactive stent activity and by the half-life of the isotopes. For an isotope such as ^{32}P (half-life : 14 days), this creates serious logistic disadvantages. Moreover, the permanent link of the isotopes with the stent structure leads to large near-field dose inhomogeneities. Lastly, existing radioactive stents and catheter-based systems use high-energetic isotopes which creates significant radiation protection constraints.

We have hypothesized that an alternative radioactive stent design could use a lower energy isotope embedded in a polymer matrix. Once the radioactive stent would be deployed, the isotope would be slowly released to irradiate the surrounding vascular tissue. This could create significant advantages in terms of near-field dosimetry. This allows also the use of longer half-life isotopes which bring significant logistic benefit. We have chosen to study the properties of a ^{45}Ca -DTPA complex. The isotope is complexed with a chelate agent that would prevent intracellular penetration of the ^{45}Ca and accelerates the elimination of the isotope complex.

The main objectives of our studies were :

- 1) To evaluate the potential target volumes for catheter-based and radioactive stent. Considering the respective vessel layer thickness would also indicate whether the requirements in terms of isotope energy would be fulfilled with ^{45}Ca . Indeed, the maximum penetration of electrons from ^{45}Ca in biological tissue has been estimated to be around 400 μm by Monte-Carlo simulations.
- 2) To study the intrinsic radiosensitivities of fibroblasts, smooth muscle cells and endothelial cells and to compare the response of human and pig cells. A critical issue is to exclude that endothelial cells are significantly more radiosensitive than smooth muscle cells or fibroblasts. Indeed, endothelial regeneration is very important to limit the risks of vessel thrombosis. We were also interested to verify that fibroblasts are not significantly more radioresistant than the other two cell lines as this could be an explanation for fibrosis development after irradiation. Finally, we wanted to determine whether the pig is well-suited as a pre-clinical model to study the early and late consequences of vascular irradiation.
- 3) To study the dose-rate effect on likely target cells using the proposed isotope complex and its role in the design of a radioactive stent.

**CHAPTER I: New Understandings and Trends in the Prevention
of Coronary Restenosis**

Introduction

The phenomenon that has plagued interventional cardiologists since the inception of percutaneous transluminal coronary angioplasty twenty years ago has been restenosis (1). Following improvements in techniques and materials, restenosis remains the greatest challenge in the advancement of percutaneous procedures. Enormous efforts and resources have been invested in the pursuit of a solution to this problem that persists in the order of 20-50% in selected patient populations (2). The elucidation of restenosis pathophysiology and the improved understanding of the pharmacology of a few original compounds have lead to promising early clinical results .

The development and application of intracoronary stents has been the first major advance to combat this problem. However, the increasing use of coronary stents has also resulted in the emergence of a new, particularly vexing problem, in-stent restenosis. The next decade will no doubt bear witness to the development and application of new stent designs, powerful pharmacological compounds and new technologies. In particular, radiation therapy appears to be the next breakthrough for the prevention and treatment of restenosis (3). Other approaches, using gene therapy or novel pharmacological agents, delivered locally or systemically, will probably become available for clinical testing in the near future.

It is the purpose of this chapter to review current understanding of the pathophysiology of restenosis, present results of new therapeutic modalities, in particular radiation therapy and define upcoming challenges for the interventional cardiologist.

New understandings in restenosis pathophysiology

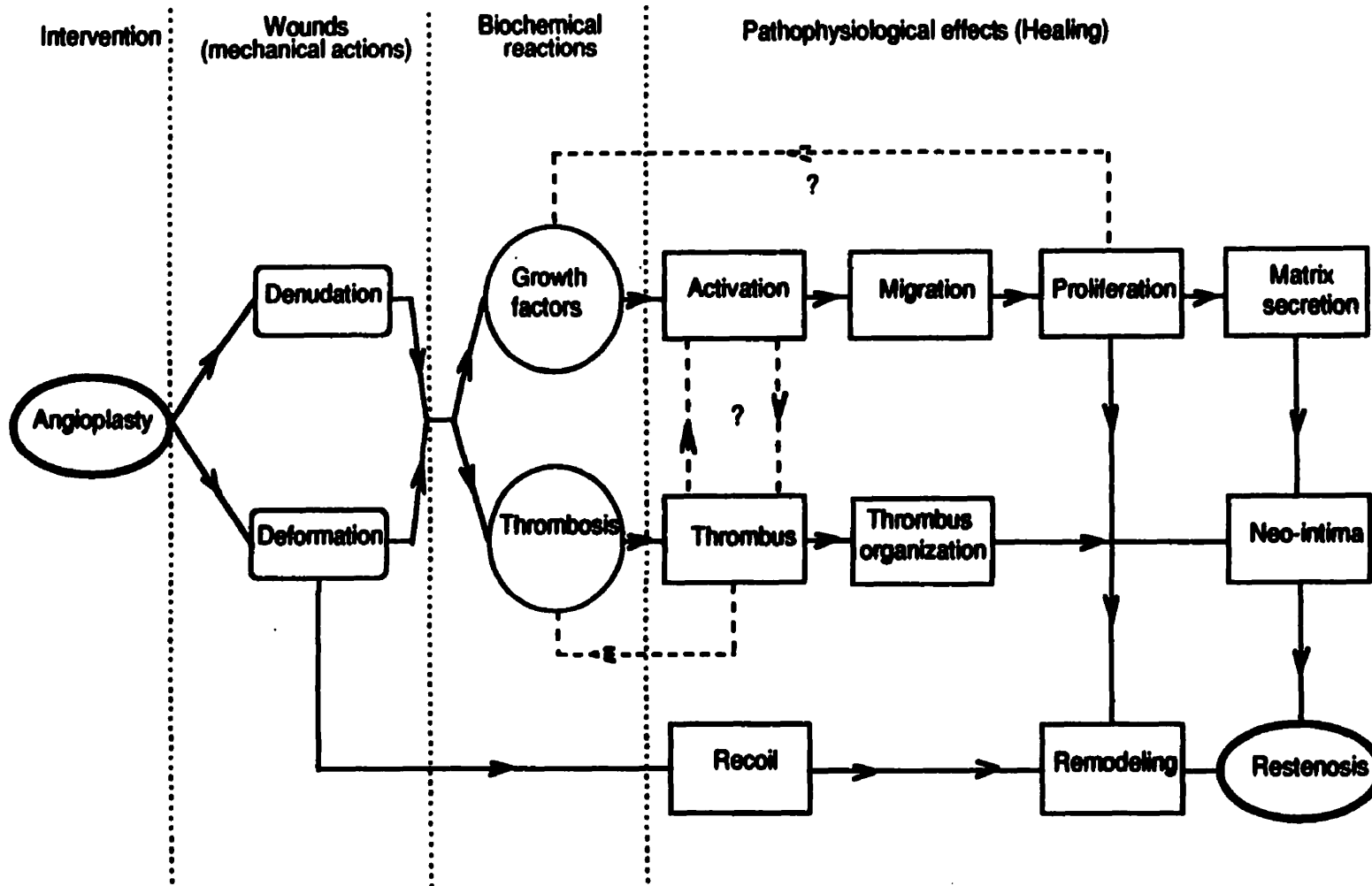
From its inception, the successful application of the new technology of percutaneous transluminal coronary angioplasty was limited by two principal problems. The first, in the acute phase, was acute or sub-acute vessel closure while the second was a delayed phenomenon, due to a more insidious recurrence of the stenosis and was rapidly termed restenosis. Acute vessel

occlusion had catastrophic results, however, with technical improvements and technique refinements this has become a relatively rare occurrence. Although the effects of restenosis are not usually fatal, it results in a significant number of patients being forced to undergo repeat procedures in the year following the initial dilatation. Careful clinical follow-up has identified the first 6 months as the critical period during which the vast majority of restenoses occur while pathologic reports helped elucidate the mechanisms of action of angioplasty (4). Balloon dilatation resulted in breaks, splits, intimal dissection, medial and adventitial tearing, vessel stretching, and plaque compression, and when pathologists had the opportunity later to examine coronary artery sections from patients who died with clinical or angiographic evidence of restenosis, they observed that a loose fibromuscular tissue obstructed a variable portion of the lumen (5-8). This tissue seemed to emerge from the previous breaks or dissections of the dilated arterial wall and contained often organized thrombus.

Major advances in the understanding of this process were made with development of animal models, initially the rat carotid artery model. Investigators convincingly demonstrated that the neointimal tissue resulted from medial smooth muscle cells migrating to the intima, undergoing a few cell divisions before resuming a quiescent state (9). This transient proliferative state was the consequence of multiple growth factors, released presumably from adhering platelets and colonizing macrophages (10, 11). This initial understanding led to the development of dozens of compounds to reduce smooth muscle cell migration or proliferation or to prevent thrombus formation. In spite of often dramatic results in animal models, these have been almost universally disappointing in human double-blind randomized trials.

The introduction of quantitative angiographic analysis performed by independent core laboratories, further contributed to our knowledge of the pathophysiology of restenosis. An important observation was that there was a spectrum of restenotic responses rather than an all or none phenomenon (12, 13).

Figure 1: Current Understanding of Restenosis Pathways



Legend: Balloon angioplasty creates endothelial denudation and vessel deformation. This will lead to thrombus formation and growth factor release by platelets and macrophages. Cells in the media and adventitia become activated and transform into myofibroblasts. Neointima is formed from myofibroblastic proliferation and extracellular matrix secretion. Vessel remodeling involves at least in part the same mechanisms.

Early autopsy reports raised the possibility that changes in vessel dimensions contribute to the restenosis process. Waller et al. first reported that less than 50% of lumen reduction could be accounted by fibro-intimal proliferation and that vessel recoil and remodeling can also play an important role (5). A more recent pathologic study also emphasized vessel remodeling as an important cause of lumen loss. Nakamura et al. found that remodeling (defined as the ratio of the artery area at the PTCA site to at the reference site < 1) was present in all restenotic segments but only rarely in vessels without restenosis (14).

In atherosclerotic rabbit iliac arteries, Kakuta et al. first established the important role of vessel size changes to explain late lumen loss after balloon angioplasty (15). By defining one group with restenosis and another without according to residual lumen area, they observed that there was no difference in intimal area between the two groups. In contrast, non-restenotic vessels had undergone sufficient compensatory enlargement to prevent luminal area reduction whereas restenotic vessels did not. Post et al. studied the effects of balloon angioplasty and thermal angioplasty in peripheral arteries of normal rabbit and normal and atherosclerotic pigs (16). In these different models, they showed that between 50-90% of late lumen loss could be explained by a reduction in vessel size. In a more recent study, they used Yucatan minipigs and intravascular ultrasound at different time intervals to further evaluate the natural history of neointimal formation and vessel remodeling (17). Lumen area decreased over time and was minimal at 42 days after balloon angioplasty. The contribution of neointima formation to lumen loss decreased over time whereas the contribution of vessel remodeling increased progressively and reached a maximal value of 78%.

Lafont et al. studied intimal, medial and adventitial changes associated with balloon angioplasty in pig coronary arteries (18). They found that residual lumen stenosis was correlated with vessel constriction but not with neointimal or adventitial growth. The degree of vessel remodeling was a continuum process and bi-directional with some arteries exhibiting constriction whereas others showed compensatory enlargement to accommodate neointima formation. These studies re-oriented restenosis pathophysiology research towards the potential role for the

adventitia, which had been long suspected to have a role in the pathogenesis of atherosclerosis and restenosis. Two different groups have demonstrated the existence of an early wave (first 3 days) of proliferation of cells characterized as myofibroblasts in the adventitia in the pig coronary model (19, 20). Subsequently, they also showed that adventitial cells in this model could contribute to neointima formation (19, 21). Geary et al. in an atherosclerotic monkey model have also demonstrated early adventitial cell proliferation (22).

Recently, using micro CT technology, Kwon et al. elegantly showed that vasa vasorum density was dramatically increased following balloon angioplasty in a pig coronary artery model (23). Pels et al. have also demonstrated early and transient adventitial neovascularization after balloon angioplasty in the same model (24). This neovascularization was maximal at 3 days and subsequently regressed. Importantly, they noted that regression of adventitial vascularization was correlated with arterial narrowing. Thus, it is now well established that balloon angioplasty induces a three layer vessel injury that heals subsequently. This bears many similarities to the processes described in wound healing.

In analyzing the restenosis process, Schwartz et al. showed that cells represented only about 11% of the neointimal volume in humans (25). This led different authors to examine the changes in extracellular matrix (ECM) associated with vessel injury. Strauss et al. examined the changes in collagen, elastin and proteoglycans in a double injury-model of rabbit iliac arteries (26). Depending on the extracellular matrix protein, they noted a two to fourfold increase in the synthesis of collagen, elastin and glycosaminoglycans after vessel injury. Synthesis peaked at one and two weeks, remained elevated at 4 weeks and then decreased to baseline levels by 12 weeks when compared with undamaged arteries. Delayed accumulation of collagen and elastin was observed at 12 weeks after injury. Karim et al. studied induction of procollagen I and III mRNA in atherosclerotic rabbit iliac arteries at 2, 7 and 30 days after angioplasty (27). They found that procollagens were transcriptionally activated early and peaked at 7 days after vessel injury. Subsequently, they also found a delayed accumulation of collagen, which doubled after 30 days

becoming the most abundant protein component of the vessel wall, representing about 50% of the vascular protein content.

Interestingly, Coats et al. found less collagen content in restenotic vessels compared with non-restenotic vessels in atherosclerotic rabbit iliac arteries, at 4 weeks after balloon angioplasty (28). They also noticed that in the neointima of non-restenotic vessels collagen fibers were thicker, more organized and contained less cells. In contrast, they did not find significant differences in gelatinase and collagenase I activities between the 2 groups. Shi et al. examined the time course and localization of collagen and elastin expression in porcine coronary arteries after balloon angioplasty (29). Procollagen α -1(I) transcripts and intracellular type I procollagen protein increased in the adventitia within 2 days after injury. At 7 to 14 days after injury, procollagen transcription decreased in the adventitia, however expression became evident in the neointima. At 1 to 3 months after vessel injury, procollagen α -1(I) mRNA expression returned to baseline in both layers. Extracellular type I collagen on the other hand demonstrated a large increase in the adventitia and neointima at 3 months after injury. An increase in tropoelastin mRNA was noted in the neointima at 1 and 3 months but not in the media or adventitia. In an atherosclerotic monkey model, Geary et al. confirmed expression of procollagen I initially in the adventitia (day 4) and then in the forming neointima (day 14) which persisted for 3 months. Elastin staining was only associated with mature neointima (22).

A series of other components (proteoglycans and glycoproteins) of extracellular matrix are also being studied in the context of vessel healing after balloon angioplasty (30, 31). Indeed, it has become clear that extracellular matrix is not only important for the strength and elasticity of the vessel wall, but it also regulates numerous biological processes through complex interactions with growth factors, cells and integrins. For example, it has been postulated that the decrease in clinical restenosis observed in the EPIC trial with Abciximab could have resulted from the blockade of interactions between vascular cells and the vitronectin receptor. Abciximab has indeed a similar affinity for the platelet glycoprotein IIb-IIIa receptor preventing fixation of

fibrinogen as it does for the other integrin $\alpha_v\beta_3$ (vitronectin receptor). Geary et al. also showed increased integrin expression after vessel injury (32). The vitronectin receptor increased early (days 2 to 7) in the injured media and was then detected in the forming neointima by day seven. Ongoing clinical trials are studying whether Abciximab may also reduce angiographic restenosis rates.

As proposed by Batchelor et al. it seems that there is an early extracellular matrix that provides environment for platelet adhesion, cellular migration and proliferation and further ECM elaboration (30). A late ECM which comprises essentially collagen, elastin and proteoglycans is then formed during weeks to months after the initial injury which undergoes as yet unidentified remodeling processes which contributes to the late geometric changes associated with restenosis. ECM formation and the changes associated with vessel injury will certainly continue to be investigated in the upcoming years and further elucidation of the different pathways of formation and degradation may lead to new therapeutic options.

Intravascular ultrasound (IVUS) has provided us with a view of living vessels that can then be correlated with pathological information from animal models and limited post mortem data, improving our understanding of the healing process after balloon angioplasty. IVUS was developed to supply detailed information not only on arterial stenosis but also on atherosclerotic plaque. Abnormalities of both the arterial lumen and vessel wall are well depicted by IVUS (33). Histologically, progressive accumulation of plaque in the intima is often associated with disruption of the internal elastic lamina and increased collagen content in the media. The resulting modifications in the echogenicity of these structures may render the identification of the intima-media border difficult. The interface between lumen and intima and the border between media and adventitia (the external elastic membrane) however, remain easily discernable and reliable. IVUS therefore allows quantitative measurement of the lumen area and of the area circumscribed by the external elastic membrane. The difference between these two areas is the intima + media + plaque, i.e. the wall area excluding the surrounding adventitia.

Di Mario et al. compared results after PTCA or directional atherectomy (DCA) by IVUS in 34 patients (34). The late lumen loss after PTCA was attributed to a decrease in vessel size as assessed by external elastic membrane (EEM) measurement with little change in vessel wall area. In contrast, restenosis following directional atherectomy resulted predominantly from an increase in arterial wall area with no reduction in vessel size. Overall, a chronic reduction in total vessel area was responsible for 67 % of late lumen loss after PTCA compared with 8% after directional atherectomy. Mintz et al. performed serial IVUS studies in 212 coronary lesions after PTCA, directional atherectomy (DCA), rotational atherectomy or excimer laser angioplasty (35). At 6-month follow-up, 73% of late lumen loss was due to a decrease in EEM. These authors also noted that vessel size changes were bi-directional. An increase in EEM was noted in 22% of lesions despite an increased vessel wall area (1.5 ± 2.5 vs. 0.5 ± 2.0 mm²) when compared with lesions, presenting with constriction or a reduction of EEM area. Kimura et al. studied 79 lesions after PTCA or DCA in the SURE trial (36). Serial IVUS examinations were conducted before intervention, immediately after, 24 hrs later, at 1 month and at 6 months. Vessel area increased after intervention and continued to enlarge at 24 hrs and at 1 month. Thereafter, between 1 month and 6 month, vessel size decreased significantly. Vessel wall area increased significantly from 24 hrs to 6 months. Of note, reference segments paralleled lesion site measurements. It was also observed that restenotic lesions presented a larger decrease in total vessel area and bigger increase vessel wall area between 1 and 6 months than non-restenotic lesions.

Lansky et al. analyzed results from the Optimal Atherectomy Restenosis Trial (OARS) trial to characterize more fully restenosis after DCA (37). They observed a decrease in vessel area at the lesion site from 19.1 ± 7.7 mm² post procedure to 16.9 ± 6.2 mm² at 6 months. This latter value was even lower than that seen before intervention (17.7 ± 5.7 mm²). In contrast, there was no significant change in vessel wall area. Overall, 22 (20%) of 104 patients had a late increase in EEM area. In patients with restenosis, a larger decrease in EEM area was demonstrated whereas there was no significant difference in vessel wall area compared with patients without restenosis. When subgroups were compared, including de novo versus restenotic lesions and DCA with and

Table I: Intravascular Ultrasound after Catheter-Based Coronary Interventions

Author (year)	Device	Area	Pre	Post	24 hrs	1 month	6 months	Δ Post/ follow-up
Di Mario <i>et al.</i> (95)	PTCA	L	-	-	-	-	-	-2.1 \pm 1.8
		EEL	-	-	-	-	-	-1.4 \pm 1.7
		P+M	-	-	-	-	-	0.7 \pm 2.9
	DCA \pm PTCA	L	-	-	-	-	-	-2.3 \pm 2.5
		P+M	-	-	-	-	-	-0.2 \pm 2.0
		EEL	-	-	-	-	-	2.1 \pm 1.8
Mintz <i>et al.</i> (96)	PTCA, Laser, DCA, Rotablator	L	1.7 \pm 0.9	6.6 \pm 2.5	-	-	4.0 \pm 3.7	-2.6 \pm 3.3
		EEL	18.5 \pm 6.3	20.1 \pm 6.4	-	-	18.2 \pm 6.4	-1.9 \pm 3.6
		P+M	16.8 \pm 6.2	13.5 \pm 5.5	-	-	14.2 \pm 5.4	0.7 \pm 2.3
Kimura <i>et al.</i> (97)	DCA	L	2.1 \pm 0.7	6.81 \pm 2.2	6.93 \pm 2.5	8.22 \pm 2.8	4.9 \pm 2.9	-1.93
		EEL	15.4 \pm 5.2	17.3 \pm 5.3	17.9 \pm 5.4	19.4 \pm 5.3	16.3 \pm 5.5	-0.99
		P+M	13.4 \pm 5.0	10.5 \pm 4.4	11.0 \pm 4.5	11.2 \pm 4.1	11.4 \pm 4.4	0.94
Lansky <i>et al.</i> (98)	DCA \pm PTCA	L	2.0 \pm 1.3	8.8 \pm 2.5	-	-	5.5 \pm 4.0	-3.3
		EEL	17.7 \pm 5.7	19.7 \pm 5.6	-	-	16.9 \pm 6.2	-2.8
		P+M	15.6 \pm 5.3	10.9 \pm 4.2	-	-	11.3 \pm 3.9	0.4
Tardif <i>et al.</i> (99)	PTCA	L	-	4.5 \pm 1.4	-	-	3.3 \pm 1.4	-1.2 \pm 1.9
		EEL	-	13.4 \pm 3.4	-	-	13.7 \pm 4.2	0.3 \pm 2.9
		P+M	-	8.8 \pm 3.0	-	-	10.3 \pm 3.9	1.5 \pm 2.5

PTCA: Percutaneous Transluminal Coronary Angioplasty, DCA: Directional Coronary Atherectomy, L: Lumen, P+M: Plaque + Media, EEL: External Elastic Lamina. All results are expressed in mm².

without adjunct PTCA, no significant differences were found with regard to neointimal proliferation or modification of vessel size. In diabetics, however, IVUS showed greater changes of vessel wall area (1.8 ± 2.0 vs. 0.3 ± 2.3 mm², $P < 0,039$) when compared with non-diabetics. Using three-dimensional reconstruction, De Vrey et al. pooled results from the SURE and the OARS trials and confirmed the significant vessel shrinkage after DCA (38).

Tardif and his group performed an IVUS substudy in the Multi-Vitamins and Probucol (MVP) trial which provided some insight into the natural history of restenosis following balloon angioplasty in de novo lesions (39). They found a minimal increase in EEM area from 13.37 ± 3.45 mm² after intervention to 13.66 ± 4.18 mm² for the control group (31 lesions) at 6 months. There was also an increase in vessel wall area from 8.85 ± 3.01 mm² immediately post procedure to 10.35 ± 3.95 mm² at 6 months. Importantly, the change in lumen area correlated with the change in EEM ($r = 0.53$, $P = 0.002$) but not with change in vessel wall area, which partly represents neointimal formation ($r = -0.13$, $P = 0.49$). This group also observed a bi-directional response of the vessels with 42 % of patients demonstrating vessel constriction and 39% in fact demonstrating compensatory vessel enlargement ≥ 1 mm² at follow-up.

In summary, these IVUS studies confirmed the role of vessel size changes or remodeling, in the restenotic process after several types of coronary catheter-based interventions. At the same time, IVUS studies have also demonstrated the almost exclusive role of neointima formation during in-stent restenosis where stenting abolishes the deleterious remodeling (40).

Novel therapies and treatment challenges in restenosis prevention

Stents

Intracoronary endoluminal prostheses, known as intracoronary stents, were initially developed and applied to angioplasty for the treatment of acute closure and dissections (41). The protection of this bailout device has allowed interventionists to perform more aggressive

angioplasty with larger final lumen diameters without the risk of severe flow-limiting dissection and subsequent surgery. These improved immediate post-angioplasty results have led to a reduction of restenosis at six months even in non-stented arteries. Intracoronary stents, however, have been shown to significantly reduce angiographic restenosis rates in selected coronary lesions compared with balloon angioplasty (42, 43). These results were correlated with a decrease in target vessel revascularization rates, ischemic complications and mortality at 6 months. This initial clinical benefit was maintained over more prolonged follow-up (44).

In a study involving 383 patients with restenosis, Erbel et al. showed that restenosis rates were significantly lower after stent deployment compared with PTCA alone (32% vs. 18%, $P = 0.03$) (45). Revascularization of the target vessel at 6 months was required in 27% of the PTCA group compared with 10% in the stent group ($P = 0.001$). This difference resulted from a larger minimum lumen diameter at 6 months after stenting compared with PTCA (2.04 ± 0.66 mm vs. 1.85 ± 0.56 mm, $P = 0.01$). The rate of event-free survival at 250 days was also significantly higher with stenting than PTCA (84% vs. 72%, $P = 0.04$). Stent thrombosis was noted in 3.9% of cases. To counter this devastating complication of stent implantation, aggressive anticoagulation was initially proposed. Investigators have subsequently demonstrated that improvements in deployment techniques, initially using IVUS guidance, and the association of the antiplatelet agents, aspirin and ticlopidine, rather than aggressive anticoagulation, resulted in impressive reduction of stent thrombosis (46).

The plethora of new stent designs and delivery systems have resulted in devices that are easier to deploy and have the technical ability to track to almost any site in the coronary tree. Numerous studies with different stent designs have shown that the vast majority of balloon expandable stents achieve similar results with regard to final lumen diameter and restenosis rates. Recent data suggests that stenting may also improve outcome in small vessels (< 3.0 mm) (47-49). Results of ongoing randomized trials comparing PTCA with several stent designs in small vessels will become available soon. Preliminary data appear encouraging for the use of stents in

this vessel subset (50). Other studies with different stents are ongoing to better define the place of stenting in treatment of long lesions, bifurcations and chronic occlusions.

There is no doubt that intracoronary stents have led to exciting improvements in restenosis prevention. Nonetheless, stents in themselves cause increased vessel damage and subsequent neointimal formation. This resultant in-stent restenosis has become an even more formidable opponent for the interventional cardiologist. The current challenges are both to prevent and to treat in-stent restenosis. Intensive research focuses presently on stent biocompatibility and new polymer coatings (51). Several pharmacologic compounds such as paclitaxel (a chemotherapeutic agent) and a combination of hirudin and prostacyclin have shown promising results in animal models and will soon progress to clinical trials (52, 53). However, currently the most promising approach to the treatment of in-stent restenosis is radiation therapy.

Radiation

Ionizing radiation has recently generated much interest as a treatment option for restenosis after vessel injury (54). Endovascular radiation can be applied using a catheter based system or alternatively with a radioactive implant, such as a stent. The first relies on high activity γ or β emitting sources such as ribbons, seeds, liquid or gas to deliver a dose of radiation locally through an endoluminal catheter in a limited period of time. Since these radioactive sources are positioned within the vessel lumen, sufficiently high energy isotopes are required to deliver an adequate dose to the vessel wall during the relatively short time frame of the procedure. The second approach uses the deployment of a radioactive stent with resultant long exposure and continuous low dose-rate treatment. Some experimental studies using external beam irradiation have been performed; however, its application appears more feasible for peripheral rather than coronary artery disease, due to the technical difficulties of treating the moving target that these arteries represent.

Ionizing radiation has multiple effects on target cells, the most obvious being cell killing. In general, less differentiated and highly proliferative cells are more sensitive than non-proliferating, well-differentiated cells. Strong evidence indicates that the nucleus and specifically the DNA structure, is the principal target for radiation-induced cell death (55). In proportion with the amount of chromosomal damage, most irradiated cells will die during or after mitosis. Radiation may also induce cell death through apoptosis, although to a much lesser extent (56). Cell killing is not the only effect of ionizing radiation. It is now well established that radiation induces early and late gene expression (57, 58). The products of these genes, specifically growth factors and cytokines, contribute to and modulate the overall response of the irradiated tissue. Growth factors that have been demonstrated to play a role in restenosis after vessel injury are also synthesized or released after radiation injury. These factors are clearly implicated in tissue reactions such as inflammation, repopulation, tissue repair and late fibrosis. It is therefore vital to appreciate that radiation injury bears some similarity with vessel injury after balloon angioplasty or stent implantation.

Several groups at Columbia University, Emory University, Baylor College of Medicine in the USA and Geneva University in Switzerland pioneered the use of endovascular radioactive sources for the prevention of restenosis after balloon angioplasty with and without stent implantation (59-62). Single doses in excess of 10 Gy produced a highly significant reduction of neointimal formation and abolished vessel constriction (54). Lower doses were either ineffective or produced paradoxically worse results than in the controls. Investigators using a γ source (¹⁹²Iridium) further described a persistent benefit to 6 months. Perivascular and intramural fibrosis was noticed in some studies and did not worsen after 6 months. Abnormalities in endothelium dependent and independent vascular reactivity have been described following vessel irradiation acutely and over longer-term follow-up. Different types of catheters, sources and isotopes including both β and γ emitters as well as x-rays continue to undergo preclinical testing.

Concurrently, significant efforts have been invested in the development of several radioactive stent prototypes. These have been evaluated in both rabbit and pig models (63, 64). With a ^{32}P phosphorous-isotope coated stent, a 30% reduction of neointima formation has been demonstrated with certain activities. This is in spite of negative results that were obtained with intermediate activity. Intensive research to develop other types of radioactive stents is currently underway (65).

Condado et al. reported the first use of an endovascular ^{192}Ir source in 21 patients after balloon angioplasty with or without stent implantation (66). The prescribed dose was 20 or 25 Gray (Gy) at 1.5 or 2 mm from the source. As there was no centering of the source and the vessel sizing was performed visually significant dose variation can be presumed. Quantitative coronary analysis revealed a significant early loss after 24 hrs but almost no late loss. With follow-up extending to 3 years, the most significant event relates to the presence of 4 coronary aneurysms. Although the late progression of these vessel abnormalities is unknown, it should be noted that post-hoc dosimetric analysis revealed that significantly higher doses were probably delivered to the arterial wall (19-55 Gy) with a potential maximum dose of up to 92 Gy. The Geneva group reported a feasibility study in 15 patients using a centering balloon and the β emitter ^{90}Y trium (67). With a target dose of 18 Gy at the luminal surface, no adverse event was reported but the angiographic restenosis rate was not reduced in 6/15 patients. It is possible that doses administered were too low to effectively curtail the restenotic response.

The Beta Energy Restenosis Trial (BERT), a feasibility study performed jointly by Emory University-Rhode Island Hospital, the Montreal Heart Institute and the Thoraxcenter recruited 85 patients to evaluate the endoluminal delivery of β radiation using the isotopes ^{90}Sr ontium/ ^{90}Y trium. Doses were randomized between 12 Gy, 14 Gy and 16 Gy at 2 mm depth. Angiographic restenosis rates among the 3 institutions were 15%, 10% and 27% respectively (68, 69). Angiographic follow-up revealed almost no late loss, significantly better than a historical

control group. An IVUS substudy performed at the Montreal Heart Institute revealed no change in vessel wall area and no change in total vessel area (68).

The first randomized trial was performed at Scripps clinic in 55 patients with restenosis (3). This patient group included post PTCA (1/3) as well as in-stent restenosis (2/3). If a coronary stent had not previously been deployed, this was performed prior to brachytherapy. The γ source ^{192}Ir was used in a non-centered catheter. Under IVUS guidance a dose of 8 Gy to the point of the EEM furthest from the catheter was prescribed (with a limiting maximum dose of 30 Gy). A restenosis rate of 17% in irradiated vessels was found, significantly less than the 55% seen in the control group. Similarly, IVUS analysis demonstrated a significant reduction in neointima volume formation at 6 months with endovascular irradiation ($15.5 \pm 22.7 \text{ mm}^3$ vs. $45.1 \pm 39.4 \text{ mm}^3$, $P = 0.01$). Two-year follow-up has recently confirmed persistence of the clinical benefit (70). Small pilot studies have also examined the potential of ^{32}P coated stents with increasing activities. Excellent feasibility has been demonstrated with no stent occlusion reported. However, so far angiographic restenosis rates have not decreased in the stents with lower activities. Furthermore the stents with higher activities have been complicated by restenosis predominating at the stent borders (the candy wrapper or edge effect) (71). Dose-finding studies continue to define the minimum effective dose. A series of large randomized trials evaluating γ and β sources for the prevention and the treatment of restenosis has now been launched and will clarify the potential of radiation therapy in the next 2 years.

Pharmacological compounds and antioxidants

Tardif et al. evaluated the potential of an antioxidant drug, probucol, alone or in combination with a multivitamins complex to reduce restenosis in 317 patients with de novo coronary artery lesions (72). Using a pre-treatment period of 30 days prior to the index procedure, patients were randomized into 4 groups: placebo, multivitamins, multivitamins + probucol and probucol. At 6 months, angiographic restenosis rate was significantly reduced with probucol compared with no probucol (21% with probucol vs. 39% without probucol, $P = 0.009$).

Unexpectedly, treatment with multivitamins partially suppressed the benefit observed with probucol. The efficacy of probucol treatment was also evident in the subgroup of smaller vessels when compared to larger vessels. In an IVUS substudy, probucol induced more vessel enlargement to accommodate neointimal growth (39). Improved geometric remodeling therefore, appears to be the mechanism by which probucol reduced restenosis. The role of oxidative stress and free radicals on restenosis is currently being investigated. Powerful antioxidants are now undergoing testing in animal models and will undoubtedly be progressed to clinical trials in the future.

Another drug, cilostazol, a phosphodiesterase inhibitor, has also shown promising early results when delivered orally in patients following coronary interventions (73-75). In all cases, it appears that scrupulous understanding of the pharmacology of these oral compounds is mandatory to anticipate a clinical benefit.

Gene Therapy

Numerous approaches using the basic techniques of gene therapy are being applied and tested for the prevention of restenosis (76). The most direct method is the incorporation of a gene into the proliferating smooth muscle cell. The gene can encode for a cytotoxic protein (e.g. herpes virus thymidine kinase), a cell cycle inhibitory protein (e.g. p53, p21, Rb, cdk), angiogenic proteins (e.g. VEGF, angiogenin, bFGF) or proteins with vasodilatory, antithrombotic or antiproliferative properties (e.g. NOS, cox-1, PAI-1) (76). Genes can be transferred using a viral vector, such as adenovirus or as naked plasmid DNA (77). Successful reduction of neointima formation using in vivo gene transfer has already been demonstrated in animal models (77). Recently, introduction of naked DNA coding for Vascular Endothelial Growth Factor (VEGF) was reported to be clinically effective in treating peripheral vascular disease with chronic ischaemia (78).

An alternative approach for limitation of restenosis has been the development of antisense oligonucleotide technology (76). These are short pieces of DNA with sequences that are complementary to specific regions of messenger RNA. Once bound to the target m-RNA, the antisense compound inhibits its interaction with ribosomes. With this technology any gene may be targeted for antisense suppression. Inhibition of production of several mediators of the cell cycle with antisense oligonucleotides has been effective in animal models of vascular injury. Most recently this technology has been applied in a single center randomized study against c-myc for prevention of in-stent restenosis following intracoronary Wallstent deployment in 84 patients (79). Initial results are not encouraging with restenosis rates of 38% and 34% in the placebo and active arms respectively. There was no evidence of a reduction of neointimal volume obstruction as measured by IVUS in this population. In spite of the lack of success in human restenosis inhibition and of the formidable obstacles to overcome, the variety of approaches and broad choice of genes for intervention leaves this field as a potentially fruitful area in the future.

Conclusion

Restenosis following percutaneous coronary interventions remains a major limiting feature of these techniques. Despite its minor contribution to cardiac mortality this problem results in significant symptomatic limitation for patients and financial drain on the health system. Historical perspectives and innovative research have resulted in multiple approaches to this problem. The most successful modality to date has been coronary stenting. In spite of this, we have found that this solution is a double-edged sword, as where it fails, the interventionist is faced with the even more vexing problem of in-stent restenosis. Numerous alternative modalities are emerging, including radiation therapy, antioxidants, novel pharmacological agents and gene therapy. Their further development and prudent application will result in a further significant reduction of restenosis, and subsequently will therefore have a profound impact on the financial drain of recurrent procedures as well as improving patient comfort.

References

1. Gruentzig A, Senning A, Siegenhaler WE. Non-operative dilatation of coronary artery stenosis: percutaneous transluminal coronary angioplasty. *N Engl J Med* 1979;301:61.
2. Bourassa MG, Lesperance J, Eastwood C, et al. Clinical, physiologic, anatomic and procedural factors predictive of restenosis after percutaneous transluminal coronary angioplasty. *J Am Coll Cardiol* 1991;18:368.
3. Teirstein P, Massulo V, Jani S, et al. Catheter-based radiotherapy to inhibit restenosis after coronary stenting. *N Engl J Med* 1997;336:1697-703.
4. Serruys PW, Luijten HE, Beutt KJ, et al. Incidence of restenosis after successful coronary angioplasty: A time-related phenomenon: A quantitative angiographic follow-up study of 342 patients at 1,2,3 and 4 months. *Circulation* 1988;77:361-71.
5. Waller BF, Gorfinkel HJ, Rogers FJ, Kent KM, Roberts WC. Early and late morphologic changes in major epicardial coronary arteries after percutaneous transluminal coronary angioplasty. *Am J Cardiol* 1984;53:42C-7C.
6. Essed CE, Van den Brand M, Becker AE. Transluminal coronary angioplasty and early restenosis. Fibrocellular occlusion after wall laceration. *Br Heart J* 1983;49:393-6.
7. Ueda M, Becker AE, Tsukada T, Numano F, Fujimoto T. Fibrocellular tissue response after percutaneous transluminal coronary angioplasty. An immunocytochemical analysis of the cellular composition. *Circulation* 1991;83:1327-32.
8. Ueda M, Becker AE, Fujimoto T, Tsukada T. The early phenomena of restenosis following percutaneous transluminal coronary angioplasty. *Eur Heart J* 1991;12:937-45.
9. Clowes AW, Reidy MA, Clowes MM. Kinetics of cellular proliferation after arterial injury: smooth muscle growth in the absence of endothelium. *Lab Invest* 1983;49:327-33.
10. Libby P, Tanka H. The molecular bases of restenosis. *Prog Cardiovasc Dis* 1997;40:97-106.
11. Libby P, Schwartz D, Brogi E, Tanaka H, Clinton SK. A cascade model for restenosis, a special case of atherosclerosis progression. *Circulation* 1992;86:47-52.

12. Kuntz RE, Gibson CM, Nobuyoshi M, Baim DS. Generalized model of restenosis after conventional balloon angioplasty, stenting and directional atherectomy. *Circulation* 1993;21:15-25.
13. Adelman AG, Cohen EA, Kimball BP, et al. A comparison of directional atherectomy with balloon angioplasty for lesions of left anterior descending coronary artery. *N Engl J Med* 1993;329:228-33.
14. Nakamura Y, Zhao H, Yutani C, Imakita M, Ishibashi-Ueda H. Morphometric and histologic assessment of remodeling associated with restenosis after percutaneous transluminal angioplasty. *Cardiology* 1998;90:115-21.
15. Kakuta T, Currier JW, Haudenschild CC, Ryan TJ, Faxon DP. Differences in compensatory vessel enlargement, not intimal formation, account for restenosis after angioplasty in the hypercholesterolemic rabbit model. *Circulation* 1994;89:2809-15.
16. Post MJ, Borst C, Kuntz RE. The relative importance of arterial remodeling compared with intimal hyperplasia in lumen renarrowing after balloon angioplasty. A study in the normal rabbit and the hypercholesterolemic Yucatan micropig. *Circulation* 1994;89:2816-21.
17. de Smet BJ, van der Zande J, van der Helm YJ, Kuntz RE, Borst C, Post MJ. The atherosclerotic Yucatan animal model to study the arterial response after balloon angioplasty: the natural history of remodeling. *Cardiovasc Res* 1998;39:224-32.
18. Lafont A, Guzman LA, Whitlow PL, Goormastic M, Cornhill JF, Chisolm GM. Restenosis after experimental angioplasty: intimal, medial, and adventitial changes associated with constrictive remodeling. *Circ Res* 1995;76:996-1002.
19. Scott NA, Cipolla GD, Ross CE, et al. Identification of a potential role for the adventitia in vascular lesion formation after balloon overstretch injury of porcine coronary arteries. *Circulation* 1996;93:2178-87.
20. Shi Y, Pieniek M, Fard A, O'Brien J, Mannion JD, Zalewski A. Adventitial remodeling after coronary arterial remodeling. *Circulation* 1996;93:340-8.
21. Shi Y, O'Brien JE, Fard A, Mannion J, Wang D, Zalewski A. Adventitial myofibroblasts contribute to neointimal formation in injured porcine coronary arteries. *Circulation* 1996;94:1655-64.

22. Geary RL, Nikkari ST, Wagner WD, Williams JK, Adams MR, Dean RH. Wound healing : a paradigm for lumen narrowing after arterial reconstruction. *J Vasc Surg* 1998;27:96-106 (-8).
23. Kwon MK, Sangiorgi G, Ritman EL, et al. Adventitial vasa vasorum in balloon-injured coronary arteries. Visualization and quantitation by a microscopic three-dimensional computed tomography technique. *J Am Coll Cardiol* 1998;32:2072-9.
24. Pels K, Labinaz M, Hoffert C, O'Brien ER. Adventitial angiogenesis early after coronary angioplasty. Correlation with arterial remodeling. *Arterioscler Thromb Vasc Biol* 1999;19:229-38.
25. Schwartz RS, Holmes DR, Topol EJ. The restenosis paradigm revisited: an alternative proposal for cellular mechanisms. *J Am Coll Cardiol* 1992;20:1284-93.
26. Strauss BH, Chisholm RJ, Keeley FW, Gotlieb AI, Logan RA, Armstrong PW. Extracellular matrix remodeling after balloon angioplasty injury in a rabbit model of restenosis. *Circ Res* 1994;75:650-8.
27. Karim MA, Miller DD, Farrar MA, et al. Histomorphometric and biochemical correlates of arterial procollagen gene expression during vascular repair after experimental angioplasty. *Circulation* 1995;91:2049-57.
28. Coats WD, Whittaker P, Cheung DT, et al. Collagen content is significantly lower in restenotic versus nonrestenotic vessels after balloon angioplasty in the atherosclerotic rabbit model. *Circulation* 1997;95:1293-300.
29. Shi Y, O'Brien JE, Ala-Kokko L, Chung W, Mannion JD, Zalewski A. Origin of extracellular matrix synthesis during coronary repair. *Circulation* 1997;95:997-1006.
30. Batchelor WB, Robinson R, Strauss BH. The extracellular matrix in balloon arterial injury: a novel target for restenosis prevention. *Prog Cardiovasc Dis* 1998;41:35-49.
31. Strauss BH, Robinson R, Batchelor WB, et al. In vivo collagen turnover following experimental balloon angioplasty injury and the role of matrix metalloproteinases. *Circ Res* 1996;79:541-50.
32. Deitch JS, Williams JK, Adams MR, et al. Effects of beta3-integrin blockade (c7E3) on the response to angioplasty and intra-arterial stenting in atherosclerotic non human primates. *Arterioscl Thromb Vasc Biol* 1998;18:1730-7.

33. Tardif JC, Lee HS. Applications of intravascular ultrasound in cardiology. In: J.H.C Reiber, E.E. van der Wall, eds. *What's new in cardiovascular imaging?* Dordrecht: Kluwer Academic Publishers, 1998:133-48.
34. Di Mario C, Gil R, Camenzind E, et al. Quantitative assessment with intracoronary ultrasound of the mechanisms of restenosis after percutaneous transluminal coronary angioplasty and directional coronary atherectomy. *Am J Cardiol* 1995;75:772-7.
35. Mintz GS, Popma JJ, Pichard AD, Kent KM, Satler L, Leon MB. Arterial remodeling after coronary angioplasty: a serial intravascular ultrasound study. *Circulation* 1996;94:35-43.
36. Kimura T, Nobuyoshi M. Remodelling and restenosis: intravascular ultrasound studies. *Sem Interv Cardiol* 1997;2:159-66.
37. Lansky A, Mintz GS, Popma JJ, et al. Remodeling after directional coronary atherectomy (with and without) adjunct percutaneous transluminal coronary angioplasty): a serial angiographic and intravascular ultrasound analysis from the Optimal Atherectomy Restenosis Study. *J Am Coll Cardiol* 1998;32:329-37.
38. De Vrey E, Mintz GS, von Birgelen C, et al. serial volumetric (three-dimensional) intravascular ultrasound analysis of restenosis after directional atherectomy. *J Am Coll Cardiol* 1998;32:1874-80.
39. Cote G, Tardif JC, Lesperance J, et al. Effects of probucol on vascular remodeling after coronary angioplasty. *Circulation* 1999;99:30-5.
40. Hoffman R, Mintz GS, Dussaillant GR, et al. Patterns and mechanisms of in-stent restenosis. A serial intravascular ultrasound study. *Circulation* 1996;94:1247-54.
41. Bertrand OF, Legrand V, Bilodeau L, Martinez CA, Kulbertus HE. Emergency coronary stenting with Wiktor stent. Immediate and late results. *J Inv Cardiol* 1997;9:2-9.
42. Fischman DL, Leon MB, Baim DS, et al. A randomized comparison of coronary-stent placement and balloon angioplasty in the treatment of coronary artery disease. *N Engl J Med* 1994;331:496-501.
43. Serruys PW, de Jaegere P, Kiemeneij F, et al. A comparison of balloon-expandable-stent implantation with balloon angioplasty in patients with coronary artery disease. *N Engl J Med* 1994;331:489-95.

44. Laham RJ, Carozza JP, Berger C, Cohen DJ, Kuntz RE, Baim DS. Long term (4- to 6-year) outcome of Palmaz-Schatz stenting: paucity of late clinical stent-related problems. *J Am Coll Cardiol* 1996;28:820-6.
45. Erbel R, Haude M, Hopp HW, et al. Coronary-artery stenting compared with balloon angioplasty for restenosis after initial balloon angioplasty. Restenosis Stent Study Group. *N Engl J Med* 1998;339:1672-8.
46. Leon MB, Baim DS, Popma JJ, et al. A clinical trial comparing three antithrombotic-drug regimens after coronary-artery stenting. Stent Anticoagulation Restenosis Study Investigators. *N Engl J Med* 1998;339:1665-71.
47. Elezi S, Kastrati A, Neumann FJ, Hadamitzky M, Dirschinger J, Schomig A. Vessel size and long-term outcome after coronary stent placement. *Circulation* 1998;98:1875-80.
48. Akiyama T, Moussa I, Reimers B, et al. Angiographic and clinical outcome following coronary stenting of small vessels: a comparison with coronary stenting of large vessels. *J Am Coll Cardiol* 1998;32:1610-18.
49. Savage MP, Fischman DL, Rake R, et al. Efficacy of coronary stenting versus balloon angioplasty in small coronary arteries. Stent Restenosis Study (STRESS) Investigators. *J Am Coll Cardiol* 1998;31:307-11.
50. Doucet S, Schlij M. Stenting of small coronary arteries: interim report of a randomized multicenter trial in patients with a vessel reference diameter of 2.3-2.9 mm (Abstract). *J Am Coll Cardiol* 1999;85:43A.
51. Bertrand OF, Sipehia R, Mongrain R, et al. Biocompatibility aspects of new stent technology. *J Am Coll Cardiol* 1998;32:562-71.
52. Suh H, Jeong B, Rathi R, Kim SW. Regulation of smooth muscle cell proliferation using paclitaxel-loaded poly(ethylene oxide)-poly(lactide/glycolide)nanospheres. *J Biomed Mater Res* 1998;42:331-8.
53. Alt E, Beilharz C, Preter D, et al. Biodegradable stent coating with polylactic acid, hirudin and prostacyclin reduces restenosis (Abstract). *J Am Coll Cardiol* 1997;29:238A.
54. Bertrand OF, Mongrain R, Lehnert S, et al. Intravascular radiation therapy in atherosclerotic disease: promises and premises. *Eur Heart J* 1997;18:1385-95.

55. Hall EJ. Radiobiology for the radiologist. 4 ed. Philadelphia: J.B. Lippincott Company, 1994.
56. Dewey WC, Ling CC, Meyn RE. Radiation-induced apoptosis: Relevance to radiotherapy. *Int J Radiat Oncol Bio Phys* 1995;33:781-96.
57. Weichselbaum RR, Hallahan DE, Sukhatme V, Dritschillo A, Sherman ML, Kufe DW. Biological consequence of gene regulation after ionizing radiation exposure. *J Natl Cancer Inst* 1991;83:480-84.
58. Weichselbaum RR, Hallahan D, Fuks Z, Kufe D. Radiation induction of immediate early genes: Effectors of the radiation-stress response. *Int. J. Radiat. Oncol. Bio. Phys.* 1994;30:229-34.
59. Verin V, Popowski Y, Urban P, et al. Intra-arterial beta irradiation prevents neointimal hyperplasia in a hypercholesterolemic rabbit restenosis model. *Circulation* 1995;92:2284-90.
60. Waksman R, Robinson KA, Croker IR, Gravanis MB, Cipolla GD, King SB. Endovascular low-dose irradiation inhibits neointima formation after coronary artery balloon injury in swine. *Circulation* 1995;91:1533-39.
61. Weinberger J, Amols H, Ennis R, Schwartz A, Wiedermann J, Marboe C. Intracoronary irradiation: Dose response for the prevention of restenosis in swine. *Int J Radiat Oncol Bio Phys* 1996;36:767-75.
62. Mazur W, Ali M, Khan M, et al. High dose rate intracoronary radiation for inhibition of neointimal formation in the stented and balloon-injured porcine models of restenosis: Angiographic, morphometric, and histopathologic analyses. *Int J Radiat Oncol Bio Phys* 1996; 36:777-88.
63. Carter A, Laird J, Bailey L, et al. Effects of endovascular radiation from a β -particle - emitting stent in a porcine coronary restenosis model. A dose-response study. *Circulation* 1996;94:2364-68.
64. Hehrlein C, Stintz M, Kinscherf R, et al. Pure β -particle-emitting stents inhibits neointima formation in rabbits. *Circulation* 1996;93:641-5.
65. Häfeli UO, Warburton MC, Landau U. Electrodeposition of radioactive rhenium onto stents to prevent restenosis. *Biomaterials* 1998;19:925-33.

66. Condado JA, Waksman R, Gurdiel O, et al. Long-term angiographic and clinical outcome after percutaneous transluminal coronary angioplasty and intracoronary radiation therapy in humans. *Circulation* 1997;96:727-32.
67. Verin V, Urban P, Popowski Y, et al. Feasibility of intracoronary β -irradiation to reduce restenosis after balloon angioplasty. A clinical pilot study. *Circulation* 1997;95:1138-44.
68. Meerkin D, Tardif JC, Crocker IR, et al. Effects of intracoronary β -radiation therapy after coronary angioplasty: an intravascular ultrasound study. *Circulation* 1999;99:1660-1665.
69. King SB, Williams DO, Chougoule L, et al. Endovascular beta-radiation to reduce restenosis after coronary balloon angioplasty: results of the Beta Energy Restenosis Trial (BERT). *Circulation* 1998;97:2025-30.
70. Teirstein PS, Massulo V, Jani S, Russo RJ, Cloutier DA. Two-year follow-up after catheter-based radiotherapy to inhibit coronary restenosis. *Circulation* 1999;99:243-7.
71. Albiero R, Di Mario C, Gregorio JD, Kobayashi N, Adamian M, Moussa I. Intravascular ultrasound (IVUS) analysis of beta-particle emitting radioactive stent implantation in human coronary arteries. Preliminary immediate and intermediate-term results of the MILAN study (Abstract). *Circulation* 1998;98:I-780.
72. Tardif JC, Côté G, Lespérance J, et al. Probucol and multivitamins in the prevention of restenosis after coronary angioplasty. *N Engl J Med* 1997;337:365-72.
73. Take S, Matsutami M, Ueda H, et al. Effect of cilostazol in preventing restenosis after percutaneous transluminal coronary angioplasty. *Am J Cardiol* 1997;79:1097-9.
74. Tsuchikane E, Katoh O, Sumitsuji S, et al. Impact of cilostazol on intimal proliferation after directional coronary atherectomy. *Am Heart J* 1998;153:495-502.
75. Sekiya M, Funada J, Watanabe K, Miyagawa M, Akutsu H. Effects of probucol and cilostazol alone and in combination on frequency of poststenting restenosis. *Am J Cardiol* 1998;82:144-7.
76. Kutryk MJB, Serruys PW. Antirestenosis alternatives for the next millenium. In: Waksman R, ed. *Vascular Brachytherapy*. New York: Futura Publishing Company, 1999:53-60.
77. French BA. Gene therapy and cardiovascular disease. *Coron Artery Dis* 1998;13:205-13.

78. Isner JM, Pieczek A, Schainfeld R, et al. Clinical evidence of angiogenesis after arterial gene transfer of phVEGF165 in patient with ischaemic limb. *Lancet* 1996;348:370-74.
79. Serruys PW, Kutryk MJB, Bruining N, et al. Antisense nucleotide against c-myc administered with the Transport delivery catheter for the prevention of in-stent restenosis. Results of the randomized ITALICS trial (Abstract). *Circulation* 1998;98:I-363.

**CHAPTER II: Intravascular radiation therapy in atherosclerotic
disease: Promises and premises**

Introduction

Since its introduction in 1977, coronary angioplasty has become an established technique for the treatment of atherosclerotic coronary disease. Currently, more than 500, 000 procedures are performed each year worldwide. However, two major problems remain unresolved. The first, post-angioplasty acute vessel closure, occurs in about 5% of cases. In this setting, intracoronary stenting has been very useful for the management of post-angioplasty dissections (1). The second problem, restenosis, occurs in 30 to 50% of cases. Thus far, drug therapy has shown little benefits in reducing the extent of this phenomenon. Recently, however, the STRESS trial showed that intracoronary stents could reduce restenosis rates from 42% to 32%, and the BENESTENT trial had an even greater reduction: from 32% to 22% (2, 3). The beneficial effect of stenting is presumably due to better vessel geometry since it induces more neointima formation than balloon angioplasty.

Balloon dilation causes vascular lesions, which include mechanical deformation, triple layer vessel injury and early thrombus formation. Mechanical injury initiates a complex process involving vasoactive hormones, growth factors, circulating cells and possibly blood lipids. The healing process is usually in three phases: thrombus formation, followed by smooth muscle cell activation and replication in the tunica media and probably in the adventitia (4,5). This is followed by intimal smooth muscle cell migration and proliferation, which precede matrix secretion (6). Thus neointima formation as a response to injury may sometimes create further coronary obstruction. The extent of smooth muscle cell proliferation, as assessed by proliferating cell nuclear antigen staining, varies between 1% and $20 \pm 18\%$ after vessel injury (7,8). The exact timing of this cellular proliferation is unknown in humans, but in animal models it may last for about 4 weeks after stent implantation (9, 10). Schwartz et al., using computer modeling, have estimated the peak post-angioplasty proliferative phase to be around 45 days in humans (11). In addition to cell proliferation, elastic recoil and vascular remodeling have also been recognized as important mechanisms to explain the restenosis phenomenon (12, 13).

Until now, drug therapy has been focused on limiting cellular proliferation and/or thrombus inhibition. Although positive effects were reported in some animal models, they were not convincingly reproduced in humans. Recently, the use of glycoprotein IIb/IIIa inhibitors has been associated with a decrease in ischaemic complications and clinical restenosis after balloon angioplasty (14, 15). There is little doubt that thrombosis prevention after balloon injury represents a major issue for the future of coronary interventions.

Drug treatment has been shown to reduce neointima formation in animals but not humans. This has been attributed, in part, to differences in tissue drug concentrations between animals and man. Thus, local drug delivery has been advocated to prevent restenosis. New catheters delivering drugs locally or regionally after angioplasty have been designed and clinical trials are ongoing (16, 17). Our understanding of the molecular biology and genetics of the restenosis mechanism has also improved, but problems remain concerning safety, cost and the handling of these genetic tools (18).

Local radiation therapy has promise, but also drawbacks and possibly serious side effects. Radiation therapy has been part of our medical armamentarium for decades and its effectiveness in controlling actively dividing tumor cells is well established. The concept of using local radiation to control smooth muscle cell proliferation is based on the assumption that ionizing radiation will kill proliferating smooth muscle cells and therefore limit neointima formation. This therapy has been applied to benign situations such as prevention of keloid scar, heterotopic bone formation or pterygium treatment as well as for the treatment of solid malignancies (19-22). Because of the biohazard, radiation therapy in clinical practice requires close collaboration between oncologists, physicists and technicians.

Brachytherapy is the term used to describe intracavitary or interstitial radiation therapy (23). Recently, this term has been used to describe endovascular radiation therapy from either radioactive sources or stents (see Appendix). We will review the current experience of using

external or endovascular radiation therapy to reduce arterial neointima formation and we will try to delineate its potential therapeutic applications and possible limitations.

External irradiation

Gellman et al. first recorded angiographic results after single doses of external irradiation in rabbit iliac arteries after balloon injury (24) (Table I). At 28 days, the angiographic lumen diameter decrease was constant in the irradiated group. Schwartz et al. obtained similar results using over-expanded stents in pig coronary arteries, submitted to increasing doses of external radiation (25) (Table II). Proliferative neointimal responses and lumen stenoses were seen in all groups, but were exaggerated in the higher dose group (8 Gy). In all three radiation groups, moderate to severe myocardial and adventitial fibrosis were present. Sudden death occurred in four irradiated pigs and all showed severe stenoses, consisting of organized neointima with fresh thrombus at the injury site. In contrast, Shefer et al. demonstrated a reduction in intimal formation after single exposure of a beta-irradiation source (9 Gy) applied against rabbit ear arteries after balloon injury (26). They observed a maximum effect when irradiation was administered 2 days post injury but no effect when applied after 7 days.

Abbas et al. studied angiographic and morphometric results 28 days after external irradiation with 6 or 12 Gy of rabbit iliac arteries after balloon angioplasty (27). Mean and minimal angiographic lumen diameters were decreased in all groups. However, in the 12 Gy treated group, lumen diameters at follow-up were not significantly different from initial values. There were minor differences in intimal hyperplasia between controls and the lower dose group. In contrast, less intimal proliferation was present in the 12 Gy treated group vs controls. Shimotakahara and Mayberg studied the effects of increasing doses and delayed administration of gamma-irradiation of rat carotid arteries (28). All groups showed a reduction in the neointimal cross-sectional area when irradiated one day after balloon injury. Significant but less prominent reductions in neointimal area were noted for all doses in arteries irradiated 2 days after injury. Extending these results, Mayberg et al. performed a detailed dose ranging study and analyzed the

Table I: External Radiation

Reference	Species	Vessel	Model	Radiation	Dose (Gy)	Dose rate (Gy . min ⁻¹)	Timing
Gellman et al. ⁽²⁴⁾	rabbit	iliac	balloon	X-rays	3 9	NA	post PTCA
Schwartz et al. ⁽²⁵⁾	pig	coronary	stent	X-rays	4 2-4 8	1	post stent
Shefer et al. ⁽²⁶⁾	rabbit	car art.	balloon	β	9	NA	variable
Abbas et al. ⁽²⁷⁾	rabbit	iliac	balloon	X-rays	6 12	2	5 days post PTCA
Shimotakahara et al. ⁽²⁸⁾	rat	carotid	balloon	γ	7.5 15 22.5	0.66	1 or 2 days post PTCA
Mayberg et al. ⁽²⁹⁾	rat	carotid	balloon	γ	1, 2.5, 5 7.5, 10, 12.5 15, 20	0.8	1, 3 or 5 days post PTCA

Table II: Histological Results after External Irradiation

References	Doses (Gy)	Irradiated	Control	P
Schwartz <i>et al.</i> ^[25]	4	0.79 ± 0.23	0.66 ± 0.23	<0.05
	2-4	0.90 ± 0.22		<0.05
Shefer <i>et al.</i> ^[26]	8	0.99 ± 0.17	0.38 ± 0.31	—
	9	0.21 ± 0.22		<0.05
		0.19 ± 0.14		<0.05
		0.08 ± 0.13		<0.05
		0.14 ± 0.11		<0.05
Abbas <i>et al.</i> ^[27]	6	0.32 ± 0.27	0.29 ± 0.05	ns
		0.32 ± 0.07		ns
		12		0.09 ± 0.02

Neointima formation after external irradiation vs control arteries. Shefer *et al.* delivered radiation dose immediately, 1 day, 2 days, 3 days and 7 days after angioplasty. Results after 4 weeks except Shefer *et al.* (2 weeks). Neointima formation expressed as: intima/media ratio for Shefer *et al.*, cross sectional area (mm²) for Abbas *et al.*, mean neointimal thickness (mm) for Schwartz *et al.*

effect of timing of irradiation (29). Irradiation administered on day 1 after injury produced a significant dose-dependent reduction of intimal hyperplasia, with a 50% decrease at 5–7.5 Gy. In contrast, radiation treatment applied 3 or 5 days after injury showed significantly less inhibition of intimal hyperplasia. Thus, external beam radiation, when the dose level and timing were optimized for the model being treated, decreased post-angioplasty neointima formation. However, no significant reduction in neointima formation has been reported to date after external irradiation of stented segments (25, 30).

Endovascular high-dose rate irradiation therapy

Wiederman et al. studied the effects of 20 Gy delivered through an Iridium-192 ribbon to the pig coronary artery immediately before overstretch balloon angioplasty (Tables III and IV) (31). Each pig received a single dose delivered over 1h. At 30 days, there was less intimal proliferation in the irradiated group but the medial layer of the vessel showed diffuse interstitial fibrosis. Overall, compared with control animals, pre-angioplasty intracoronary irradiation reduced the bulk of neointima proliferation by 71% and percent area stenosis by 63%. In a follow-up study performed at 180 ± 8 days, it was found that the benefit seen at 30 days had been maintained (32). In contrast, when using a dose of 10 Gy, they described a 123% increase in neointima formation as compared with controls (33). Addressing the long-term effect, these authors described diffuse interstitial fibrosis throughout the medial and adventitial layers (33). Intimal proliferation consisted of equal proportions of smooth muscle cells and zones of diffuse fibrosis. There was no ultrastructural evidence of malignant or pre-malignant transformation in any cell lines, and vessels distal to the irradiation site were intact.

The same model was used for a study of the effects of gamma-irradiation (20 Gy) on vasomotor function, both acutely and later (32 days) (34). Early, irradiated segments were vasoconstricted in response to acetylcholine and did not vasodilate after nitrate infusion. When studied later, the vasodilatory response to acetylcholine was found to be restored but loss of dilation after nitrates persisted. The endothelium was intact but the media throughout the

Table III: Endovascular Radiation

References	Species	Vessel	Model	Radiation	Isotope	Dose (Gy)	Dose rate (Gy . min ⁻¹)	Timing
Wiedermann et al. ^(31,33)	pig	coronary	balloon	γ	Ir 192	10	0.66	pre-PTCA
						15		
						20		
Mazur et al. ⁽³⁵⁾	pig	coronary	balloon stent	γ	Ir 192	10	2.5	pre-PTCA pre-stent
						15		
						25		
Waksman et al. ⁽³⁶⁾	pig	coronary	balloon	γ	Ir 192	3.5	0.36-0.43	post-PTCA and 2 days post-PTCA
						7		
						14		
Sarac et al. ⁽³⁷⁾	rat	carotid	balloon	γ	Ir 192	5	3-6.7	post-PTCA
						10		
						15		
Waksman et al. ⁽³⁸⁾	pig	coronary	stent	γ,β	Ir 192 Sr90/Y	14	0.5-0.7 4.2	pre-stent
						4.2		
Wiedermann et al. ⁽³⁹⁾	pig	coronary	stent	γ	Ir 192	20	NA	pre-stent
Hehrlein et al. ⁽⁴⁰⁾	rabbit	iliac	stent	γ,β	NA	1.2	0.4	post-stent
Verin et al. ⁽⁴¹⁾	rabbit	iliac carotid	balloon	β	Y90	6	3.1	post-PTCA
						12		
						18		
Waksman et al. ⁽⁴²⁾	pig	carotid	balloon	β	Sr90/Y	7	4.6	post-PTCA
						14		
						28		
						56		

When necessary, dose rates have been extrapolated from doses and treatment time

Table IV: Histological Results after Endovascular Irradiation

References	Doses (Gy)	Irradiated	Control	P
Wiedermann et al. ^(31,33)	10	1.87 ± 1.30	0.84 ± 0.60	<0.05
	15	0.35 ± 0.23		<0.05
	20	0.24 ± 0.13		0.01
Mazur et al. ⁽³⁵⁾	10	0.50 ± 0.15	0.53 ± 0.15	ns
	15	0.20 ± 0.11		<0.001
	25	0.15 ± 0.20		<0.001
Waksman et al. ⁽³⁶⁾	3.5	1.23 ± 0.47	0.96 ± 0.70	ns
	7	0.70 ± 0.44		<0.0001
	7 delayed	0.48 ± 0.25		<0.0001
	14	0.33 ± 0.35		<0.0001
Sarac et al. ⁽³⁷⁾	5	0.01 ± 0.01	0.12 ± 0.02	<0.01
	10	0.02 ± 0.01		<0.01
	15	0.05 ± 0.02		<0.01
Waksman et al. ⁽³⁸⁾	14 (Ir)	1.98 ± 0.78	3.82 ± 1.23	<0.005
	14 (Si/Yt)	2.53 ± 1.03		<0.03
Wiedermann et al. ⁽³⁹⁾	20	4.00 ± 1.55	3.44 ± 0.76	ns
Hehrlein et al. ⁽⁴⁰⁾	1.2	0.70 ± 0.30	1.00 ± 0.30	ns
Verin et al. ⁽⁴¹⁾	6	79 ± 43	891 ± 415	<0.0002
	12	192 ± 264		
	18	22 ± 13		
Waksman et al. ⁽⁴²⁾	7	0.81 ± 0.49	1.09 ± 0.70	0.03
	14	0.58 ± 0.54		<0.0001
	28	0.47 ± 0.55		<0.001
	56	0.10 ± 0.15		<0.000001

Neointima formation after irradiation versus control arteries. Results after 4 weeks except Verin *et al.* (8 days), Waksman *et al.* (2 weeks), Sarac *et al.* (3 weeks). Neointima formation expressed in neointima area (mm²) except Verin *et al.* (total SMC/cm of inner arterial circumference) and Mazur *et al.* (maximal intimal thickness, mm).

irradiated segment was focally dependent and replaced by loose connective tissue, collagen and fibroblasts. Interestingly, some mild neointimal proliferation, albeit less than in control vessels, occurred eccentric to the vessel. As the ribbon was not centered in the vessel, this might suggest that the irradiation dose was not uniformly distributed throughout the length of the target vessel.

Mazur et al. studied the effects of intracoronary irradiation delivered through an Iridium-192 source connected with an afterloader (35). After balloon overstretch and oversized stent injury, incremental doses from 10 Gy to 25 Gy were applied to pig coronary arteries. At 28 days, maximal intimal thickness was significantly reduced in the 15 Gy and 25 Gy treated groups. Of note, there was no beneficial effect at any dose in the stented right coronary segments. The absence of source centering and the constant bending of the right coronary artery were the main reasons advanced to explain the lack of efficacy (35). Medial fibrosis was recognized in all groups, but the extent of adventitial fibrosis, hemorrhage and thrombus formation were radiation dose-dependent.

Waksman et al. and Sarac et al., using gamma irradiation with slightly lower doses, confirmed these positive effects in pig and rat models and Waksman et al. showed an improved benefit when the same dose (7 Gy) was administered 2 days after injury (36, 37). A long-term beneficial effect was observed at 6 months, without any morphological differences in the media or adventitia being observed between the irradiated and control groups (36). The same investigators studied the effects of irradiation with Iridium-192 or strontium-yttrium-90 prior to slotted tube stent implantation in porcine coronary arteries (38). The dose was estimated at 14 Gy at a depth of 2 mm and exposure time lasted between 28-38 min for gamma irradiation and 192 s for beta-irradiation. At 28 days, irradiated stented arteries exhibited significantly less neointima formation than controls. Many segments showed inflammatory infiltrates surrounding the stent wires, but these were less extensive in the treated arteries compared to the control arteries. Wiederman et al. using a similar experimental model and a dose of 20 Gy prior to stent implantation but with a different stent design (coil) failed to confirm these positive effects (39). Hehrlein et al. using an

activated guide-wire failed to demonstrate a significant reduction in neointima formation after irradiation post stent implantation, although there was a positive trend (40).

Verin et al. delivered intra-arterial radiation through pure Yttrium coils and a centering balloon catheter in hypercholesterolaemic rabbits (41). Using doses from 6 to 18 Gy, they treated carotid and iliac arteries after de-endothelialization and dilation. At 8 days, all irradiated groups showed a decreased number of neointima cells. However, at 6 weeks, percent area stenosis and mean number of neointimal cell layers were significantly reduced only in the group with 18 Gy irradiation. Waksman et al., using a similar pure beta-source, performed a range of dose studies in pig coronary arteries after balloon injury (42). All doses from 7 Gy to 56 Gy induced a significant reduction in neointima formation and the level of response was dose-dependent. Moreover, arteries receiving higher doses had an increased diameter, suggesting that irradiation could also interact with vessel remodeling (42).

Radioactive stents

Hehrlein et al. described the first intra-arterial use of radioactive stents produced by particle bombardment in a cyclotron (Table V and VI) (43). Activated stents were created, emitting gamma and beta isotopes of half-lives up to 2-7 years. Three series of stents of increasing radioactivities from 3.9 μ Curie to 35 μ Curie were produced. At 4 weeks, exposure to the two higher dose levels caused a significant reduction in neointima formation, while in all three groups there was a significant reduction in proliferating cell nuclear antigen positive cells (16% in non-radioactive stents vs 0.8% in 35 μ Ci stents) and smooth muscle cell counts (705 ± 23 SMCs/0.1 mm^2 in non-radioactive stents vs 229 ± 9 SMCs/0.1 mm^2 in the 35 μ Ci activity group). This reduction was maintained over a year.

These authors also assessed vascular re-endothelialization, which occurred despite prolonged irradiation. After a week, arteries with non-radioactive stents began to endothelialize but the process was delayed in a dose-dependent fashion in vessels with radioactive stents.

Table V: Radioactive Stent

References	Species	Vessel	Activity	Radiation	Main Isotopes	Dose (Gy)	
Hehrlein et al. ⁽⁴³⁾	rabbit	iliac	3.9	β, γ	Co ^{55,56} , Ci ⁵¹	—	
			17.5			Mn ⁵²	—
			35			Ni ⁵⁷ , Fe ⁵⁵	16 in 5 days*
Laird et al. ⁽⁴⁴⁾	mini-swine	iliac	0.14	β, γ	P ³² +?	3 in 4 weeks**	
Hehrlein et al. ⁽⁴³⁾	rabbit	iliac	4	β	P ³²	—	
Carter et al. ⁽⁴⁶⁾	pig	coronary	13	β	P ³²	<2 in 4 weeks***	
			0.15-0.5			1	40 in 4 weeks
			3-23			3-23	>100 in 4 weeks

*A dose of 16 Gy at 1 mm distance from the stent wire was delivered in the first 5 days.

**Total radiation dose at the surface of a stent wire over the lifetime period of the ³²P.

***Carter *et al.* estimated a tissue dose below 2 Gy after 4 weeks in the group with a maximum activity of 0.5 μ Curie, 40 Gy with the 1 μ Curie stent and a dose above 100 Gy in the group with a maximum activity of 23 μ Curie.

Table VI: Histological Results after Radioactive Stent Implantation

References	Activity (μ Curie)	Irradiated	Control	P
Hehrlein et al. ^[43]	3.9	0.90 \pm 0.20	0.70 \pm 0.10	ns
	17.5	0.40 \pm 0.10		<0.001
	35	0.20 \pm 0.10		<0.001
Laird et al. ^[44]	0.14	1.76 \pm 0.37	2.81 \pm 1.22	0.05
Hehrlein et al. ^[45]	4	0.30 \pm 0.06	1.00 \pm 0.20	<0.001
	13	0.20 \pm 0.06		<0.001
Carter et al. ^[46]	0.15-0.5	1.63 \pm 0.67	2.40 \pm 0.87	0.024
	1	4.67 \pm 1.50		<0.0001
	3-23	1.73 \pm 0.97		0.04

Neointima formation (mm²) after irradiation vs controls. Results after 4 weeks

Endothelial cell coverage of non-radioactive stents was completed within 4 weeks, while 12 weeks were required for $\geq 95\%$ endothelialization in the group with the highest activity stent. After 4 weeks, the collagen content had increased in the lowest activity group and was more pronounced in the two higher activity groups. Again this was maintained over one year. The exact significance of this collagen accumulation is unknown, but it could result from growth factor release associated with prolonged irradiation exposure.

Laird et al. studied the effects of Strecker stents, ion-implanted with ^{31}P beneath the surface, in porcine iliac arteries (44). Stents were made radioactive by exposure for several hours to a neutron flux which converted about 1/100 000 ^{31}P atoms to ^{32}P and generated other radioisotopes estimated to be short-lived. Twenty-eight days' exposure to radioactive stents with an initial activity of 0.014 μCurie caused a significant reduction in neointimal area (37%) and percent area stenosis (32%) compared to the effects of control non-radioactive stents. There was no difference between the two groups in terms of smooth muscle cell proliferation as assessed by the proliferating cell nuclear antigen technique. Scanning electron microscopy showed complete endothelialization of arteries with control and radioactive stents except at the proximal and distal ends of the stents.

In a subsequent study, a pure beta-emitter stent was developed by Hehrlein et al. (45). ^{32}P , produced by neutron bombardment, was ionized and ion-implanted beneath the outer surface of titanium-nickel stents using a specially designed reactor. ^{32}P emitting stents with 4 and 13 μCurie as initial activities, were implanted in rabbit iliac arteries and histomorphometry was performed at 4 and 12 weeks (45). At 4 weeks, both groups showed significant reductions in neointima formation and in smooth muscle cell density. Twelve weeks after implantation, only the group receiving the highest radiation dose showed a significant reduction in neointima formation and in smooth muscle cell density compared with non-radioactive stents. Neointima formation appears to have been only delayed in the low dose group. Endothelial cell coverage was present after 4 weeks, in all groups albeit less complete in arteries implanted with radioactive stents.

Recently, Carter et al., using a similar radioactive stent, studied responses to 0.1 to 23 μCi stents (46). Neointima formation was reduced with low (0.15–0.5 μCi) activity and high (3–23 μCi) activity stents, but increased neointima formation was observed with stents of 1 μCi initial activity. This highlights the complexity of the response of organized tissues such as the vascular system to ionizing radiation.

Human experience with endovascular radiation

The Frankfurt group reported the use of endovascular high-dose rate brachytherapy for recurrent stenosis or occlusion in stented femoral arteries (Table VII) (47-49). Because of fear of radiation-induced malignancy, only patients older than 65 years were selected. The procedures were started in the radiology department where a 9 Fr catheter was placed at the stent site. A 5 Fr applicator was then carefully positioned inside the catheter and fixed. The patients were transferred to the radiotherapy unit and the applicator was connected to an Iridium-192 afterloading machine. The average dose was 12 Gy at 3 mm depth delivered in about 200 s (48). All 28 patients supported the treatment without side-effects. With a follow-up ranging from 8–71 months, the authors demonstrated four reocclusions out of 25 controlled patients (16%). In the remaining 21 patients, none showed evidence of restenosis as assessed by Doppler ultrasound (49).

Condado et al. reported preliminary data in 22 coronary arteries irradiated with an Iridium-192 source which delivered 20 Gy or 25 Gy in 5 to 15 min (50). A few patients experienced chest pain, and mild spasm occurred in the majority of treated coronary arteries (51). After a mean follow-up of 260 days, 20 out of 22 treated arteries remained patent. However, in the group who received 25 Gy, seven out of eight treated arteries showed tiny aneurysm-like irregularities and one artery developed an aneurysm (52). In the group with 20 Gy, four out of 12 treated arteries developed restenosis. The occurrence of these coronary aneurysms is certainly

Table VII: Human Experience

References	Vessel	Patients	Radiation	Isotope	Dose (Gy) Mean/range	Dose rate (Gy · min ⁻¹)
Botcher et al. ⁽⁶⁷⁾	Femoral artery	n = 28	γ	Ir 192	12/8-28	2.4-8.4
Condado et al. ⁽⁵⁸⁾	Coronary artery	n = 22	γ	Ir 192	20 25	1.33-4
Popowski et al. ⁽⁵⁴⁾	Coronary artery	n = 15	β	Yt 90	18	1.4-7
Waksman et al. ⁽⁵⁹⁾	Arterio/venous fistulas	n = 11	γ	Ir 192	14	.
Jani et al. ⁽⁵⁹⁾	Coronary artery/ saphenous vein	n = 55	γ	Ir 192	8/7-26	0.20-0.73

alarming but later re-calculation of the administered doses found significant discrepancies and raised the possibility that doses up to 50 Gy had in fact been given in a short time (53).

The Geneva group, using a centering balloon and beta-radiation with Yttrium, performed a feasibility trial in 15 patients using a target dose of 18 Gy to the inner vessel wall (54). No adverse events were reported but the restenosis rate remained in the usual range after balloon angioplasty. (Data presented at the 1st Thoraxcenter course on highlights in intracoronary radiation therapy, Rotterdam, 10–11 December 1996). Teirstein et al. at Scripps Clinic treated 55 patients with restenosis with Iridium-192 seeds embedded in a nylon ribbon (55-58). Radiation was delivered after Palmaz–Schatz stent implantation in coronary arteries or vein grafts. An average dose of about 8 Gy was delivered to the medial layer in 25–40 min (56). No significant adverse event has been reported thus far and initial results suggest a beneficial short-term effect with a restenosis rate of 17% in the irradiated vessels. (Data presented at the 1st Thoraxcenter course on highlights in intracoronary radiation therapy, Rotterdam, 10–11 December 1996). Angiographic follow-up showed an improved 6 month minimal lumen diameter in the irradiated group as compared with controls (2.43 mm Vs 1.85 mm, $P = 0.02$) (57). Similarly, intravascular ultrasound analysis demonstrated a significant reduction in neointima formation at 6 months after endovascular irradiation ($16 \pm 22 \text{ mm}^3$ vs $45 \pm 39 \text{ mm}^3$, $P = 0.0088$) (58). Waksman et al. used an Iridium-192 source connected to a high dose rate afterloader to treat narrowed arterio-venous grafts in 11 chronic dialysis patients (59). During a mean follow-up of 5 months, all but one graft remained patent, as assessed by ultrasound.

Summary of the unresolved issues

Mechanisms of action

Ionizing radiations have a number of effects on target cells, the most obvious of which is cell killing (60). For highly differentiated cells which do not divide (neurons or secretory cells), cell death is defined as a loss of specific function and in general, a very high radiation dose

(approximately 100 Gy) is required to kill cells in a non-proliferating system. For proliferating cells, cell death occurs at a much lower dose and there is strong evidence that the nucleus, specifically DNA, is the principal target for radiation-induced cell lethality (61). There is an inverse relationship between cell survival and the number of lethal, asymmetrical exchange type chromosome aberrations observed per cell. When the cell divides, chromosome abnormalities induced earlier by radiation may be so severe as to prevent completion of division. Other cells may divide successfully and even complete several cycles before dying during subsequent mitosis due to the cumulative effects of chromosome damage.

Radiation damage not expressed as lethal changes may result in mutagenic and carcinogenic changes in the descendants of irradiated cells. A number of biological factors influence cell survival, the most important of which in the context of this review is repair of sublethal damage. This process reflects the repair of DNA damage which may take place before interactions between damaged sites can produce lethal chromosome aberrations. As a result, low-dose rate or fractional radiation causes less cell killing because sublethal damage can be repaired between dose fractions or during prolonged radiation exposure (62). Fractionation is an integral part of clinical radiation treatment practice, largely because it reduces the severity of normal tissue damage. Obviously, fractionated intravascular radiation therapy would be an unrealistic approach in the prevention of coronary restenosis.

In addition to reproductive cell death, ionizing radiation may induce programmed cell death or apoptosis in normal tissue and in tumors. Apoptosis is activated by a specific signal which initiates a cascade of biochemical and morphological events culminating in cell death. It occurs in a number of situations during normal development and can also be induced by cytotoxic drugs and radiation (63). However, the effect of radiation-induced apoptosis on the overall radiation response of normal tissues and tumor is still unclear (64). It has recently become apparent that cell killing, whether the result of reproductive death or by apoptosis is not the sole reason for the derangement of function observed in organized tissues following radiation. Radiation can result in the induction of early and late response genes, and the gene products,

specifically cytokines and growth factors may influence the radiation response of the tissue (65). Experimental findings indicate that growth factors are synthesized de novo and secreted by cells which survive irradiation (66). Growth factor-like molecules can promote proliferation of smooth muscle cells and participate in abnormal proliferation of endothelial cells and the initiation of fibrosis characteristic of late radiation response. Therefore, similarities exist between radiation-induced late responses and restenosis which partly involves abnormal proliferation of smooth muscle cells after vessel injury.

Control of restenosis by vascular irradiation is based on the simple premise that the target population, proliferating smooth muscle cells, can be eliminated or controlled by radiation. Simple calculations based on the size of the population suggest that single doses required to do so would probably be unacceptably large because of the risks of late complications (67). The risks associated with high radiation dose could be offset to some extent by localizing the radiation to the target population and/or by reduction of dose rate. The radiation doses which would not exceed normal tissue tolerance might be expected, based on the radiobiology and cell kinetics, to cause delay in restenosis but not elimination of the process, at least if smooth muscle cells continue to proliferate at the same rate indefinitely (67). As yet unexamined mechanisms which might influence this response would be the withdrawal or reduction of the factors which stimulate proliferation of smooth muscle cells and the possibility that these smooth muscle cells which normally divide very slowly will reach the limit of their capacity to undergo further division. In that context, endothelial regeneration is probably a key issue (68).

Gamma or beta irradiation

Beta particles have the same characteristics as electrons which have a limited tissue depth penetration. When they are slowed down by nuclei interactions, they give rise to high penetration X-rays, called bremsstrahlung (69). Because the mass of tissue involved in the restenotic process is on a millimeter scale, it seems appropriate to favor beta-radiation. The range of gamma-radiation and X-rays is usually greater than that of β -particles and strict radioprotective measures

are required. It should not be concluded, however, that manipulation of beta-emitters does not require special attention. Depending on the energy, β -particles can travel a significant distance through air, and therefore, precautions are required to limit the risks of source escape. In addition, secondary X-ray emission after ionization by beta rays is proportional to the atomic number of the interacting matter and covers the entire energy spectrum of the beta isotope. For example, bremsstrahlung of yttrium will generate a few X-rays with a mean energy of 300 Kev and a maximum energy of 2.3 Mev (70). Lead shielding (high atomic number), commonly used to stop gamma radiation or X-rays, is not appropriate for β radiation protection and therefore lucite or plastic (low atomic number) protectors are also required. Moreover, during the procedure secondary emission resulting from interactions of beta-rays and the patient's body will result in scattered radiation.

Waksman et al. compared the total effective body dose to the patient using gamma and beta irradiation (42). Using a delivered target dose of 14 Gy at 2 mm depth (in 30 min with ^{192}Ir source and 4 min with $^{90}\text{Sr}/\text{Yt}$), the body dose was estimated at 0.19 mSivert (mSv) for the beta emitter and 100 mSv for the gamma emitter. In contrast, it has been estimated that a patient receives a total effective dose of about 20 mSv per angioplasty procedure (71). By comparison, a thallium scan (100 MBq) will give a patient dose of 25 mSv and a Mibi scan (1110 MBq), a dose of 9 mSv (71). Johns et al. have also estimated the total effective dose received by the cardiologist and the scrub nurse during angioplasty procedure at the Montreal Heart Institute. On average, a cardiologist receives 0.003 mSv per procedure, to give an annual dose of 1.7 mSv, while the nurse receives 0.9 mSv/year (72). In contrast, the cardiologist during a brachytherapy procedure with $\text{Sr}/\text{Yttrium}$, which delivers a target dose of 14 Gy at 2 mm depth, will receive a dose of 0.009 mSv (42). Therefore, the cardiologist will receive a total dose four times higher than usually received for a standard balloon angioplasty.

Nevertheless, these doses remain below the maximal permissible effective personal dose of 20 mSv/year set by the International Commission of Radiation Protection (ICRP)(73).

However, it should be remembered that no dose of radiation is known to be safe and the ICRP has thus recommended adoption of the ALARA (As Low As Reasonably Achievable) principle in order to limit radiation exposure to workers (74).

Administered doses

Dual effects are observed following both external and endovascular irradiation. At lower doses, dose effects are consistent with increased neointima formation (24, 25, 33-35). Higher doses are associated with less neointima formation, less smooth muscle cell proliferation and increased lumen diameters (27-38). At the present time, it is unclear whether the adverse effects are related to increased smooth muscle cell proliferation and/or greater extracellular matrix secretion (24, 25, 33, 35). Interestingly, Herhlein et al. showed a dose dependent increase in collagen content after radioactive stent implantation (43). As already discussed, gene induction could be responsible for the dual reaction observed after vascular irradiation (65). For example, TGF- β , which is thought to play a role in matrix secretion during restenosis, is released from mesangial cells after ionizing radiation exposure and could also affect the radiation response of adjacent cells (75, 76). These factors complicate prediction of the optimal dose of ionizing radiation to reduce smooth muscle cell proliferation, and the effects on the other vascular cells remain to be determined. In addition, the timing of the radiation delivery, as described in a previous section, is also important. Recently, Waksman et al. were unable to reproduce positive results when the radiation dose was administered after stent implantation (77).

High dose-rate vs low dose-rate

Catheters and radioactive stents deliver radiation at different dose-rates. Catheter studies employing Ir-192 or St/Yt-90 delivered the dose between 3 min and 1 h, and dose-rates varied from 0.23 to 6.67 Gy . min⁻¹. With X-rays and gamma-rays, the dose-rate effect is an important parameter determining the biological consequences of the absorbed dose (62). As a rule in radiobiology, the biological effect of a given dose is lowered if the dose-rate is reduced and the overall exposure time is increased (62). The dose rate effect is significant between 0.1 Gy . h⁻¹

and several Gy . min⁻¹. Above and below that range, differences in response for different dose-rates are negligible. The magnitude of the dose-rate effect varies dramatically among different types of cells and between species. Comparing different human cell lines in culture, Hall et al. showed that differences in dose response for different cell lines was greatest at low dose-rates. At high dose-rates, there is a moderate effect due to variations in intrinsic cell radiosensitivities, whereas at lower dose rates, there is a wider range of response since different cell lines repair sublethal damage to different degrees (78). This observation is important to keep in mind when speculating about the late effects of endovascular radiation therapy. Dose-rate responses could be ultimately an important factor determining which technology between catheter-based endovascular brachytherapy (high dose-rate) and radioactive stent (low dose-rate) would offer the best therapeutic ratio.

Delayed effects

Potential adverse effects are essential to keep in mind when one considers the use of endovascular ionizing radiations. Restenosis is not, in the majority of cases, a life-threatening condition and therefore the treatment itself should not carry a significant risk to the patient and the hospital staff. Ionizing radiation produce DNA damage resulting in cell death, mutagenetic and carcinogenetic changes. However, carcinogenesis is a multistage process and probabilities are sufficiently low to consider the risk as negligible after endovascular radiation.

The cell depletion effect, which paradoxically may ultimately lead to excess cell proliferation, could be more of a problem (23, 82). In the basal state, turnover of smooth muscle and endothelial cells in the vascular wall is very low (68, 79-81). After angioplasty, however, smooth muscle cells from the media de-differentiate, migrate and proliferate. It is hypothesized that the acute killing effect of radiation would limit smooth muscle proliferation in the neointima. However, radiation affects all cells of the vascular wall and late effects could be related to the delayed depletion of some cells (adventitial cells, fibroblasts) with subsequent overshoot of re-population (82). Smooth muscle cells from the media could be progressively replaced by

fibroblasts and extracellular matrix (fibrosis) and progressive cellular depletion of the vascular wall could lead to aneurysm formation. Wiederman et al. studied pig coronary arteries 6 months after a delivered dose of 20 Gy and described fibrosis and loose interconnective tissue in the media and in the adventitia (32). Condado et al. described human coronary aneurysms as early as 6 months after a delivered dose of 20 Gy (52). Recently Waksman et al. described pseudoaneurysm formation after irradiation of a subclavian vein (83). No fibrosis or coronary aneurysms have been described to date after radioactive stent implantation. This could be due in part to the sparing effect of low dose-rates which tend to limit the adverse side effects of normal tissue irradiation. Nevertheless, delayed fibrosis is probably the most important side effect which should be excluded in order to consider endovascular radiation as a possible treatment modality for restenosis.

Conclusion

Endovascular irradiation represents a new field of investigation for the cardiologist. Obviously, endovascular brachytherapy will require intense collaboration between radiobiologists, oncologists, physicists and interventional cardiologists before being an approved therapeutic option. If the potential has already been demonstrated, many questions remain unanswered, such as optimal dose, timing of delivery, best device (catheter high dose-rate vs stent low dose-rate) and long-term effects. In the present state of knowledge, these unanswered questions require more experimental work before endovascular brachytherapy could be routinely applied to human patients for the prevention of coronary restenosis. Nevertheless, as some pathophysiological links seem to exist between cancer, atherosclerosis and perhaps restenosis, it is possible that careful analysis of the radiation effects on vascular cells in the context of restenosis prevention will provide new insight into these clinical syndromes (84).

References

1. Bertrand OF, Legrand V, Bilodeau L, Martinez C, Kulbertus H. Emergency coronary stenting with Wiktor stent. Immediate and late results. *J Inv Cardiol* 1997; 9: 2-9.
2. Fischman DL, Leon MB, Baim DS et al. A randomized comparison of coronary-stent placement and balloon angioplasty in the treatment of coronary artery disease. *N Engl J Med* 1994; 331: 496-501.
3. Serruys PW, de Jaegere P, Kiemeneij F et al. A comparison of balloon-expandable-stent implantation with balloon angioplasty in patients with coronary artery disease. *N Engl J Med* 1994; 331: 489-95.
4. Scott NA, Cipolla GD, Ross CE et al. Identification of a potential role for the adventitia in vascular lesion formation after balloon overstretch injury in porcine coronary arteries. *Circulation* 1996; 93: 2178-87.
5. Wilcox JN, Waksman R, King SB, Scott NA. The role of the adventitia in the arterial response to angioplasty: The effect of intravascular radiation. *Int J Radiat Oncol Biol Phys* 1996; 36: 789-96.
6. Forrester JS, Fishbein M, Helfant R, Fagin J. A paradigm for restenosis based on cell biology: Clues for the development of new preventive therapies. *J Am Coll Cardiol* 1991; 17: 758-69.
7. O'Brien ER, Alpers CE, Stewart DK et al. Proliferation in primary and restenotic coronary atherectomy tissue: Implications for antiproliferative therapy. *Circ Res* 1993; 73: 223-31.
8. Pickering J, Weir L, Jakanowski J, Kearney M, Isner J. Proliferative activity in peripheral and coronary atherosclerotic plaque among patients undergoing percutaneous revascularization. *J Clin Invest* 1993; 91: 1469-80.
- VIII. Bai H, Massuda J, Sawa Y et al. Neointima formation after vascular stent implantation. Spatial and chronological distribution of smooth muscle cell proliferation and phenotypic modulation. *Arterioscler Thromb* 1994; 14: 1846-53.

10. Carter A, Laird JR, Farb A, Kufs W, Wortham DC, Virmani R. Morphologic characteristics of lesion formation and time course of smooth muscle cell proliferation in a porcine proliferative restenosis model. *J Am Coll Cardiol* 1994; 24: 1398-405.
11. Schwartz RS, Chu A, Edwards WD et al. A proliferation analysis of arterial neointimal hyperplasia: Lessons for anti-proliferative restenosis therapies. *Int J Card* 1996; 53: 71-80.
12. Post MJ, Borst C, Kuntz RE. The relative importance of arterial remodeling compared with intimal hyperplasia in lumen renarrowing after balloon angioplasty. A study in the normal rabbit and the hypercholesterolemic Yucatan micropig. *Circulation* 1994; 89: 2816-21.
13. Mintz GS, Popma JJ, Pichard AD et al. Arterial remodeling after coronary angioplasty: a serial intravascular ultrasound study. *Circulation* 1996; 94: 35-43.
14. EPIC Investigators. Use of monoclonal antibody directed against the platelet glycoprotein IIB/IIIa receptor in high-risk coronary angioplasty. *N Engl J Med* 1994; 330: 956-61.
15. Topol EJ, Califf RM, Weisman HF et al. Randomized trial of coronary intervention with antibody against platelet IIB/IIIa integrin for reduction of clinical restenosis: Results at six months. *Lancet* 1994; 343: 881-6.
16. Cammenzind E, Vrolix M, Hanet C et al. Local heparin delivery following balloon angioplasty to prevent restenosis: Preliminary results of an open multicenter registry (Abstract). *Circulation* 1995; 92: I-346.
17. Pavlides GS, Barath P, Manginas A, Vassilikos V, Cokkinos DV, O'Neill W. Intramural delivery of low molecular weight heparin by direct injection within the arterial wall with a novel infiltrator catheter. Acute results and follow-up in patients undergoing PTCA or stenting (Abstract). *Circulation* 1996; 94: I-615.
18. Bennett MR, Schwartz SM. Antisense therapy for angioplasty restenosis. Some critical considerations. *Circulation* 1995; 92: 1981-93.
19. Borok T, Bray M, Sinclair I. Role of ionizing irradiation for 393 keloids. *Int J Radiat Oncol Biol Phys* 1988; 15: 865-70.
20. Kovalic J, Perez C. Radiation therapy following keloidectomy: A 20-year experience. *Int J Radiat Oncol Biol Phys* 1989; 17: 77-80.

21. Walter WL. Another look at pterygium surgery with postoperative Beta radiation. *Ophthalmic Plast Reconstr Surg* 1994; 10: 247-52.
22. Blount LH, Thomas BJ, Tran L, Selch MT, Sylvester JE, Parker RG. Postoperative irradiation for the prevention of heterotopic bone: Analysis of different dose schedules and shielding considerations. *Int J Radiat Oncol Biol Phys* 1991; 19: 577-81.
23. Hall EJ. *Radiobiology for the radiologist*, 4 edn. Philadelphia: J. B. Lippincott Company, 1994: 121.
24. Gellman H, Healey G, Quingsheng C, Tselentakis MJ. The effect of very low dose irradiation on restenosis following balloon angioplasty. A study in the atherosclerotic rabbit. *Circulation* 1991; 84 (Suppl II): II-46-59.
25. Schwartz RS, Koval TM, Edwards WD. Effect of external beam irradiation on neointimal hyperplasia after experimental coronary artery injury. *J Am Coll Cardiol* 1992; 19: 1106-13.
26. Shefer A, Eigler NL, Whiting JS, Litvak FI. Suppression of intimal proliferation after balloon angioplasty with local beta irradiation in rabbits (Abstract). *J Am Coll Cardiol* 1993; 21: 185A.
27. Abbas MA, Afshari NA, Stadius ML, Kernoff RS, Fiscell TA. External beam irradiation inhibits neointimal hyperplasia following balloon angioplasty. *Int J Cardiol* 1994; 44: 191-202.
28. Shimotakahara S, Mayberg MR. Gamma irradiation inhibits neointimal hyperplasia in rats after arterial injury. *Stroke* 1994; 25: 424-8.
29. Mayberg MR, Luo Z, London S, Gajdusek C, Rasey JS. Radiation inhibition of intimal hyperplasia after arterial injury. *Radiat Res* 1995; 142: 212-20.
30. Hehrlein C, Kaiser S, Kollum M, Kinscherf R, Fehsenfeld P. Effects of very low dose endovascular via an activated guidewire on neointima formation after stent implantation (Abstract). *Circulation* 1995; 92(Suppl I): I-146.
31. Wiedermann JG, Marboe C, Amols H, Schwartz A. Intracoronary irradiation markedly reduces restenosis after balloon angioplasty in a porcine model. *J Am Coll Cardiol* 1994; 23: 1491-8.

32. Wiedermann JG, Marboe C, Amols H, Schwartz A, Weinberger J. Intracoronary irradiation markedly reduces neointimal proliferation after balloon angioplasty in swine: Persistent benefit at 6-month follow-up. *J Am Coll Cardiol* 1995; 25: 1451-6.
33. Weinberger J, Amols H, Ennis RD, Schwartz A, Wiedermann JG, Marboe C. Intracoronary irradiation: Dose response for the prevention of restenosis in swine. *Int J Radiat Oncol Biol Phys* 1996; 36: 767-75.
34. Wiedermann JG, Leavy JA, Amols H et al. Effects of high-dose intracoronary irradiation on vasomotor function and smooth muscle histopathology. *Am J Physiol* 1994; 267 (1 Pt 2): H125-32.
35. Mazur W, Ali MN, Khan MM et al. High dose rate intracoronary radiation for inhibition of neointimal formation in the stented and balloon-injured porcine models of restenosis: angiographic, morphometric and histopathologic analyses. *Int J Radiat Oncol Biol Phys* 1996; 36: 777-88.
36. Waksman R, Robinson KA, Croker IR, Gravanis MB, Cipolla GD, King SB. Endovascular low-dose irradiation inhibits neointima formation after coronary artery balloon injury in swine. *Circulation* 1995; 91: 1533-9.
37. Sarac TP, Riggs PN, Williams JP et al. The effects of low-dose radiation on neointimal hyperplasia. *J Vasc Surg* 1995; 22: 17-24.
38. Waksman R, Robinson KA, Crocker IR et al. Intracoronary radiation before stent implantation inhibits neointima formation in stented porcine coronary arteries. *Circulation* 1995; 92: 1383-6.
39. Wiedermann JG, Marboe C, Amols H, Schwartz A, Weinberger J. Intracoronary irradiation fails to reduce neointimal proliferation after oversized stenting in a porcine model (Abstract). *Circulation* 1995; 92 (Suppl I): I-146.
40. Hehrlein C, Kaiser S, Kollum M, Kinscherf R, Fehsenfeld P. Effects of very low dose endovascular irradiation via an activated guide-wire on neointima formation after stent implantation. *Circulation* 1995; 92: I-69.
41. Verin V, Popowski Y, Urban P et al. Intra-arterial beta irradiation prevents neointimal hyperplasia in a hyper-cholesterolemic rabbit restenosis model. *Circulation* 1995; 92: 2284-90.

42. Waksman R, Robinson K, Crocker IR et al. Intracoronary low-dose β -irradiation inhibits neointima formation after coronary artery balloon injury in the swine restenosis model. *Circulation* 1995; 92: 3025-31.
43. Hehrlein C, Gollan C, Dönges K et al. Low-dose radioactive endovascular stents prevent smooth muscle cell proliferation and neointimal hyperplasia in rabbits. *Circulation* 1995; 92: 1570-5.
44. Laird JR, Carter A, Kufs WM et al. Inhibition of neointimal proliferation with low-dose irradiation from a β -particle-emitting stent. *Circulation* 1996; 93: 529-36.
45. Hehrlein C, Stintz M, Kinscherf R et al. Pure β -particle-emitting stents inhibits neointima formation in rabbits. *Circulation* 1996; 93: 641-5.
46. Carter A, Laird J, Bailey L et al. Effects of endovascular radiation from a β -particle-emitting stents in a porcine coronary restenosis model. A dose-response study. *Circulation* 1996; 94: 2364-8.
47. Bottcher HD, Schopohl B, Liermann D, Kollath TJ, Adamietz IA. Endovascular irradiation - A new method to avoid recurrent stenosis after stent implantation in peripheral arteries: Technique and preliminary results. *Int J Radiat Oncol Biol Phys* 1994; 29: 183-6.
48. Liermann D, Bottcher HD, Kollath J et al. Prophylactic endovascular radiotherapy to prevent intimal hyperplasia after stent implantation in femoro-popliteal arteries. *Cardiovasc Intervent Rad* 1994; 17: 12-16.
49. Schopohl B, Liermann D, Pohlitz LJ et al. ^{192}Ir endovascular brachytherapy for avoidance of intimal hyperplasia after percutaneous transluminal angioplasty and stent implantation in peripheral vessels: 6 years of experience. *Int J Radiat Oncol Biol Phys* 1996; 36: 835-40.
50. Condado JA, Gurdiel O, Espinoza R et al. Percutaneous transluminal coronary angioplasty (PTCA) and intracoronary radiation therapy (ICRT): A possible new modality for the treatment of coronary restenosis: A preliminary report of the first 10 patients treated with intracoronary radiation therapy (Abstract). *J Am Coll Cardiol* 1995; (Special issue): 288A.

51. Condado JA, Gurdiel O, Espinoza R et al. Tolerance of intracoronary radiation therapy (IRCT) after percutaneous revascularization procedures (Abstract). *J Inv Cardiol* 1995; 7 (Suppl C): 25C.
52. Condado JA, Gurdiel O, Espinosa R et al. Late follow-up after percutaneous transluminal coronary angioplasty and intracoronary radiation therapy. In: King SB, Waksman R, Crocker IR, eds. *Discoveries in Radiation for Restenosis*. Atlanta: Emory School of Medicine Press; 1996: 105.
53. Waksman R. Local catheter-based intracoronary radiation therapy for restenosis. *Am J Cardiol* 1996; 78 (Suppl 3A): 23-8.
54. Popowski Y, Verin V, Urban P. Endovascular β -irradiation after percutaneous transluminal coronary balloon angioplasty. *Int J Radiat Oncol Biol Phys* 1996; 36: 841-5.
55. Jani SK, Massulo V, Tripuraneni P, Teirstein P. Irradiation using manually loaded Ir-192 ribbons to inhibit restenosis after stenting: Procedural aspects of a pilot study (Abstract). *Int J Radiat Oncol Biol Phys* 1996; 36 (Suppl I): 147.
56. Teirstein P, Massulo V, Jani S et al. Radiation therapy following coronary stenting – 6-month follow-up of a randomized trial (Abstract). *Circulation* 1996; 94: I-210.
57. Teirstein PS, Massulo V, Jani S et al. Radiotherapy reduces coronary restenosis: Late follow-up (Abstract). *J Am Coll Cardiol* 1997; (Special issue): 397A.
58. Mintz GS, Massulo V, Popma JJ et al. Transcatheter iridium-192 irradiation reduces in-stent neointimal tissue proliferation: A serial volumetric intravascular ultrasound analysis from the SCRIPPS trial (Abstract). *J Am Coll Cardiol* 1997; (Special issue): 60A.
59. Waksman R, Crocker IR, Kikeri D et al. Endovascular low dose radiation for prevention of restenosis following angioplasty for treatment of narrowed dialysis arterio venous grafts (Abstract). *J Am Coll Cardiol* 1996; (Special issue): 14A.
60. Bacq Z, Alexander P. *Fundamentals of Radiobiology*, 2 edn. New York, Oxford, London, Paris: Pergamon Press. *Pure and Applied Biology: Modern Trends in Physiological Sciences*, 1961.

61. Hall EJ. Molecular biology in radiation therapy: The potential impact of recombinant technology on clinical practice. *Int J Radiat Oncol Biol Phys* 1994; 5: 1019-28.
62. Hall EJ, Brenner DJ. The dose-rate effect revisited: Radiobiological considerations of importance in radiotherapy. *Int J Radiat Oncol Biol Phys* 1991; 21: 1403-14.
63. Lowe SW, Ruley HE, Jacks T, Housman DE. P53-dependent apoptosis modulates the cytotoxicity of anticancer agents. *Cell* 1993; 74: 957-67.
64. Dewey WC, Ling CC, Meyn RE. Radiation-induced apoptosis: Relevance to radiotherapy. *Int J Radiat Oncol Biol Phys* 1995; 33: 781-96.
65. Weichselbaum RR, Hallahan DE, Sukhatme V, Dritschillo A, Sherman ML, Kufe DW. Biological consequences of gene regulation after ionizing radiation exposure. *J Natl Cancer Inst* 1991; 83: 80-4.
66. Witte L, Fuks Z, Haimovitsz-Friedman A, Vlodavsky I, Goodman DW, Eldor A. Effects of irradiation on the release of growth factors from cultured bovine, porcine, and human endothelial cells. *Cancer Res* 1989; 49: 5066-72.
67. Brenner DJ, Miller RC, Hall EJ. The radiobiology of intravascular irradiation. *Int J Radiat Oncol Biol Phys* 1996; 36: 805-9.
68. Scott-Burden T, Vanhoutte PM. The endothelium as a regulator of vascular smooth muscle proliferation. *Circulation* 1993; 87 (Suppl V): V-51-55.
69. Dutreix J, Marinello G, Wambersie A. *Dosimétrie en Curiethérapie*. Paris: Masson, 1982.
70. Brodsky AB. Selected particle and photon spectral data. In: Brodsky AB, ed. *Handbook of Measurement and Protection*, section A, vol. 1. West Palm Beach, CRC Press, 1978: 391.
71. International Commission on Radiological Protection. Publication 62. Radiological protection in biomedical research. Addendum to publication 53. Oxford: Pergamon Press, 1993: 28.
72. Johns PC, Renaud L. Radiation risk associated with PTCA. *Primary Card* 1994; 20: 27-31.
73. Recommendations of the International Commission on Radiological Protection. ICRP-60. London: Pergamon Press, 1991.

74. Recommendations of the International Commission on Radiological Protection. IRCP-26. London: Pergamon Press, 1977.
75. Sigel AV, Centrella M, Eghballi-Webb M. Regulation of proliferative response of cardiac fibroblasts by transforming growth factor- β 1. *J Mol Cell Cardiol* 1996; 28: 1921-9.
76. Wang J, Robbins MEC. Radiation-induced alteration of rat mesangial cell transforming growth factor- β and expression of the genes associated with the extracellular matrix. *Rad Res* 1996; 146: 561-8.
77. Waksman R, Robinson K, Crocker IR, Gravanis MB, Palmer SJ, Cipolla GD. Intracoronary beta radiation before versus after stent implantation for inhibition of neointima formation in the porcine model (Abstract). *Circulation* 1996; 94: I-619.
78. Hall EJ, Marchese M, Hei TK, Zaider M. Radiation response characteristics of human cells *in vitro*. *Radiat Res* 1988; 114: 415-24.
79. Wright HP. Mitosis pattern in aortic endothelium. *Atherosclerosis* 1972; 15: 93-100.
80. Ross R. The pathogenesis of atherosclerosis. An update. *N Engl J Med* 1986; 314: 488-500.
81. Schwartz SM, Campbell GR, Campbell JH. Replication of smooth muscle cells in vascular disease. *Circ Res* 1986; 58: 427-44.
82. Fowler JB. What next in fractionated radiotherapy. *Br J Cancer* 1984; 49 (Suppl VI): 285S-300S.
83. Waksman R, Crocker IR, Lumsden AB, MacDonald J, Keker D, Martin LG. Long-term results of endovascular radiation therapy for prevention of restenosis in the peripheral vascular system (Abstract). *Circulation* 1996; 94: I-300.
84. Trosko J, Chang C. An integrative hypothesis linking cancer, diabetes and atherosclerosis: The role of mutations and epigenetic changes. *Med Hypoth* 1980; 6: 455-68.

Appendix: Radiation glossary

Absorbed dose. The mean energy imparted by ionizing radiation to an irradiated medium per unit mass. Units: Gray (Gy), rad.

Activity. The number of nuclear disintegrations occurring in a given quantity of material per unit time.

Becquerel (Bq). SI unit of radioactivity. $1 \text{ Bq} = 1 \cdot \text{s}^{-1}$ (read as 1 nuclear disintegration per second).

Beta particle. Charged particle emitted from the nucleus of an atom during radioactive decay. A negatively charged beta particle is identical to an electron.

Bremsstrahlung. Electromagnetic (X-ray) radiation produced by the deposition of charged particles in matter. Usually associated with energetic beta emitters, e.g. phosphorus-32.

Curie (Ci). A unit of activity equal to 3.7×10^{10} disintegrations $\cdot \text{s}^{-1}$.

Effective dose equivalent. The sum of the products of the dose equivalent to the organ or tissue and the weighting factors applicable to each of the body organs or tissues that are irradiated.

Gamma radiation. Also gamma rays; short wavelength electromagnetic radiation of nuclear origin, similar to X-ray but usually of higher energy (100 keV to 9 MeV).

Gray (Gy). The new international system unit (SI unit) of absorbed dose of radiation, $1 \text{ Gy} = 1 \text{ J kg}^{-1} = 100 \text{ rad}$.

Half-life, radioactive. Time required for a radioactive substance to lose 50% of its activity by decay.

Ionizing radiation. Radiation sufficiently energetic to dislodge electrons from an atom. Ionizing radiation includes x and gamma radiation, electrons (beta radiation), alpha particles (helium nuclei), and heavier charge atomic nuclei.

Rad. A unit of absorbed dose. Replaced by the gray in SI units.

Radioactivity. The property of some nuclides of spontaneously emitting particles or gamma radiation, emitting x radiation after orbital electron capture, or undergoing spontaneous fission.

Radioisotope. A nuclide with an unstable ratio of neutrons to protons placing the nucleus in a state of stress. In an attempt to reorganize to a more stable state, it may undergo various types of

rearrangement that involve the release of radiation. Almost identical chemical properties exist between isotopes of a particular element.

Sievert (Sv). The special name for the SI unit of dose equivalent. One sievert equals one joule per kilogram. The previously used unit, rem, is being replaced by the sievert. One sievert is equal to 100 rem.

X radiation. Also X-rays; penetrating electromagnetic radiation, usually produced by bombarding a metallic target with fast electrons in a high vacuum.

CHAPTER III: Biocompatibility Aspects of New Stent Technology

Abstract

Stent implantation represents a major step forward since the introduction of coronary angioplasty. As indications continue to expand, better understanding of the early and late biocompatibility issues appears critical. Persisting challenges to the use of intracoronary stents include the prevention of early thrombus formation and late neointima development. Different metals and designs have been evaluated in animals models and subsequently in patients. Polymer coatings have been proposed to improve the biocompatibility of metallic stents or to serve as matrix for drug delivery and they are currently undergoing clinical studies. The promises of a biodegradable stent have not yet been fulfilled although encouraging results have recently been reported. Lastly, continuous low-dose rate brachytherapy combining the scaffolding effect of the stent with localized radiation therapy has witnessed the development and early clinical testing of radioactive stents. The combined efforts of basic scientists and clinicians will undoubtedly contribute to the improvement of stent biocompatibility in the future.

Introduction

During the last 20 years, major technological advances have been achieved and new devices for coronary interventions have been tested. Among these, stents recently modified standard practice by affording a highly effective and safe method to tackle dissections occurring after balloon angioplasty. Two landmark studies have shown that slotted tube, stainless-steel, balloon-expandable stents could significantly decrease restenosis rates in selected lesions (1, 2). Multidisciplinary efforts have subsequently been put into stent research and as a result, new designs and different materials and coatings have been proposed to further improve the performance of these prostheses. The purpose of this review is to address some issues of stent design and materials, to review recent experience with various stent coatings and biodegradable stents and to describe recent research data involving surface modifications to increase biocompatibility and possibly reduce neointima formation.

Coronary Stents: Material and Design

Metallic characteristics, bulk and surface properties, design and chemistry are all important factors to consider in the conception of an optimal stent. Materials to be used as stent backbone must fulfill stringent physical, mechanical and chemical properties. The metal of an expandable stent must have enough plasticity to remain at the required size when deployed. Self-expanding stents, in addition, must be prepared from metals with sufficient elasticity so they can be compressed and then expanded and retain sufficient radial hoop strength to prevent vessel recoil or closure once in place (3). First generation coronary stents were made of surgical grade stainless-steel or tantalum although several authors have also suggested the use of temporary or permanent nitinol stents due to the super-elastic and thermal shape memory properties of that alloy (4, 5, 6).

Among chemical characteristics, corrosion properties are paramount. Formation of a surface metal oxide-film retards corrosion, and for some metals, such as chromium and titanium, this passivation is highly effective.

However, saline liquids (such as blood) will destabilize the oxide layer on many metals. Although not yet investigated with stents, it has been shown that corrosion particles might migrate from metallic implants to other parts of the body (3). Long-term results with stainless-steel or tantalum coronary prostheses do not suggest so far any signs of local or distant toxicity (7). Most presently available stents are manufactured in 316L stainless steel with L indicating the low (0.03 % wt) carbon content. This alloy is predominantly iron (60-65%) mixed with chromium (17-18%) and nickel (12-14%) (8). The chromium content affords a very good corrosion protection in addition to contributing to strength and hardness (8, 9). Thus, 316L stainless steel provides good resistance to corrosion and excellent mechanical properties although biocompatibility remains limited by the thrombosis issue (3, 8, 9). Nickel (\cong 55%)-titanium (\cong 45%) (Nitinol) stents may offer some advantages which have not yet been fully explored in the clinical setting (9). Nitinol alloy has also proved to have good early biocompatibility. Some concern exists that nickel leakage from these alloys could lead to immunogenic reactions (8, 10, 11).

Tantalum confers several theoretical advantages over stainless steel in terms of radiopacity, biocompatibility, mechanical properties and lack of ferromagnetism. It is regarded as a biologically inert material. After implantation, the tantalum stent wire undergoes oxidation resulting in an oxide which is very stable and extremely resistant to degradation (3). In the circulation, the thin layer of inert tantalum peroxide creates an electrically negative charge which might reduce adhesion of negatively charged platelets (12). However, in clinical practice, tantalum has not been shown to decrease stent thrombosis in comparison with stainless-steel stents. This may be partly due to the activation of the coagulation cascade by negatively charged surfaces (13). Therefore, whether the metallurgic properties may confer an advantage in vivo is still unknown. Scott et al. found no difference in platelet deposition and fibrin accumulation

between identical coil stents made of tantalum or stainless-steel in baboon arteriovenous shunts and in porcine coronary arteries (14). Rogers et al. compared vascular injury, thrombosis rates and neointima formation between stainless steel slotted tube (Palmaz-Schatz) and stainless steel corrugated ring stents (Multilink) in rabbit iliac arteries (15). These two stents have distinct designs but identical metals and metal to surface ratios. Overall neointima formation was proportional to vessel injury and corrugated ring stents created 42% less arterial injury and 38% less neointimal hyperplasia than slotted tube stents. Polymer coating (Thrombosshield) had no effect on vessel injury or neointima formation but significantly decreased thrombosis rates. Altering the stent surface with a polymer coating virtually eliminated thrombotic occlusion in corrugated ring stents and significantly reduced thrombosis rates in coated versus uncoated slotted-tube stents (8 % vs 42 % respectively).

Barth et al. performed paired comparisons of vascular wall reactions after implantation of 3 different stents in dog peripheral arteries (16). Neointima formation was significantly higher with Strecker stents than with Wallstent or Palmaz stents. Sheth et al. described less thrombosis and vessel injury after implantation of slotted tube nitinol stents in rabbit carotid arteries as compared with Palmaz-Schatz stents (17). In an attempt to separate the multiple factors involved in stent performance, Fontaine et al. compared similarly designed tantalum coil stents with different rigidity (18). The more rigid stents induced more vessel injury and created more neointima than the flexible design. Buchwald et al. compared regular and short-wave Wiktor stents implanted in mini-pig coronary arteries (19). Although neointimal area was reduced at 4 weeks in the short-wave group, no difference subsisted in neointimal or lumen area between the 2 groups at 12 weeks. Therefore, the increased metal mass (15%) associated with the short-wave design did not lead to increased neointima formation. Many factors such as blood rheology, longitudinal flexibility, metal hoop-strength and coverage may interfere with and complicate the objective evaluation of stents with different designs.

Furthermore, surface treatment has also been shown to modify the performance of stents. Makkar et al. compared the effects of mechanical polishing to decrease surface irregularities, on

thrombosis in an ex-vivo porcine arteriovenous shunt model (20). Polished nitinol slotted-tube and Palmaz-Schatz stents exhibited a drastic reduction in thrombus formation as compared with unpolished nitinol stents. De Scheerder et al., using electrochemical polishing of stainless-steel stents, showed a significant reduction in early thrombosis in a rat A-V shunt model and less neointima formation in a pig coronary model as compared with untreated stents (21). Other authors have also tested noble metal coatings to improve the corrosion properties (22, 23). However, no distinct advantages in terms of thrombus or neointima formation were found between metal coatings by galvanization or ion implantation as compared with uncoated stents. Thus, experimental data suggest that stent design and surface properties may influence early and late results of stenting in animal models. Ongoing randomized trials comparing various stent designs will soon confirm whether this translates into different clinical outcomes.

Polymer Coatings

Polymers are long-chain molecules that consist of small repeating units (8). Several polymers with previous medical or dental use have been evaluated to cover stents or to coat stent struts (Table I).

Non biodegradable synthetic polymers

Van der Giessen et al. compared thrombosis rates and neointima formation using uncoated and coated Wallstents with Biogold (Plasma Carb Inc.)(24). Despite suppression of early thrombosis with the coating, neointima formation remained similar in both groups after 12 weeks. A large group of investigators have evaluated 3 synthetic non biodegradable coatings covering partially coil tantalum stents (25). Three different non sterile polymers were implanted in a pig coronary model: Polyurethane, poly (dimethyl) siloxane (silicone) and polyethene terephthalate (dacron). All but one of the silicone coated stents (1/20), remained patent at 4 weeks.

All polymers elicited intense inflammatory responses with presence of multinucleated giant cells and macrophages surrounding proteinaceous debris and thrombus remnants. De

Table I: Polymers used as stent coatings

Author (ref)	Stent	Material	Polymer	Biodegradable	Thickness (µm)	Model
Van Der Giessen et al. (24)	Wallstent	Stainless-steel	Biogold	no	-	Pig coronary
Van Der Giessen et al. (25)	Wiktor	Tantalum	PGLA PCL PHBV POE PEO/PBTP PUR SIC PETP	yes yes yes yes yes no no no	75-125	Pig coronary
de Scheerder et al. (59)	Wiktor	Tantalum	POP	no	20	Pig coronary
de Scheerder et al. (26)	-	Stainless-steel	POP PUR	no	23	Pig coronary
Fontaine et al. (27)	Fontaine-Dake	Tantalum	PUR	no	-	Pig shunt
Rechavia et al. (28)	-	Nitinol	PUR	no	-	Rabbit carotid
Chronos et al. (29)	-	-	MPC/LM	no	-	Arteriovenous baboon shunt
Malik et al. (30)	Dyvisio	Stainless-steel	PC XL-PC	no	-	Pig coronary
Nordrehaug et al. (31)	-	Stainless-steel	PC	no	-	Rabbit iliac
Amon et al. (32)	-	Tantalum	Silicone carbide	no	-	Pig femoral
Ozbek et al. (33)	-	Stainless-steel	Silicone carbide	no	-	Human coronary
Lincoff et al. (34)	Wiktor	Tantalum	PLLA	yes	11-27	Pig coronary
Schwartz et al. (35)	Wiktor	Tantalum	PPE	-	-	Pig coronary
Holmes et al. (36)	Wiktor	Tantalum	FIB PUR	yes no	120 70-120	Pig coronary
Kipshidze et al. (38)	-	Titanium	FIB	yes	40 ± 6	Dog iliac artery
	Palmaz-Schatz	Stainless-steel	FIB	yes	40 ± 6	Dog iliac artery
Lambert et al. (57)	Harts	Ni/Ti	PUR	no	50	Rabbit carotid
Cox et al. (53)	Coil	Tantalum	CEL	yes	-	Pig coronary
Folts et al. (69)	Palmaz-Schatz	Stainless-steel	PSNO-BSA	yes	80-1000	Pig caroud
Prietzl et al. (63)	Palmaz-Schatz	Stainless-steel	PLLA	yes	10	Pig coronary
Aggarwal et al. (66)	Cook	Stainless steel	CEL	yes	30	rabbit iliac

PGLA: polyglycolic/lactic acid, PCL: polycaprolactone, PHBV: polyhydroxybutyrate/valerate, POE: polyorthoester, PEO/PBT: polyethyleneoxide/polybutylene terephthalate, SIL: silicone, PETP: polyethylene terephthalate, POP: polyorganophosphazene, PUR: polyurethane, PPE: polyphosphate ester, MPC/LM: methacryloylphosphorylcholine/laurylmethacrylate, PC: phosphorylcholine, XL-PC: Cross-linked phosphorylcholine, FIB: fibrin, COLL+LAM: collagene/laminin, H: heparin, CEL: Cellulose, PSNOBSA: polynitrosated NO albumin, PLLA: poly-L-lactic acid.

Scheerder et al. compared 2 different polymer coatings of stainless steel slotted tube stents in normal porcine coronary arteries. Stents were coated with either a biodegradable poly(organo)phosphazene (POP) or a biostable polyurethane (26). While 3 of 6 pigs with uncoated stents died of acute stent occlusion, only one (1/4) POP-coated stent was found occluded at follow-up angiography. No difference in neointima proliferation was found between bare and polyurethane stents. However, in the POP-coated stent group, severe intimal proliferation of histiolympocytic tissue was noted. Fontaine et al. compared platelet adhesion between uncoated and polyurethane-coated tantalum stents implanted in a swine arterio-venous shunt (27). Radiolabeled platelet accumulation in the uncoated stent group was already more severe after 5 min and remained higher after 60 to 120 min. In rabbit carotid arteries, Rechavia et al. observed identical tissue reaction between polyurethane coated and uncoated nitinol stents (28).

Chronos et al. used a copolymer of methacryl-phosphorylcholine and laurylmethacrylate to coat stainless steel stents. In a baboon A-V shunt model, they observed an early decrease in platelet deposition at 60 and 120 min as compared with bare-stents (29). Subsequently, Malik et al. evaluated phosphorylcholine (a component of cell membrane) or cross-linked phosphorylcholine coated on stainless steel stents in a pig coronary model (30). No stent thrombosis occurred in any group and there was no excess neointima formation in coated compared with uncoated stents. Identical results have been obtained in rabbit iliac arteries with phosphotidylcholine by Nordrehaug and colleagues (31). Amon et al. used a newly designed tantalum stent with a silicon carbide coating (32). In vivo testing in a pig model showed the absence of thrombus formation. Ozbek et al. using the same coating applied on Palmaz-Schatz stents reported the first clinical use in bail-out stenting (33). Among 44 patients who received 58 silicon-carbide coated stents, 21% (9/42) had restenosis at 6 month follow-up and stent thrombosis was suspected in two patients. Thus, these results do not seem to suggest a clinical advantage for these silicone-carbide coated stents. Therefore, it remains unclear whether any polymer coating may improve the stent biocompatibility per se but recent data suggest that some polymers such as polyurethane or phosphorylcholine could serve as effective drug delivery systems.

Biodegradable synthetic polymers

Van der Giessen et al. studied 5 polymer-coated stents implanted in pig coronary arteries (25). Polyglycolic/polylactic acid copolymer (PG/LA), polycaprolactone (PCL), polyhydroxybutyrate/valerate copolymer (PHBV), polyorthoester (POE) and polyethyleneoxide/polybutylene terephthalate copolymer (PEO/PBTP) were used as strips covering 90 degrees of a Wiktor stent circumference. In contrast with similar studies using non biodegradable polymers, 3 stents with PHBV (3/7) and 3 with PEO/PBTP (3/10) occluded within hours after implantation. A wide range of inflammatory response was also demonstrated. Lincoff et al. evaluated low (80 kD) and high molecular weight (321 kD) Poly-L-lactic acid (PLLA) coated onto Wiktor stents again in pig coronary arteries (34). In the group with low molecular weight PLLA, severe acute and chronic signs of inflammation were recognized with a variable destruction of the vessel architecture. In contrast, in the group with high molecular weight PLLA (slower degradation), there was no evidence of acute or chronic inflammation and the neointima was similar to that noticed in the control group. A single preliminary study reported no thrombosis and little inflammation after polyphosphate ester coated tantalum stents were implanted in pig coronary arteries (35). Among these biodegradable polymers, PLLA remains high in the list to serve as a temporary matrix for drug release.

Natural coated and covered stents

Natural products offer the theoretical advantage of minimizing the inflammatory response. Holmes et al. compared fibrin-covered with polyurethane-covered tantalum stents in a pig coronary artery model (36). Polymerization of fibrin produced a film completely encasing the stent. In addition, fibrin-covered stents were soaked in a heparin solution for 3 hours. In the other group, stents were covered with biostable medical grade polyurethane. Three (3/34) fibrin-covered stents occluded within 48 hours. After 4 weeks, all stents were endothelialized. In contrast, in the group with polyurethane covering, 6 out of 12 stents occluded within 48 hours. In addition, after 4 weeks, neointimal proliferation in the group with polyurethane coating

completely obliterated the lumen of the remaining stents. Histology documented an intense foreign-body reaction with multinucleated giant cells. Baker et al. using a similar fibrin coating on self-expanding titanium stents and balloon-expandable Palmaz-Schatz stents reported a significant reduction in platelet deposition after 2 hours in an in vitro model (37). Subsequently implanted in canine iliac arteries, 3 out of 7 uncoated stents thrombosed after 8 weeks while no coated stent presented signs of thrombosis. In addition, foreign body reaction was observed in 2 uncoated stents but not in fibrin-coated stents. Endothelial coverage was also higher in the fibrin-coated group, suggesting that fibrin could also allow rapid endothelialization of the stent struts (38). Stefanidis et al. introduced the concept of a conventional stent completely covered by an autologous vein or arterial graft. In a pig iliac artery model, they inserted 27 regular or vein covered stents. Two uncovered stents developed subacute thrombosis. With a follow-up extending up to 6 months, covered stents showed only minimal hyperplasia (39). These results prompted the investigators to use the same technique in patients and preliminary clinical results are encouraging (40). In view of its relative complexity, the potential long-term benefit will be the primary factor that will determine the place of this technique.

Heparin-Coated Stents

Bonan et al. were first to use heparin-coated (a preliminary version of Carmeda coating) zig-zag stents in canine coronary arteries (41) (Table II). Neither thrombosis nor neointima formation was different between coated and uncoated groups. Several preliminary reports however suggested that heparin-coating could reduce early thrombosis (42, 43, 44). The Rotterdam group reported experimental and early clinical results with heparin-coated (Carmeda) Palmaz-Schatz stents (45, 46). In their experimental series, stent thrombosis occurred in 37 % of pigs receiving uncoated stents while no coated stent with either moderate or high heparin activity presented thrombosis. After 4 weeks, histomorphometric analysis showed a slight but significant increase in neointimal thickness in the group with highest heparin activity. However, after 12 weeks, the difference was no longer significant. Heparin-coating induced a decreased endothelial cell covering of the coated stents, possibly by an effect of heparin on cell attachment and growth.

Table II: Heparin-coated stents

Author	Model	Stent	Coating	Control	Thrombosis reduction	Neointima reduction
Bonan et al. (41)	Dog coronary	Zig-Zag	-	bare stent	no	no
Stradienko et al. (42)	Rabbit iliac	Palmaz-Schatz	-	bare-stent	yes	-
Bailey et al. (43)	Rabbit iliac	Palmaz-Schatz	Proprietary	bare stent	nes	no
Sheth et al. (44)	Rabbit carotid	Harts	SPUU- PEO-Hep	bare-stent	yes	-
Hardhammar et al. (45)	Pig coronary	Palmaz-Schatz	Carmeda	bare stent	yes	no
Sernuys et al. (46)	Human coronary	Palmaz-Schatz	Carmeda	-	yes	-
Chronos et al. (47)	Baboon carotid	Cordis	-	bare-stent	yes	yes
Chronos et al. (48)	Baboon A-V shunt	Palmaz-Schatz	Carmeda	bare-stent	yes	-
Zidar et al. (50,51)	Dog coronary	Cordis	-	bare-stent	-	no
de Scheerder et al. (52)	Pig coronary	Self-designed	Duraflow	bare stent	yes	no
Jeong et al. (54)	Porcine carotid	Wallstent	-	bare-stent	yes	-
Vrolix et al.(56)	Human coronary	Wiktor	Hepamed	-	-	-

SPUU-PEO-H: Polyurethaneurea-polyethylene oxide-heparin, H: Heparin

The Carmeda coating seems also highly effective to reduce platelet deposition when stents are not completely deployed (47).

Using heparin-bonded tantalum coil stents Chronos et al. showed similarly less early thrombosis and subsequent neointima formation in baboon carotid arteries (48, 49). In contrast, Zidar et al. implanted heparin-bonded tantalum coil stents in dog coronary arteries and found no difference in early thrombosis or neointima formation between coated and uncoated stents (50, 51). De Scheerder et al. performed a detailed experimental study to evaluate the immediate and delayed effects of heparin-coating. After 30 min in a rat A-V shunt model, thrombus weight, radiolabeled platelets and fibrinogen were significantly reduced in the Duraflo II coated stent group (52). However, when subsequently implanted in pig coronary arteries, there was no reduction in neointima proliferation in the group with heparin-coating as compared with control stents. Cox et al. evaluated the potential of heparin release from a cellulose-coated coil stent to reduce neointima formation (53). In porcine coronary arteries, there was no significant difference at 4 weeks between coated and uncoated stents. Jeong et al. evaluated heparin release from coated Wallstent in a porcine carotid model (54). After 1 week, all uncoated stents were occluded whereas all coated stents remained widely patent. Therefore, in animal models, various heparin coatings have been shown effective to reduce thrombosis whereas a benefit on neointima formation remains to be established.

Serruys et al. reported initial clinical experience with Carmeda heparin-coated Palmaz-Schatz stents (46). Overall, this study showed no stent thrombosis and restenosis rates remained low decreasing from 15 % in the group with conventional anticoagulation to 6 % in patients with an association of ticlopidine-aspirin. In the recently completed Benestent II trial comparing heparin-coated stents with balloon angioplasty, 413 patients received a stent and thrombosis occurred in only 1 case (55). Vrolix et al. also reported preliminary results with a heparin-covalently bound (Hepamed) Wiktor stent in 100 patients (56). Given the better stent deployment technique and the clinical effectiveness of ticlopidine-aspirin regimen that both helped to

dramatically reduce stent thrombosis, the exact role of heparin-coating for stents remains to be established.

Drug-Eluting Stents

Much interest has been focused on loading a drug on a stent to limit the early thrombogenicity and late neointima formation (Table III). Drugs might be released by diffusion mechanisms or during polymer breakdown. Lambert et al., by using forskolin loaded into a polyurethane (Tecoflex) coated nitinol stent, reported a decrease in thrombosis in rabbit carotid arteries (57). The same group compared drug release between forskolin and etedrinatate (58). Levels of etedrinatate in the vessel wall peaked at 24 hours and remained high up to 72 hours after placement. Levels of forskolin peaked within 2 hours of stent placement but rapidly fell during the first 24 hours. About 50 % of the original etedrinatate remained in the stent at 72 hours compared to about 5 % of forskolin at 24 hours. Ratios of drug levels in the vessel wall to that in blood peaked at 6000 for etedrinatate and at 780 for forskolin.

This study confirmed the feasibility and efficiency of the concept of a drug eluting stent and demonstrated the variability in release kinetics according to the chemical characteristics of the selected compounds. De Scheerder et al. showed an improved biocompatibility of POP coating by loading the polymer with methylprednisolone or angiopeptin (59, 60). Cellulose ester has been used in one study as a coating for tantalum stents with heparin and/or methotrexate bound to the polymer (53). In porcine coronary arteries, there was no difference in neointima formation between drug-coated and uncoated stents. Lincoff et al. loaded dexamethasone onto PLLA matrices that were coated on Wiktor stents (34). In a low molecular weight PLLA group, dexamethasone reduced the inflammatory response observed in the PLLA group whereas in the high molecular weight PLLA group, there was no difference in neointima formation between polymer-coated and bare stents. At 28 days, the tissue concentration in dexamethasone was still 3000 higher than in the blood, confirming the possibility of slow-drug release from a polymer matrix coated on a stent. Eccleston et al., using the same model eluting colchicine also obtained

Table III: Drug-eluting stents

Author (ref)	Polymer	Drug	Amount	Release/ Kinetics	Control	Thrombosis reduction	Neointima reduction
Lambert et al. (57)	PUR	Forskolin	1.58 mg	95% in 24 hrs	-	yes	-
Dev et al. (58)	PUR	Forskolin	1.5 mg	95% in 24 hrs	-	-	-
		Etedinate	2.8 mg	50.5% in 72 hrs			
de Scheerder et al. (59)	POP	Methylprednisolone	300 µg	86% in 24hrs	POP-stent	-	yes
Cox et al. (53)	CELLULOSE	Heparin, Methotrexate, Heparin + Methotrexate	-	-	bare-stent	-	no
Lincoff et al. (34)	PLLA	Dexamethasone	0.8 mg	> 50% in 2-3 days	PLLA bare-stent	-	no
Eccleston et al. (61)	PLLA	Colchicine	3.96 mg 0.99 mg	50% in 28 days <10% in 28 days	-	-	-
Schmidmaier et al. (64)	PLLA	PEG-hirudin PGI ₂	-	52.8% in 30 days 11.8% in 30 days	bare-stent	yes	-
Alt et al. (62)	PLLA	PEG-hirudin PGI ₂	10 µg 2 µg	-	bare-stent	-	yes
Aggarwal et al. (66)	CELLULOSE	IIb-IIIa inhibitors		60% in 14 days	CELLULOSE +/- anti CMV	yes	no
Aggarwal et al. (67)	CELLULOSE	IIb-IIIa-UK	-	-	CELLULOSE	yes	-
Folts et al. (69)	PSNO-BSA	NO	-	-	bare-stent	yes	yes
Baker et al. (71)	FIBRIN	RGD peptide	-	-	bare-stent	-	yes
Santos et al. (72)	PLLA	L 703,801	40 w %	-	PLLA bare-stent	no yes	- -

PUR: Polyurethane, POP: Polyorganophosphazene, PLLA: Poly-L-lactic acid, PSNO-BSA: Polynitrosated Albumin, CMV : Cytomegalovirus.

similar results at 28 days (61). More recently, other investigators using PLLA matrix loaded with prostacyclin and PEG-hirudin coated onto Palmaz-Schatz stents described less early thrombosis and neointima formation in porcine coronary arteries compared with uncoated stents (62-65).

Aggarwal et al. showed decreased early stent thrombogenicity using cellulose matrix loaded with GPIIb-IIIa inhibitors or a complex of GPIIb-IIIa-Urokinase (66, 67). No reduction in neointima formation was subsequently demonstrated. Recent data, however, showed that increased loading could be achieved and it is thus possible that higher local doses can produce a greater biological effect (68). Folts et al. used a polynitrosated albumin NO donor coated onto Palmaz-Schatz stents that were implanted in pig coronary arteries (69, 70). Preliminary results suggest an early decrease in thrombosis and less neointimal hyperplasia. Baker et al. using a fibrin covered Peak stent loaded with an RGD peptide in an atherosclerotic rabbit model described significantly less smooth muscle cell proliferation, inflammation and neointima formation in the coated group (71). Santos et al. used a composite polymer-metal stent loaded with a non-peptide tirofiban analogue and showed a significant reduction of platelet deposition after 2 hrs as compared with bare stents in canine coronary arteries (72). Although the concept of a drug delivery stent is appealing, the challenges to define the right pharmacologic agent and its release kinetics further complicate the polymer issues.

Polymeric Stents

The group from the Mayo Clinic first reported initial results using a dacron tubing mesh self-expanding stent (73) (Table IV). Two animals sacrificed after 24 hours confirmed the correct mechanical stent deployment within the coronary vessel. However, all animals sacrificed 4-6 weeks after implantation showed a stent occluded by neointimal proliferation. In addition, there was a marked chronic foreign body inflammatory response with lymphocytes, eosinophils and giant cells. In contrast, the Rotterdam group, using a similar stent implanted in peripheral porcine arteries, described higher patency rates at 4 weeks (74). Histologic analysis displayed complete endothelial cell coverage and minimal intimal thickness. A foreign body inflammatory response

Table IV: Polymeric stents

Author (ref)	Design	Auto-expanding Balloon-expandable	Polymer	Model	Evaluation	Remarks
Murphy et al. (73)	Mesh	Auto	PETP	Porcine coronary	24 hrs, 4-6 weeks	all stents occluded at 6 weeks
van der Giessen et al. (74)	Mesh	Auto	PETP	Porcine femoral	4 weeks	7/8 patent
Susowa et al. (75)	Knitted	Balloon	PGA	Dog coronary	3 hrs, 1, 2, 8 weeks	15/15 patent at 3 h
Zidar et al. (76)	Diamond braided	Auto	PLLA	Dog femoral	2 hrs, 2, 4 days, 1, 2, 12 weeks, 18 months	10/11 patent at 18 months
Bier et al. (77)	-	Balloon	Collagen I	In vitro	-	-
Gregory et al. (78)	Sheet-tube	Laser energy	Elastin	Porcine aorta	-	-
Gao et al. (79)	Film		PCL/D,L PLA	Porcine carotid	1, 2 months	-
Landau et al. (80)	Tubular Coil	Balloon	PLLA-PCL	Rabbit carotid	5 days	carriers for adenovirus vectors

hrs: hours, PETP: Polyethylene terphthalate, PGA: Polyglycolic acid, PLLA: Poly-L-lactic acid, PCL/D,L-PLA: Polycaprolactone/D,L-lactic acid, PLLA/PCL: Poly-L-lactic acid/polycaprolactone.

was noted in the neointima of all vessels and additional inflammation was noted in the media of the occluded vessels. It is therefore possible that a contaminant was present in the non-sterilized stents used by the group at the Mayo Clinic.

Investigators at Kyoto University developed a biodegradable stent in polyglycolic acid. All stents were successfully implanted in 15 dogs (75). Fresh thrombus was present in some struts at 3 hours. Endothelialization of the stent surface occurred between 2 and 8 weeks. However, at 1 and 2 weeks, stent degradation began to occur and foreign body reaction was recognized. Stack and colleagues at Duke University have accumulated a wide experience in the development of biodegradable stents (76). Using PLLA designs, their stents have shown promising in vitro mechanical properties. In vivo testing in dog femoral arteries confirmed excellent scaffolding properties. The degradation was nearly complete by 9 months with minimal inflammatory response. To assess thrombogenicity and biocompatibility, 11 polymeric stents, sterilized by polyethylene oxide, were implanted after 5 minutes of heparin soaking, in a canine femoral artery model. Only 2 stent occlusions were observed due to traumatic implantation. After 18 months, limited neointima formation was present, but there was no chronic inflammatory response.

Bier et al. developed bioabsorbable stents in collagen I (77). Preliminary in vitro data showed that the majority of these stents could be expanded against porcine arteries when correctly matched to vessel size. Gregory et al. evaluated an elastin based material as a means to seal the artery (78). Absorption of the material into porcine arterial wall was obtained using thermal bonding with laser energy. Gao et al. developed a balloon expandable biodegradable stent made of a copolymer of coprolactone and D,L lactide impregnated with heparin (79). This stent could withstand collapse pressures of 300-700 mmHg at 38°C. After preheating at 51°C, stents were implanted in mini-swine carotid arteries. No thrombosis or foreign body reaction was noticed after 2 months. Recently, Landau and his group developed coil and tubular stents in copolymers of poly-L-lactic acid and polycoprolactone (80). They served also as carriers for recombinant adenovirus vectors and were implanted in rabbit carotid arteries. Clearly the efforts to develop a fully biodegradable stent have been slowed down by the technical complexities and by the

positive long term results of metallic stents. The concept however, together with the possibility to locally deliver large amount of drug for an extended period of time remains appealing.

Endothelial Cell Seeding

Another interesting approach is to provide a natural coating by using genetically engineered endothelial cells. This technique has previously been used for endovascular graft coatings. In addition, these cells might be genetically modified to generate increased local fibrinolytic activity (81, 82). However, initial results were marked by limited cell retention after stent expansion and pulsatile flow exposure (82, 83). To overcome some technical limitations of cells seeding, Bailey et al. used local delivery of endothelial cells after stent implantation in rabbit iliac and porcine coronary arteries (84). After 4 hrs, both models displayed a large number (> 75%) of attached endothelial cells onto implanted stents. By 14 days, endothelial cell coverage was > 90% in both treated and untreated segments. Interestingly, it has recently been shown that local delivery of vascular growth factor (VEGF₁₆₅) could increase endothelial regeneration after vessel injury (85). Van belle et al. showed that a single dose of VEGF administered locally could enhance endothelial regeneration after stent implantation in rabbit iliac arteries (86). Moreover, this accelerated endothelization was correlated with a decrease in thrombosis and intimal thickening after 28 days (86).

Radioactive Stents

Besides the use of single doses of γ or β rays delivered at high dose-rates by intravascular catheters, radioactive stents present the radiobiological advantage of delivering radiation at continuous low-dose rates (87). Using stents radioactivated by particle bombardment, Herhlein et al. showed a significant reduction in neointima formation in a rabbit iliac artery model despite the fact that extended follow-up revealed that neointima formation was only delayed in the low-activity stent groups (88). Later, the same group and investigators at Walter Reed Army Medical Center developed a β -emitting stent by ion-implantation of ^{32}P (89, 90). Studies in pig coronary

arteries and rabbit iliac arteries confirmed earlier positive results, although they also noticed delayed reendothelialization of the stented segments and increased neointima formation with certain radioactivities (89, 90). Ion-implantation of noble metals has been proposed to improve the corrosion properties of metal alloys (8, 23).

However, to obtain the required initial radioactivity with an isotope such as ^{32}P , would raise the quantity of phosphorus above the recommended maximum limit of 316L stainless-steel (91). As a consequence, the corrosion properties of the resulting stent surface would be changed. Thus, it is possible that the surface characteristics of ^{32}P ion-implanted or particle bombarded Palmaz-Schatz stents would be modified leading to reduced long-term biocompatibility. Another alternative would be to use an eluting system to deliver a chosen isotope from a stent platform (92).

Discussion

Biocompatibility has evolved from the previous notion of inert material to a more recent concept based upon the ability of a material to perform with an appropriate host response in a specific environment (93). Stent implantation adds to tissue compatibility the enormous challenge of hemocompatibility. As we have described, there are several important factors involved in the design of an optimal coronary stent. Most of the mechanical properties are related to the bulk characteristics of the metal or polymer and those related to biocompatibility are linked to surface properties. Early biocompatibility problems with stents are associated with thrombosis, inflammation and neointima formation. Late problems with stents can be divided in 2 broad categories: Mechanical failure due to material fatigue resulting from the considerable stress imposed to stents by cardiac contractions, and chemical failure where corrosion or depolymerisation can release potential toxic substances such as nickel, degradation products or contaminants (8, 94). To date, long-term clinical follow-up of first generation stents has not

revealed signs of mechanical failure or toxicity, although some longer stent designs showed early fatigue when implanted in animal models and during in vitro testing (unpublished results).

Stent implantation leads to greater vessel injury than balloon dilatation and can be followed by inflammation, wound healing and sometimes foreign body reaction. Recent data suggest that the stent design itself may influence the extent of injury (15, 17). Metallic stents have elicited a rather limited inflammatory response while coated and polymeric stents have shown more severe responses with histiolympocytic infiltrates, macrophages and giant cells typical of foreign body reaction (25, 26). Reports, however, suggest that this inflammatory response can be modulated by drug release or polymer modification. In addition, the accumulation of inflammatory cells may stimulate growth factor and cytokine release and in turn promote neointima formation. Drug eluting stents could provide, therefore, an ideal tool to limit the inflammatory reaction and possibly the neointima formation.

The basic tenet of blood-stent interactions is that circulating cells do not react directly with the coating or the metallic stent surface (8, 13, 95). Within minutes after stent implantation, soluble proteins will adhere to it and rapidly form a monolayer at the surface of the foreign material. It is therefore fundamental to understand, at the molecular level, the dynamic process which regulates protein adsorption. Indeed, proteins will adhere according to their plasma concentrations but also depending upon their surface affinity (13, 95). Therefore, there will be a competition between numerous proteins to adhere to the foreign surface. Some surfaces may preferentially absorb albumin whereas others will tie fibrinogen. The former may promote passivation of the stent surface while the latter may lead to thrombus accumulation. Protein adhesion leads to conformational changes in the protein structure initiating cell adhesion while soluble proteins do not interact with circulating cells (13, 95). This field is currently under active investigation, especially since the discovery of the integrin family.

Heparin coatings have been developed to provide permanent fixation or slow-release from the material surface (8). There are basically three different approaches to achieve heparin coating.

First, heparin may be bound by ionic interaction (49). Then, heparin is slowly released and interacts with anti-thrombin III to neutralize thrombin. A second approach is to incorporate heparin by blending it with a polymer. In this case, heparin is released by leaching or biodegradation of the polymer (53). The third approach such that developed by Carmeda consists of heparin immobilization using end-point attachment of heparin fragments to polyamine-dextran sulfate layers which have adsorbed on the stent surface (45, 46). The Medtronic (Hepamed) coating uses a similar approach where unfractionated heparin is attached to a polyamine layer. This layer has been previously covalently linked to a hydrogel deposited on the stent surface (M Verhoeven, personal communication). With the first two techniques, the release kinetics and concentration of heparin determine the clinical lifetime of the coating. With the last technology, the active site of heparin remains free and heparin functions as a catalyzer to permit repetitive inactivation of thrombin by ATIII. It has been shown that immobilized heparin retains its ability to bind thrombin for more than 4 months (8). Other anticoagulants such as hirudin have been tested, although immobilized hirudin binds thrombin indefinitely and therefore a cycle of inactivation cannot be entertained. Other research avenues involve slow-release hirudin, immobilized fibrinolytic enzymes or new antiplatelet agents such as GPIIb-IIIa inhibitors or GPIb antagonists. Whether early reduction in thrombogenicity will translate into reduction in neointima formation and ultimately restenosis remains, however, to be demonstrated.

Conclusion

Stents represent a major advance since the introduction of coronary angioplasty. As stents may be, in the near future, implanted in smaller vessels and in more complex lesions, the biocompatibility aspects will need to be further analyzed and mastered. There is little doubt that the next decade will witness the emergence of much less thrombogenic coronary endoprostheses capable of being accepted and tolerated by the body environment. Indeed, the research in the direction of reduction in stent thrombogenicity and in providing better tissue compatibility may have a significant impact on stent effectiveness in a variety of clinical conditions and may further expand the use of stents.

References

1. Fischman D, Leon M, Baim D, et al. A randomized comparison of coronary-stent placement and balloon angioplasty in the treatment of coronary artery disease. *N Engl J Med* 1994;331:496-501.
2. Serruys P, de Jaegere P, Kiemeneij F, et al. A comparison of balloon-expandable stent implantation with balloon angioplasty in patients with coronary disease. *N Engl J Med* 1994;331:489-95.
3. Taylor A. Metals. In: Sigwart U, ed. *Endoluminal stenting*. London, Philadelphia, Toronto, Sydney, Tokyo: WB Saunders, 1996: 28-33.
4. Dotter C. Transluminally placed coilspring endarterial tube grafts, long term patency in canine popliteal artery. *Invest Radiol* 1969;4:329.
5. Beyar R, Roguin A. Self expandable nitinol stent for cardiovascular applications: canine and human experience. *Cath Cardiovasc Diagn* 1994;32:162-70.
6. Eigler N, Litvak F, Whitlow P. Temporary stents. In: Topol E, ed. *Textbook of Interventional Cardiology*. Philadelphia, London, Toronto, Montreal, Sydney, Tokyo: W.B. Saunders, 1994: 766-775.
7. Robinson K, Roubin G, King S. Long-term intracoronary stent placement: arteriographic and histologic results after 7 years in a dog model. *Cathet Cardiovasc Diagn* 1996;38:32-7.
8. Ratner B, Hoffman A, Schoen F, Lemons J, eds. *An introduction to materials in medicine*. San Diego, London, Boston, New York, Sydney, Tokyo, Toronto: Academic Press, 1996.
9. Park JB. Metallic Biomaterials. In: Branzino JD, ed. *The biomedical engineering handbook*. Boca Raton: CRC Press, 1995: 537-71.
10. Ryhanen J, Niemi E, Serlo W, Niemela E, Sandvik P, Pernu H, Salo T. Biocompatibility of nickel-titanium shape memory metal and its corrosion behavior in human cell cultures. *J Biomed Mater Res* 1997;35:451-57.
11. Castelman L, Motzkin S, Aricandri F, et al. Biocompatibility of nitinol alloy as an implant material. *J Biomed Mater Res* 1976;10:695-731.

12. Zitter H, Plenk H. The electromechanical behavior of metallic implant material as an indicator of their biocompatibility. *J Biomed Mater Res* 1987;21:881-896.
13. Salzman EW, Merrill EW, Kent KC. Interaction of blood with artificial surfaces. In: Colman RW, Hirsh J, Marder VJ, Salzman EW, ed. *Hemostasis and thrombosis: basic principles and clinical practice*. Philadelphia: J.B. Lippincott Company, 1994: 1469-1485.
14. Scott N, Robinson K, Nunes G, et al. Comparison of the thrombogenicity of stainless steel and tantalum coronary stents. *Am Heart J* 1995;129:866-72.
15. Rogers C, Edelman E. Endovascular stent design dictates experimental restenosis and thrombosis. *Circulation* 1995;91:2995-3001.
16. Barth K, Virmani R, Froelich J, et al. Paired comparison of vascular wall reactions to Palmaz stents, Strecker tantalum stents, and Wallstents in canine iliac and femoral arteries. *Circulation* 1996;93:2161-69.
17. Sheth S, Litvak F, Dev V, Fishbein M, Forrester J, Eigler N. Subacute thrombosis and vascular injury resulting from slotted-tube nitinol and stainless steel stents in a rabbit carotid artery model. *Circulation* 1996;94:1733-40.
18. Fontaine A, Spigos D, Eaton G et al. Stent-induced intimal hyperplasia: are there fundamental differences between flexible and rigid stent designs? *J Vasc Interv Radiol* 1994;5:739-44.
19. Buchwald A, Stevens J, Zilz M, et al. Influence of increased wave density of coil stents on the proliferative response in a minipig coronary stent-angioplasty model (Abstract). *Eur Heart J* 1997;18:152.
20. Sheth S, Litvak F, Fishbein M, Forrester J, Eigler N. Reduced thrombogenicity of polished and unpolished nitinol vs stainless steel slotted-tube stents in a pig coronary artery model (Abstract). *J Am Coll Cardiol* 1996;27:197A.
21. De Scheerder I, Sohier J, Wang K, et al. Metallic surface treatment using electrochemical polishing decreases thrombogenicity and neointimal hyperplasia after coronary stent implantation in a porcine model (Abstract). *Eur Heart J* 1997;18:153.

22. Hermann R, Schmidmaier G, Alt E, et al. Comparison of the thrombogenicity of steel and gold-surface coronary stents with a biodegradable drug releasing coating in a human stasis model (Abstract). *Eur Heart J* 1997;18:152.
23. Hehrlein C, Zimmerman M, Metz J, Ensinger W, Kubler W. Influence of surface texture and charge on the biocompatibility of endovascular stents. *Coronary Artery Dis* 1995;6:581-86.
24. van der Giessen W, van Beusekom H, van Houten C, van Woerkens L, Verdouw P, Serruys P. Coronary stenting with polymer-coated and uncoated self-expanding endoprostheses in pigs. *Coronary Artery Dis* 1992;3:631-40.
25. van der Giessen W, Lincoff A, Schwartz R, et al. Marked inflammatory sequelae to implantation of biodegradable and nonbiodegradable polymers in porcine coronary arteries. *Circulation* 1996;94:1690-97.
26. De Scheerder I, Wilczek K, Verbeken E, et al. Biocompatibility of polymer-coated oversized metallic stents implanted in normal porcine coronary arteries. *Atherosclerosis* 1995;114:105-114.
27. Fontaine A, Koelling K, Clay J. Decreased platelet adherence of polymer-coated tantalum stents. *J Vasc Interv Radiol* 1994;5:567-72.
28. Rechavia E, Fishbien M, DeFrance T, Nakamura M, Litvak F, Eigler N. Vascular injury triggered by temporary and permanently implanted polyurethane coated and uncoated stents in rabbit carotid arteries (Abstract). *Circulation* 1996;94:I-88.
29. Amon M, Winkler S, Dekker A, Bolz A, Mittermayer C, Schaldach M. Introduction of a new coronary stent with enhanced radioopacity and hemocompatibility. *IEEE Eng Med Biol Soc* 1995;7:120-1.
30. Özbek C, Heisel A, Grob B, Bay W, Schieffer H. Coronary implantation of silicone-carbide-coated Palmaz-Schatz stents in patients with high risk of stent thrombosis without oral anticoagulation. *Cathet Cardiovasc Diagn* 1997;41:71-8.
31. Chronos N, Robinson K, Kelly A, et al. Thromboresistant phosphorylcholine coating for coronary stents (Abstract). *Circulation* 1995;92:I-685.

32. Malik N, Gunn J, Sheperd L, Newman C, Crossman D, Cumberland D. Phosphorylcholine-coated stents in porcine coronary arteries: angiographic and morphometric assessment (Abstract). *Eur Heart J* 1997;18:152.
33. Nordrehaug J, Chronos N, Sigwart U. A biocompatible phosphotidylcholine coating applied to metallic stents (Abstract). *J Am Coll Cardiol* 1994; 23:5A.
34. Lincoff A, Furst J, Ellis S, Tuch R, Topol E. Sustained local delivery of dexamethasone by a novel intravascular eluting stent to prevent restenosis in the porcine coronary injury model. *J Am Coll Cardiol* 1997;29:808-16.
35. Staab ME, Holmes DR, Schwartz RS. Polymers. In: Sigwart U, ed. *Endoluminal stenting*. London: W.B. Saunders, 1996: 34-44.
36. Holmes D, Camrud A, Jorgenson M, Edwards W, Schwartz R. Polymeric stenting in the porcine coronary artery model: differential outcome of exogenous fibrin sleeves versus polyurethane-coated stents. *J Am Coll Cardiol* 1994;24:525-31.
37. Baker J, Horn J, Nikolaychik V, Kipshidze N. Fibrin stent coatings. In: Sigwart U, ed. *Endoluminal Stenting*. London, Philadelphia, Toronto, Sydney, Tokyo: W.B. Saunders Comapany Ltd, 1996:84-9.
38. Kipshidze N, Baker J, Nikolaychik N. Fibrin coated stents as an improved vehicle for endothelial cell seeding (Abstract). *Circulation* 1994;90:I-597.
39. Stefanidis C, Toutouzas K, Vlachopoulos C, et al. Stents wrapped in autologous vein: An experimental study. *Circulation* 1996;28:1039-46.
40. Stefanidis C, Toutouzas K, Tsiamis E, et al. Preliminary results by using the autologous arterial graft-coated stent for the treatment of coronary artery disease (Abstract). *Eur Heart J* 1997;18:154.
41. Bonan R, Bhat K, Lefèvre T. Coronary artery stenting after angioplasty with self-expanding parallel wire metallic stents. *Am Heart J* 1991;121:1522-30.
42. Stratienco A, Zhu D, Lambert C, Palmaz J, Schatz R. Improved thromboresistance of heparin coated Palmaz-Schatz coronary stents in an animal model (Abstract). *Circulation* 1993;88:I-596.

43. Bailey S. Coating of endovascular stents in *Textbook of interventional cardiology*. Topol E ed. 1994,754-765.
44. Sheth S, Dev V, Jacobs H, Forrester J, Litvak F, Eigler N. Prevention of subacute stent thrombosis by polymer-polyethylene oxide-heparin coating in the rabbit carotid artery (Abstract). *J Am Coll Cardiol* 1995;25:348A.
45. Hardhammar P, Van Beusekom H, Emanuelsson H, et al. Reduction in thrombotic events with heparin-coated Palmaz-Schatz stents in normal coronary arteries. *Circulation* 1996;93:423-30.
46. Serruys P, Emanuelsson H, Van der Giessen W, et al. Heparin-coated Palmaz-Schatz stents in human coronary arteries: Early outcome of the Benestent-II pilot study. *Circulation* 1996;93:412-22.
47. Chronos N, Robinson K, White D, et al. Heparin coating dramatically reduces platelet deposition on incompletely deployed Palmaz-Schatz in the baboon A-V shunt (Abstract). *J Am Coll Cardiol* 1996;27:84A.
48. Chronos N, Robinson K, Kelly A, et al. Thrombogenicity of tantalum stents is decreased by surface heparin bonding: Scintigraphy of ¹¹¹In-platelet deposition in baboon carotid arteries (Abstract). *Circulation* 1995;92:I-490.
49. Chronos N, Robinson K, Kelly A, et al. Neointima formation in stented baboon carotid arteries is reduced by bonded heparin: Correlation with decreased thrombogenicity (Abstract). *J Am Coll Cardiol* 1996;27:85A.
50. Zidar J, Virmani R, Culp S, et al. Quantitative histopathologic analysis of the vascular response to heparin coating of the Cordis stent (Abstract). *J Am Coll Cardiol* 1993;21:336A.
51. Zidar J, Jackman J, Gammon R, et al. Serial assessment of heparin coating on vascular responses to a new tantalum stent (Abstract). *Circulation* 1992;89:I-185.
52. de Scheerder I, Wang K, Wilczek K, et al. Experimental study of thrombogenicity and foreign body reaction induced by heparin-coated coronary stents. *Circulation* 1997;95:1549-53.
53. Cox D, Anderson P, Roubin G, Chou C, Agrawal S, Cavender J. Effects of local delivery of heparin and methotrexate on neointimal proliferation in stented porcine coronary arteries. *Coron Art Dis* 1992;3:237-48.

54. Jeong M, Owen W, Staab M, et al. Does heparin release coating of the Wallstent limit thrombosis and platelet deposition? Results in a porcine carotid injury model (Abstract). *Circulation* 1995;92:I-37.
55. Legrand V, Serruys PW, Emanuelsson H, et al. Benestent II trial- Final results of visit 1 : A 15-day follow-up (Abstract). *J Am Coll Cardiol* 1997;29:170A.
56. Vrolix M, Grollier G, Legrand V, et al. Heparin-coated wire coil (Wiktor) for elective stent placement-The MENTOR trial (Abstract). *Eur Heart J* 1997;18:155.
57. Lambert T, Dev V, Rechavia E, Forrester J, Litvak F, Eigler N. Localized arterial wall drug delivery from a polymer-coated removable metallic stent: Kinetics, distribution, and bioactivity of forskolin. *Circulation* 1994;90:1003-11.
58. Dev V, Eigler N, Sheth S, Lambert T, Forrester J, Litvak F. Kinetics of drug delivery to the arterial wall via polyurethane-coated removable nitinol stent: Comparative study of two drugs. *Cathet Cardiovasc Diagn* 1995;34:272-278.
59. de Scheerder I, Wang K, Wilczek K, et al. Local methylprednisolone inhibition of foreign body response to coated intracoronary stents. *Coronary Artery Dis* 1996;7:161-6.
60. de Scheerder I, Wilczek K, Van Dorpe J. Angiopeptin loaded stents inhibit the neointimal reaction induced by polymer coated stents implanted in porcine coronary arteries (Abstract). *Circulation* 1994;90:I-597.
61. Eccleston D, Lincoff A, Furst J. Administration of colchicine using a novel prolonged delivery stent produces a marked local biological effect within the porcine coronary artery (Abstract). *Circulation* 1995;92:I-67.
62. Alt E, Beilharz C, Preter G, et al. Biodegradable stent coating with polylactic acid, hirudin and prostacyclin reduces restenosis (Abstract). *J Am Coll Cardiol* 1997;29:238A.
63. Prietzel K, Pasquantonio J, Fliedner T, Stemberger A, Janczewski M. Inhibition of neointimal proliferation with a novel hirudin/prostacyclin analog eluting stent coating in an animal overstretch model (Abstract). *Circulation* 1996;94:I-260.
64. Schmidmaier G, Stemberger A, Alt E, Gawaz M, Neumann F, Schömig A. A new biodegradable polylactic acid coronary stent-coating, releasing PEG-Hirudin and a prostacycline

analog, reduces both platelet activation and plasmatic coagulation (Abstract). *J Am Coll Cardiol* 1997;29:354A.

65. Schmidmaier G, Stemberger A, Alt E, Gawaz M, Schömig A. Time release characteristics of a biodegradable stent coating with polylactic acid releasing PEG-hirudin and PGI₂-analog (Abstract). *J Am Coll Cardiol* 1997;29:94A.

66. Aggarwal R, Ireland D, Azrin M, Ezekowitz M, De Bono D, Gershlick A. Antithrombotic potential of polymer-coated stents eluting platelet glycoprotein IIb/IIIa receptor antibody. *Circulation* 1996;94(12):3311-7.

67. Aggarwal R, Ireland D, Azrin M, de Bono D, Gershlick A. Reduction in thrombogenicity of cellulose polymer-coated stents by immobilization of platelet-targeted urokinase (Abstract). *J Am Coll Cardiol* 1997;29:353A.

68. Baron J, Aggrawal R, de Bono D, Gershlick A. Adsorption and elution of c7E3 Fab from polymer-coated stents in-vitro (Abstract). *Eur Heart J* 1997;18:503.

69. Folts J, Maalej N, Keaney J, Loscalzo J. Coating Palmaz-Schatz stents with a unique NO donor renders them much less thrombogenic when placed in pig carotid arteries (Abstract). *Circulation* 1995;92:I-670.

70. Folts J, Maalej N, Keaney J, Loscalzo J. Palmaz-Schatz stents coated with a NO donor reduces reocclusion when placed in pig carotid arteries for 28 days (Abstract). *J Am Coll Cardiol* 1996;27:86A.

71. Baker J, Nikolaychik V, Zulich A, Komorowski R, Kipshidze N. Fibrin coated stents as depot to deliver RGD peptide inhibit vascular reaction in atherosclerotic rabbit model (Abstract). *J Am Coll Cardiol* 1996;27:197A.

72. Santos R, Tanguay J, Kruse K, et al. Local administration of L-703,801 with a composite polymer stent reduces platelet deposition in canine coronary arteries (Abstract). *J Am Coll Cardiol* 1997;29:418A.

73. Murphy J, Schwartz R, Edwards W, Camrud A, Vliestra R, Holmes D. Percutaneous polymeric stents in porcine coronary arteries. *Circulation* 1992;86:1596-604.

74. Van der Giessen W, Slager C, Gussenhoven E, et al. Mechanical features and in vivo imaging of a polymer stent. *Int J Card Imag* 1993;9(219-26).

75. Susawa T, Shiraki K, Shimizu Y. Biodegradable intracoronary stents in adult dogs (Abstract). *J Am Coll Cardiol* 1993;21:483A.
76. Zidar J, Lincoff A, Stack R. Biodegradable stents. In: Topol E, ed. *Textbook of Interventional Cardiology*. Philadelphia, London, Toronto, Montreal, Sydney, Tokyo: W.B. Saunders, 1994: 787-802.
77. Bier J, Zalesky P, Sasken H, Williams D. A new bioabsorbable intravascular stent: in vitro assessment of hemodynamic and morphometric characteristics (Abstract). *Circulation* 1991;84:II-197.
78. Gregory K, Grunkemeier J. Internal elastic lamina replacement with a new elastin stent biomaterial (Abstract). *Circulation* 1994;90:I-596.
79. Gao R, Shi R, Qiao S, Song L, Li Y. A novel polymeric local heparin delivery stent: Initial experimental study (Abstract). *J Am Coll Cardiol* 1996;27:85A.
80. Ye Y, Landau C, Meidell RS, Willard J, Moskowitz A, Aziz S, Carlisle E, Nelson K, Eberhart RC. Improved bioresorbable microporous intravascular stents for gene therapy. *ASAIO J* 1996;42:M823-27.
81. Dichek D, Neville R, Zwiebel J, Freeman S, Leon M, Anderson W. Seeding of intravascular stents with genetically engineered endothelial cells. *Circulation* 1989;80:1347-53.
82. Flugelman M, Virmani R, Leon M, Bowman R, Dichek D. Genetically engineered endothelial cells remain adherent and viable after stent deployment and exposure to flow in vitro. *Circulation* 1992;70:348-54.
83. Scott N, Candal F, Robinson K, Ades E. Seeding of intracoronary stents with immortalized human microvascular endothelial cells. *Am Heart J* 1995;129:860-6.
84. Bailey SR, Decento YJ, Sprague E. Endothelial seeding: Intraprocedural replacement of endothelial cells on endovascular stents (Abstract). *Circulation* 1997;94:I-261.
85. Van Belle E, Tio F, Couffinhall T, Maillard L, Passeri J, Isner J. Stent endothelialization. Time course, impact of local catheter delivery, feasibility of recombinant protein administration and response to cytokine expedition. *Circulation* 1997;95:438-448.

86. Van Belle E, Tio F, Chen D, et al. Passivation of metallic stents after arterial gene transfer of p^h VEGF₁₆₅ inhibits thrombus formation and intimal thickening. *J Am Coll Cardiol* 1997;29:1371-9.
87. Bertrand OF, Mongrain R, Lehnert S, et al. Intravascular radiation therapy in atherosclerotic disease: promises and premises. *Eur Heart J* 1997;18:1385-95.
88. Hehrlein C, Gollan C, Dönges K et al.. Low-dose radioactive endovascular stents prevent smooth muscle cell proliferation and neointimal hyperplasia in rabbits. *Circulation* 1995;92:1570-5.
89. Hehrlein C, Stintz M, Kinscherf R et al. Pure β -particle emitting stents inhibits neointima formation in rabbits. *Circulation* 1996;93:641-5.
90. Carter A, Laird J, Bailey L et al. Effects of endovascular radiation from a β -particle-emitting stent in a porcine coronary restenosis model. A dose-response study. *Circulation* 1996;94:2364-8.
91. American Society for Testing and Materials, eds. *Annual Book of ASTM Standards*, 1992;13:F139-86.
92. Bertrand OF, Mongrain R, Bilodeau L, Tanguay JF. Radioactivity local delivery system. In: PCT patent application (CA97/00262).
93. Williams D. *Definitions in biomaterials*. Consensus Conference of the European Society for Biomaterials. Chester: Elsevier, 1987.
94. Stokes K. Biodegradation. *Cardiovasc Pathol* 1993;2(3):111S-119S.
95. Horbett T. Principles underlying the role of adsorbed plasma proteins in blood interactions with foreign materials. *Cardiovasc Pathol* 1993;2(3):137S-148S.

**CHAPTER IV: Early and Late Effects of Radiation Therapy
for Prevention of Coronary Restenosis: A Critical Appraisal.**

Introduction

Radiation therapy represents a new and promising approach for prevention of restenosis after coronary interventions (1, 2). Restenosis results from a complex interplay between thrombosis, vessel remodeling and neointima formation. Although the exact contribution of each process is still debated, neointima formation has been shown to play a major role in humans after balloon angioplasty and more recently after stent implantation. It is now admitted that vessel shrinkage plays a predominant role in restenosis after catheter-based coronary interventions whereas in-stent restenosis seems exclusively due to neointima formation (3, 4). Neointima formation results mainly from the accumulation of proliferating smooth muscle cells (SMCs) and extracellular matrix (ECM) secretion. Adventitial myofibroblast proliferation and ECM deposition may also play a role in vessel shrinkage in a way similar to scar retraction after skin injury (5).

Radiation therapy holds the promise to reduce or prevent SMCs and myofibroblast proliferation and thus to interfere with vessel remodeling and neointima formation. There are currently two different approaches to deliver endovascular irradiation. One is based on γ or β sources which are positioned locally through a catheter, to deliver single doses at high dose-rate in a limited period of time. The other uses radioactive stents for continuous low dose-rate therapy. Both techniques have undergone extensive animal testing and initial pilot studies have confirmed the potential. However, in addition to cytotoxicity, ionizing radiations have a number of biological effects that complicate the prediction of an optimal dose for restenosis prevention. In this article, we apply fundamental concepts and recent findings in radiation biology to the interpretation of the early and late consequences of radiation therapy used for restenosis prevention.

Cellular effects of radiation therapy

Available data describing neointimal cell proliferation are mostly qualitative and relatively little is known about the absolute number of proliferating cells associated with human restenosis. The recruitment of quiescent cells into the proliferating pool seems to differ significantly among different animal models currently used to study the pathophysiology of restenosis (6). In humans, however, the extent of SMC proliferation varied from 1 % to 25% after vessel injury (7, 8, 9). It has also been proposed that SMCs undergo a few proliferation cycles before resuming a quiescent state (6).

The volume associated with neointima formation after vessel injury is rather limited. Using arterial sections of human coronary vessels with restenosis, we found that neointima area represented about 10% of the total vessel area (10). In the Scripps trial, Teirstein et al. randomized 55 patients with restenosis or in-stent restenosis for either conventional treatment or endovascular radiation therapy with an ^{192}Ir source (1). Results at 6 months were impressive with a 65% reduction in restenosis rate after irradiation. The initial clinical benefit seems to be maintained at 2 years (11). Using intravascular ultrasound imaging, they measured an in-stent neointimal growth volume of $45 \pm 39 \text{ mm}^3$ in the control group. After delivery of a mean dose of 8 Gy to the medial layer, the neointimal growth volume was reduced to $16 \pm 23 \text{ mm}^3$ (1). Consequently, this suggests that a limited dose of irradiation is indeed effective in reducing neointima formation.

Using different animal models, several investigators have shown that single doses in excess of 10 Gy significantly reduce neointima formation after balloon angioplasty or before stent implantation (2). These results have been observed after short-term follow-up (usually between 2 and 4 weeks), although persistent benefit at 6 months using ^{192}Ir has subsequently been reported (12, 13). In humans, preliminary experience using prescribed doses from 8 to 25 Gy to the vessel wall have also shown positive early results with limited angiographic late loss (1, 14, 15).

The response of normal tissues to ionizing radiation varies according to the type of cellular organization. For some tissues, such as the skin, organization is hierarchical with cells responsible for proliferation and function in separate compartments. A stem cell compartment consists of pluripotent clonogenic cells which proliferate and sometimes mature into differentiating transit cells, which ultimately lose their ability to divide and become functional cells of limited life span. Under normal conditions, there is an equilibrium between cell proliferation and cell loss. The cellular effects of ionizing radiation on this type of tissue are thus a direct results of the number of stem cells that are sterilized by radiation.

In contrast, coronary artery walls consist of 3 different layers which contain variable numbers of SMCs, fibroblasts, macrophages and inflammatory cells, the inner part of the vascular wall being lined by a monolayer of endothelial cells. These cells represent differentiated functional cells with a very long but finite lifetime. Under steady state conditions, fibroblastic, SMC and endothelial cell proliferation in vascular wall is extremely low but may increase in response to appropriate stimuli. These cells may retain latent injury (i.e. irreversible DNA damage) for a long time until it is expressed at mitosis. One can assume that a dose of ionizing radiation delivered at the time of vessel injury will affect several cell types. As a result of irreversible DNA damage, cells having received a lethal dose of radiation will die when they attempt to divide. This means, in the context of restenosis, that a significant number of proliferating cells will die early after the coronary intervention.

It is possible, after high doses, that the rate of expression of the irreversible DNA damage could accelerate to the point where there would be an « avalanche » effect progressively amplifying the rate of cellular depletion (16). Later effects may thus, originate from progressive cell depletion of the vascular wall resulting from delayed cell division. This ultimately could create significant wall thinning with the possibility of aneurysm development. Aneurysm formation has already been demonstrated in humans after endovascular irradiation. Condado et al. reported that 4 out 20 patients treated with a single dose of radiation developed coronary aneurysm after a mean follow-up of 2 years (14). Waksman et al. reported the occurrence of a

subclavian vein aneurysm after endovascular treatment with an ^{192}Ir source and more recently in a peripheral artery (presented at Cardiovascular Radiation Therapy III, Washington, February 99) (17). In the European arm of the BERT study using a $^{90}\text{Sr}/\text{Y}$ source, the Rotterdam group also has noticed the emergence of a coronary aneurysm (P. Serruys, personal communication). In contrast, cell death and medial thinning have also been described in atherosclerotic coronary arteries and yet, coronary aneurysms are uncommon (18). These post-irradiation aneurysms could also be the consequence of dissections which have been prevented from complete healing by the radiation effects and subsequently, enlarge as false aneurysms. Indeed, Meerkin et al. using intravascular ultrasound imaging found less dissection resolution after endovascular radiation therapy compared with a control group (19). In that context, endothelial regeneration appears critical in preventing cells of the vascular wall from entering cell cycle and maintaining steady state conditions in the media and the adventitia (20). Intravascular ultrasound imaging may also help to differentiate true and false aneurysms since their prognosis appears different (21).

Waksman et al. showed a significant reduction in myofibroblastic proliferation in the adventitia of irradiated pig coronary arteries (22). On this basis, radiation therapy has been hypothesized to prevent negative vascular remodeling. This has also been suggested by recent intravascular ultrasound studies in human coronary arteries, 6 months after endovascular radiation therapy, which revealed little change in vessel dimensions, indicating that radiation therapy could counteract negative vessel remodeling early after coronary intervention (23).

Besides cell death during mitosis, radiation therapy also induces apoptosis (24). Apoptotic cells have also been demonstrated after coronary balloon angioplasty and in human restenotic lesions (25). To date, however, endovascular radiation therapy has not been proved to increase apoptosis early after vessel injury and its role in this process remains undefined (22).

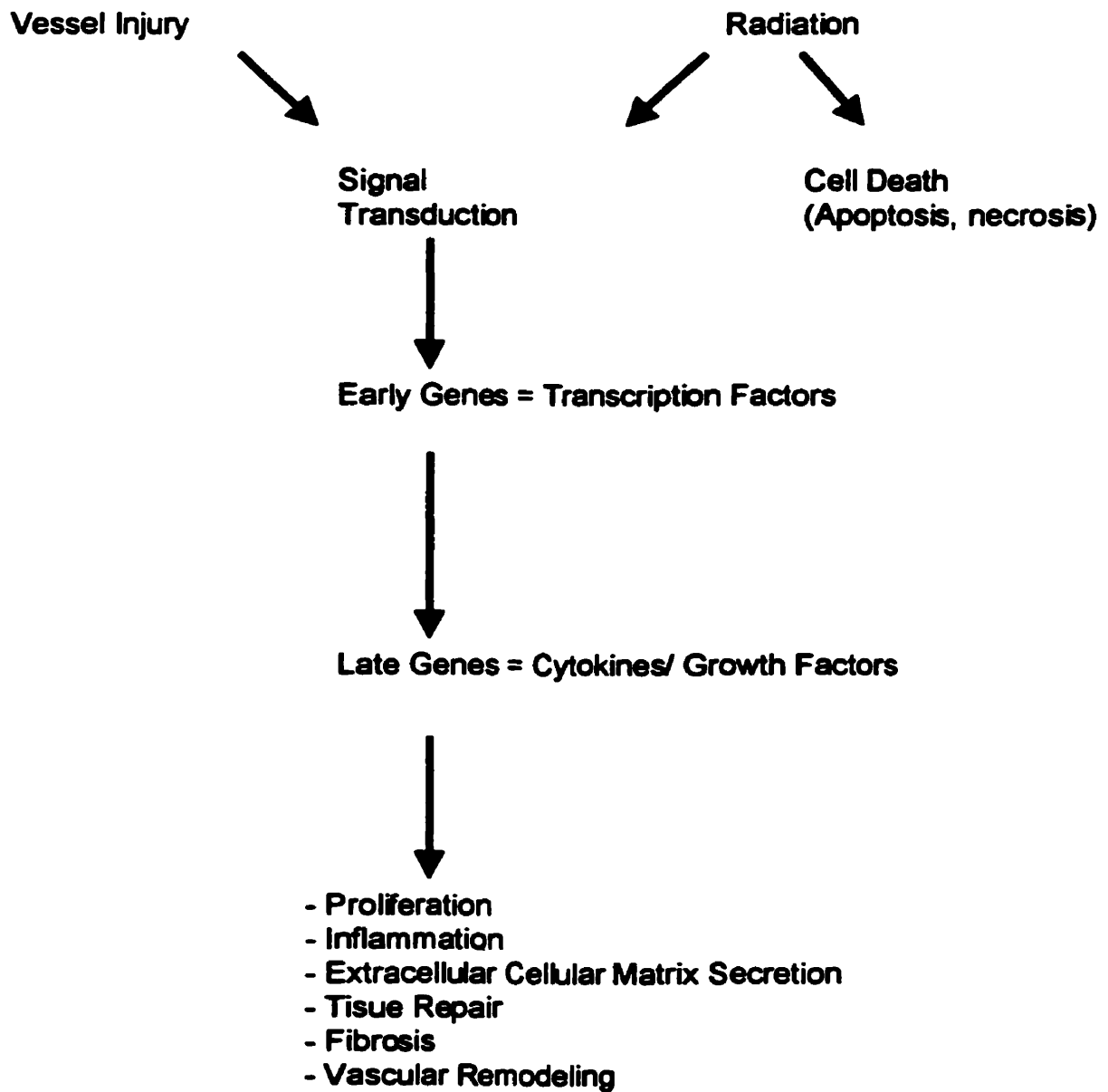
It is noteworthy that all radiation doses do not always produce the desired effect. A number of animal studies have reported a delayed or increased neointima formation with lower doses (2, 26, 27). Some investigators have also observed a beneficial effect at early follow-up

which was later lost (26). In the pilot trial performed at the Montreal Heart Institute using single prescribed doses between 12-16 Gy, 1 patient presented with a late restenosis at 1 year which was not present at the 6 month angiographic follow-up. It is worth mentioning that this recurrent stenosis was highly resistant and required cutting balloon angioplasty. This at least may suggest a fibrotic component. The emerging edge problem with restenosis occurring at the borders of the irradiated zones or at the radioactive stent extremities, so-called "candy-wrapper effect" is also probably a manifestation of a low-dose stimulatory effect (28). This apparent paradoxical effect deserves some attention. If sufficient clonogenic (with an intact potential to divide) cells survive radiation exposure, they can divide and repopulate the tissue. Cellular depletion below a critical level may also initiate an accelerated rate of proliferation resulting from an increase in the rate of stem cell division or recruitment of resting cells into the cell cycle. This process is well known to radiation oncologists as the response of certain tumors and normal tissues to fractionated irradiation (29). In the case of normal tissue such as the vascular system, this could explain delayed obstruction or border zone restenosis (30). It is likely that this process results also in part from growth factor release from intact or injured cells.

Gene regulation after radiation therapy

Early and late gene induction have been well described after vessel injury. Early gene transcription produces regulatory DNA binding proteins which possess multiple roles. The transcription factors encoded by these genes are critically involved in the entry of the cell into the G1 phase (first phase before DNA synthesis (S) and mitosis (G2-M)) of the cell cycle. In the basal state, most vascular cells are in the quiescent or G0 phase and some of these become activated soon after injury. In the rat carotid model, for instance, this corresponds with an entry into the cell cycle of 20-40% of medial SMCs in the 48 hrs after balloon injury (6). Late gene induction promotes the expression and secretion of several cytokines, growth factors and hormones. More than a decade of research has established the role of bFGF, PDGF, TGF- β , IGF and the interleukins in the inflammatory and growth processes leading to intimal thickening after vessel injury (31).

Figure 1: Similar Pathways after Vessel Injury and Radiation Therapy



Radiation therapy holds the promise to block the final effector of restenosis, namely proliferating SMCs and myofibroblasts. However, it has recently become apparent that the cellular response to damaging agents such as ionizing radiation is also complex and involves many genes and multiple regulatory mechanisms. Radiation induces gene products particularly important to radiation response. First, transcription factors involved in DNA repair and second, cytokines and growth factors, which play a role in inflammation and in the late effects of radiation therapy (32). Thus gene induction after vessel injury shares some similarity with radiation response (Figure 1). While little is known yet about gene induction after radiation therapy in the context of restenosis prevention, gene activation and cytokine/growth factor release are likely to play a critical role in the overall effect of endovascular radiation therapy.

Among early response genes that code for transcription factors and are activated by vessel injury and irradiation, the regulation of p53 deserves special attention. After irradiation, intracellular p53 protein level is increased through post-transcriptional mechanisms (33). P53 is critically involved in the activation of distinct pathways leading to cell cycle arrest and/or apoptosis (34). P53 is indeed the most frequently mutated gene in human cancer and mutated p53 has been implicated in the cellular radiation response. Furthermore, a role for p53 in restenosis has been proposed recently (35). Apoptotic cells have been identified in atherosclerotic plaques and restenotic lesions and a link with p53 mutation has been postulated (36). Hannan et al. described increased radiosensitivity for fibroblasts cultured from patients with overt coronary atherosclerosis (37). The possibility that atherosclerosis induces genotypic modifications that will alter radiation response is a fascinating hypothesis that needs to be explored further.

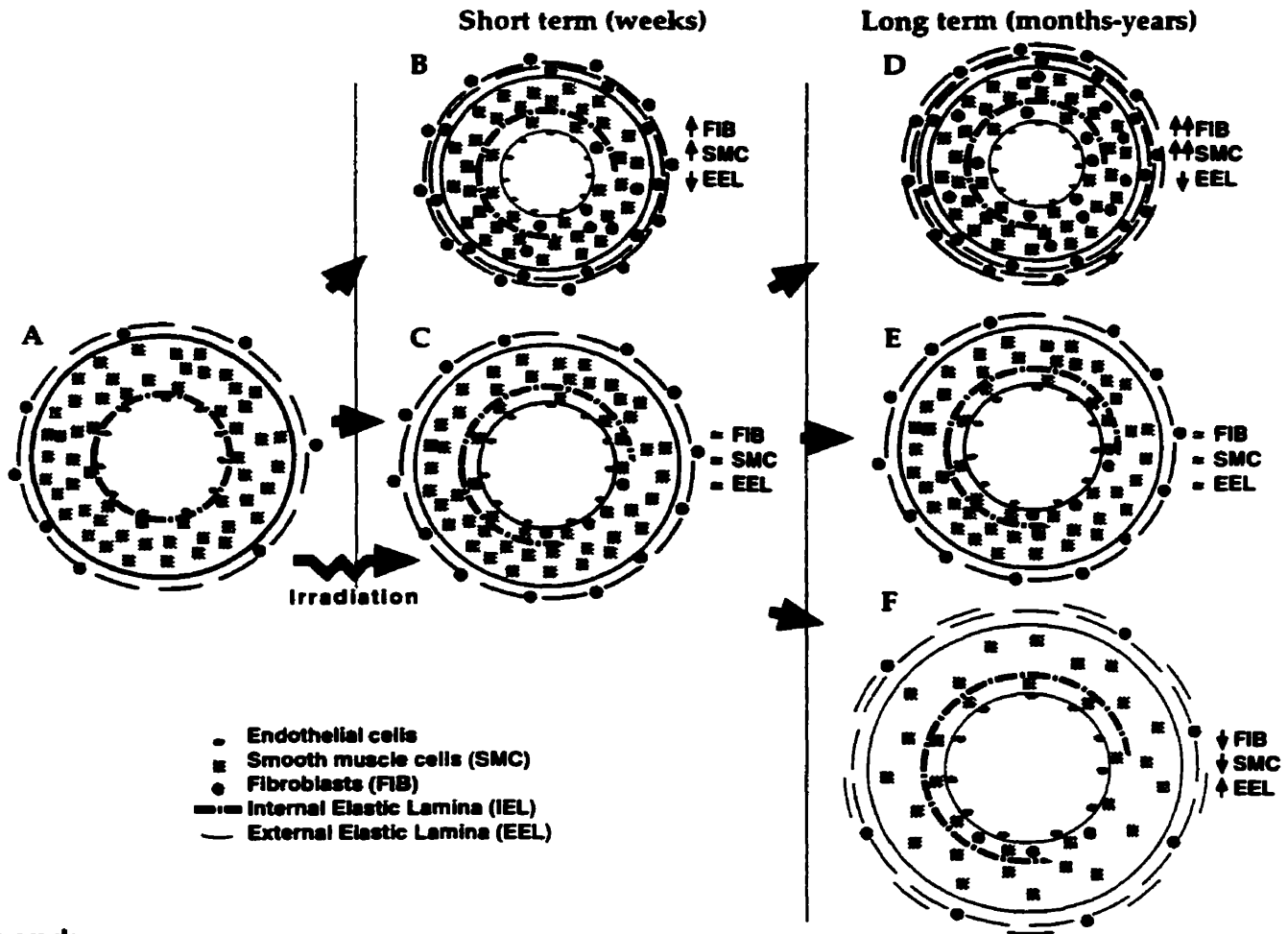
Experimental data indicate that growth factors and cytokines are synthesized de novo and secreted by vascular cells which survive irradiation. Witte et al. exposed endothelial cells to single doses of ionizing radiation and showed a dose-related increase in growth factor activity identified as bFGF and PDGF-related (38). Later, it was shown that bFGF through protein kinase C is

implicated in the protection of endothelial cells against radiation-induced apoptosis (39). Another cytokine, TNF- α is also induced by ionizing radiation and has been shown to sensitize cells to the lethal effects of irradiation (40). Thus, cytokines appear also to modulate the acute radiation response. This interaction could play a role, particularly after radioactive stent implantation and longer radiation exposure.

Normal human cell lines have also been shown, in response to radiation, to secrete factors which may influence the delayed response of the vascular system. Among others, TGF- β is released after irradiation exposure (41). Exploring radiation-induced lung fibrosis, Rubin et al. described a biphasic release of TGF- β and PDGF which was correlated with the fibrogenic response (42). In addition, they showed a similar time-related phenomenon for several types of collagen and for fibronectin (42). Hehrlein et al. showed a dose-related increase in collagen 1 deposition after radioactive stent implantation in rabbit iliac arteries (43). Interestingly, Rubin et al. described PDGF release after vessel injury in rat carotid arteries which was reduced in radiation-treated animals (44). They also postulated that radiation could act by reducing the number of macrophages which are known to release several growth-factors (44). Exposing SMC to γ -irradiation, Martin et al. showed that there was an extensive accumulation of extracellular matrix containing elastin between the cell layers (45). Therefore, experimental data strongly suggest that irradiation of vascular cells may also induce profibrogenic cytokine synthesis and secretion which in turn could produce abnormal cell proliferation and ECM secretion.

Fibrosis, a well-known consequence of external vascular irradiation, has also been described by some investigators in the different vascular layers after endovascular radiation therapy for restenosis prevention (13, 46). Therefore, it may be that if an optimal dose has been delivered after vessel injury, initial positive effects of a significant reduction in neointima formation and absence of negative vessel remodeling will persist during long term follow-up beyond 2 or 3 years.

Figure 2: Hypothetical Pathways after Radiation Therapy for Restenosis



Legend:

- A. Before vessel injury
- B. Restenosis after vessel injury is created by neointima formation and vessel remodeling
- C. Early effect after ionizing radiation, neointima formation and negative vessel remodeling are limited
- D. Late effect after ionizing radiation, if proliferation and cell proliferation are predominant, vessel shrinkage and delayed obstruction may develop
- E. If an optimal therapeutic window exists, persistent benefit will be maintained
- F. If cell depletion is predominant, vessel wall may weaken and progressively enlarge (aneurysm)

However, outside this presumed therapeutic window, at least two types of vessel remodeling are likely to occur (Figure 2). First, if cell depletion is the predominant radiation effect, the irradiated vascular segment may progressively enlarge and the arterial wall become thinned and lead to aneurysm formation. Intravascular ultrasound imaging has an important role to play in differentiating these malformations into true or false aneurysms as their respective prognosis appears different. Second, if fibrosis is predominant there is a potential risk of vascular wall thickening with negative remodeling and further lumen reduction. Preliminary data from clinical experience as described above suggest that these mechanisms can also be operative after irradiation of atherosclerotic coronary arteries. Again, successive intravascular ultrasound examinations of irradiated segments will provide new clues to assess potential late effects of endovascular radiation therapy. Stent implantation is also likely to influence delayed effects of radiation by preventing late vessel remodeling (11, 47). Indeed, no vessel aneurysm or delayed restenosis have been described so far in irradiated stented vessels.

In summary, radiation therapy for restenosis prevention seems an attractive new approach to counteract the most vexing problem for interventional cardiologists since the introduction of balloon angioplasty. Early clinical results have confirmed impressive short term experimental data and there is some evidence to suggest that endovascular radiation therapy will have a therapeutic window for restenosis prevention. Dose-finding clinical trials and long term follow-up studies are clearly required to better establish the therapeutic benefit. However, it is likely that limitations will continue to emerge with accumulating experience and long term follow-up. In particular, we propose that the cytokine cascade model postulated in both restenosis and radiation-induced fibrosis may explain some early adverse results and long term side-effects of radiation therapy when used for prevention of restenosis (42, 48).

References

1. Teirstein P, Massulo V, Jani S, et al. Catheter-based radiotherapy to inhibit restenosis after coronary stenting. *N Engl J Med* 1997;336:1697-703.
2. Bertrand O, Mongrain R, Lehnert S, et al. Intravascular radiation therapy in atherosclerotic disease: promises and premises. *Eur Heart J* 1997;18:1385-95.
3. Mintz GS, Popma JJ, Pichard AD, Kent KM, Satler L, Leon MB. Arterial remodeling after coronary angioplasty: a serial intravascular ultrasound study. *Circulation* 1996;94:35-43.
4. Hoffman R, Mintz GS, Dussailant GR, et al. Patterns and mechanisms of in-stent restenosis. A serial intravascular ultrasound study. *Circulation* 1996;94:1247-54.
5. Shi Y, Pieniek M, Fard A, O'Brien J, Mannion JD, Zalewski A. Adventitial remodeling after coronary arterial remodeling. *Circulation* 1996;93:340-8.
6. Clowes AW, Reidy MA, Clowes MM. Kinetics of cellular proliferation after arterial injury: smooth muscle growth in the absence of endothelium. *Lab Invest* 1983;49:327-33.
7. O'Brien E, Alpers C, Stewart D, et al. Proliferation in primary and restenotic coronary atherectomy tissue: implications for antiproliferative therapy. *Circ Res* 1993;73:223-31.
8. Pickering J, Weir L, Jakanowski L, Kearney M, Isner J. Proliferative activity in peripheral and coronary atherosclerotic plaque among patients undergoing percutaneous revascularization. *J Clin Invest* 1993;91:1469-72.
9. Kearney M, Pieczek A, Haley L, et al. Histopathology of in-stent restenosis in patients with peripheral artery disease. *Circulation* 1997;95:1998-2002.
10. Bertrand OF, Brunette J, Mongrain R, Leung TK, Lehnert S. Histo-morphology of coronary restenosis in humans. relevance for radiation therapy. In: Waksman R, ed. *Cardiovascular Radiation Therapy III*. Washington, 1999:66.
11. Teirstein PS, Massulo V, Jani S, Russo RJ, Cloutier DA. Two-year follow-up after catheter-based radiotherapy to inhibit coronary restenosis. *Circulation* 1999;99:243-7.
12. Waksman R, Robinson KA, Croker IR, Gravanis MB, Cipolla GD, King SB. Endovascular low-dose irradiation inhibits neointima formation after coronary artery balloon injury in swine. *Circulation* 1995;91:1533-39.

13. Wiedermann JG, Marboe C, Amols H, Schwartz A, Weinberger J. Intracoronary irradiation markedly reduces neointimal proliferation after balloon angioplasty in swine: Persistent benefit at 6-month follow-up. *J Am Coll Cardiol* 1995;25:1451-6.
14. Condado JA, Waksman R, Gurdziel O, et al. Long-term angiographic and clinical outcome after percutaneous transluminal coronary angioplasty and intracoronary radiation therapy in humans. *Circulation* 1997;96:727-32.
15. King SB, Williams DO, Chougoule L, et al. Endovascular beta-radiation to reduce restenosis after coronary balloon angioplasty: results of the Beta Energy Restenosis Trial (BERT). *Circulation* 1998;97:2025-30.
16. Nias AH. *An introduction to radiobiology*. Chichester, New York, Brisbane, Toronto, Singapore: John Wiley & Sons, 1990.
17. Waksman R, Robinson KA, Croker IR, Gravanis MB, Cipolla GC, King SB. Long term efficacy and safety of endovascular low dose irradiation in a swine model of restenosis after angioplasty. *J Am Coll Cardiol* 1995.
18. Mitchinson JM, Hardwick SJ, Bennett MR. Cell death in atherosclerotic plaques. *Curr Opin Lipid* 1996.
19. Meerkin D, Bonan R, Bertrand OF, Vincent J, Paiement P, Tardif JC. Radiation effects on dissection resolution: an IVUS study. In: Waksman R, ed. *Cardiovascular radiation therapy III*. Washington, 1999:64.
20. Scott-Burden T, Vanhoutte PM. The endothelium as a regulator of vascular smooth muscle proliferation. *Circulation* 1993;87:V51-5.
21. Bertrand OF, Mongrain R, Soualmi L, et al. Development of coronary aneurysm after cutting balloon angioplasty: assesment by intracoronary ultrasound. *Cathet Cardiovasc Diagn* 1998;44:449-52.
22. Waksman R, Rodriguez JC, Robinson KA, et al. Effect of intravascular irradiation on cell proliferation, apoptosis, and vascular remodeling after balloon overstretch injury of porcine coronary arteries. *Circulation* 1997;96:1944-52.

23. Meerkin D, Tardif JC, Crocker IR, et al. Effects of intracoronary β radiation therapy after coronary angioplasty: an intravascular ultrasound study. *Circulation* 1999;99:1660-65..
24. Dewey WC, Ling CC, Meyn RE. Radiation-induced apoptosis: Relevance to radiotherapy. *Int J Radiat Oncol Bio Phys* 1995;33:781-96.
25. Isner J, Kearney M, Bortman S, Passeri J. Apoptosis in human atherosclerosis and restenosis. *Circulation* 1995;91:2703-11.
26. Verin V, Popowski Y, Urban P, et al. Intra-arterial beta irradiation prevents neointimal hyperplasia in a hypercholesterolemic rabbit restenosis model. *Circulation* 1995;92:2284-90.
27. Weinberger J, Amols H, Ennis R, Schwartz A, Wiedermann J, Marboe C. Intracoronary irradiation: Dose response for the prevention of restenosis in swine. *Int J Radiat Oncol Bio Phys* 1996;36:767-75.
28. Albiero R, Di Mario C, Gregorio JD, Kobayashi N, Adamian M, Moussa I. Intravascular ultrasound (IVUS) analysis of beta-particle emitting radioactive stent implantation in human coronary arteries. Preliminary immediate and intermediate-term results of the MILAN study (Abstract). *Circulation* 1998;98:I-780.
29. Dorr W, Emmendorfer H, Haide E, Kummermehr J. Proliferation equivalent of accelerated repopulation in mouse oral mucosa. *Int J Radiat Biol* 1994;66:157-67.
30. Brenner D, Miller R, Hall E. The radiobiology of intravascular irradiation. *Int J Radiat Oncol Bio Phys* 1996;36:805-10.
31. Libby P, Tanka H. The molecular bases of restenosis. *Prog Cardiovasc Dis* 1997;40:97-106.
32. Weichselbaum RR, Hallahan DE, Sukhatme V, Dritschillo A, Sherman ML, Kufe DW. Biological consequence of gene regulation after ionizing radiation exposure. *J Natl Cancer Inst* 1991;83:480-84.
33. Bunz F, Dutriaux A, Lenganer C, et al. Requirement for P53 and P21 to sustain G2 arrest after DNA damage. *Science* 1998;282:1497-501.
34. Ko L, Prives C. p53: puzzle and paradigm. *Gen Devel* 1996;10:1054-72.

35. Speir E, Modali R, Huang E, et al. Potential role of human cytomegalovirus and p53 interaction in coronary restenosis. *Science* 1994;265:391-4.
36. Bennett MR, Littlewood TD, Schwartz SM, Weissberg PL. Increased sensitivity of human vascular smooth muscle cells from atherosclerotic plaques to p53-mediated apoptosis. *Circ Res* 1997;81:591-99.
37. Hannan M, Khougeer F, Halees Z, Sanei AM, Khan BA. Increased radiosensitivity and radioresistant DNA synthesis in cultured fibroblasts from patients with coronary atherosclerosis. *Arterioscl Thromb*. 1994;14:1761-66.
38. Witte L, Fuks Z, Haimovitz-Freidman A, Vloday I, Goodman DS, Eldor A. Effects of radiation on the release of growth factors from cultured bovine porcine and human endothelial cells. *Cancer Res* 1989;489:5066-72.
39. Haimovitz-Friedman A, Balaban N, McLoughlin M, et al. Protein kinase C mediates basic fibroblast growth factor protection of endothelial cells against radiation-induced apoptosis. *Cancer Res* 1994;54:2591-7.
40. Hallahan DE, Spriggs DR, Beckett MA, Kufe DW, Weichselbaum RR. Increased tumor necrosis factor alpha mRNA after cellular exposure to ionizing radiation. *Proc Natl Acad Sci USA* 1989;86:10104-7.
41. Martin M, Lefaix JL, Pinton P, et al. Temporal modulation of TGF- β 1 and β -actin gene expression in pig skin and muscular fibrosis after ionizing radiation. *Radiat Res* 1993;134:63-70.
42. Rubin P, Johnston CJ, Williams JP, McDonald S, Finkelstein JN. A perpetual cascade of cytokines postirradiation leads to pulmonary fibrosis. *Int J Radiat Oncol Biol Phys* 1995;33:99-109.
43. Hehrlein C, Gollan C, Dönges K, et al. Low-dose radioactive endovascular stents prevent smooth muscle cell proliferation and neointimal hyperplasia in rabbits. *Circulation* 1995;92:1570-75.
44. Rubin P, Williams J, Riggs P, et al. Cellular and molecular mechanisms of radiation inhibition of restenosis. Part I: role of the macrophage and platelet-derived growth factor. *Int J Radiat Oncol Bio Phys* 1998;40:929-41.

45. Martin BM, Ritchie AR, Toselli P, Franzblau C. Elastin synthesis and accumulation in irradiated smooth muscle cell cultures. *Connect Tissue Res* 1992;28:181-9.
46. Mazur W, Ali M, Khan M, et al. High dose rate intracoronary radiation for inhibition of neointimal formation in the stented and balloon-injured porcine models of restenosis: Angiographic, morphometric, and histopathologic analyses. *Int J Radiat Oncol Bio Phys* 1996;36:777-88.
47. Schopohl B, Liermann D, Pohlitz L, et al. ¹⁹²Ir endovascular brachytherapy for avoidance of intimal hyperplasia after percutaneous transluminal angioplasty and stent implantation in peripheral vessels: 6 years of experience. *Int J Radiat Oncol Bio Phys* 1996;36:835-40.
48. Libby P, Schwartz D, Brogi E, Tanaka H, Clinton SK. A cascade model for restenosis, a special case of atherosclerosis progression. *Circulation* 1992;86:47-52.

**CHAPTER V: Histo-morphologic Aspects of Coronary Restenosis after
Balloon Angioplasty in Humans: Relevance for Radiation Therapy**

Abstract

Radiation Therapy is undergoing clinical testing as a new therapy for the prevention and the treatment of restenosis after percutaneous coronary artery intervention. To better define the critical volume and target cells, we reviewed histo-morphometric data of human coronary restenosis.

We analyzed pathologic coronary specimens from 7 patients who died 8 ± 10 months after balloon angioplasty and presented histologic evidence of restenosis. Color images were digitized and analyzed using semi-automated image analysis software.

Total vessel area (TVA) averaged $12.6 \pm 2.5 \text{ mm}^2$. The residual lumen was $0.67 \pm 0.63 \text{ mm}^2$. Atherosclerotic plaque occupied a large portion of the vessel area with an average value of $5.9 \pm 1.6 \text{ mm}^2$ (50 % of TVA). Media and adventitia layers, which represent potential target zones, occupied about 33% of TVA. Depending on segment lengths (20-35 mm), targeted volumes using adventitial limits are estimated to be between 245 and 429 mm^3 . Using the external elastic lamina limit, which can be identified clinically by intravascular ultrasound imaging, about 80% of the vessel area would be covered. Adventitial and medial thickness were measured at $0.26 \pm 0.14 \text{ mm}$ and $0.15 \pm 0.06 \text{ mm}$ respectively. The distance between lumen center to the outer vessel limits averaged $1.99 \pm 0.56 \text{ mm}$. The media layer was the most cellular with $2,018 \pm 719 \text{ cells/mm}^2$, followed by the neointima with $1,444 \pm 598 \text{ cells/mm}^2$. The atherosclerotic plaque and adventitia were less cellular with $765 \pm 391 \text{ cells/mm}^2$ and $944 \pm 428 \text{ cells/mm}^2$ respectively. Total vessel density was estimated to be at 817 cells/mm^2 for normal vessels and 1023 cells/mm^2 for a restenotic vessel.

Our results indicate that target volumes for endovascular brachytherapy using media and adventitia limits are small. The presence of atherosclerotic plaque is likely to influence medial and adventitial dose distribution especially for β -emitters. Given the large differences in morphological characteristics, it seems that intravascular ultrasound imaging remains essential in the clinical evaluation of endovascular brachytherapy.

Introduction

Ionizing radiation has been recently proposed as a novel therapy for the prevention and/or the treatment of restenosis after vessel injury (1). There are actually two different approaches. One is based on the introduction, through small catheters, of very active γ or β sources (ribbon, liquid or seeds) to deliver the dose locally in a few minutes. Several isotopes such as ^{192}Ir , $^{90}\text{Sr/Y}$, ^{186}Re , ^{188}Re , and ^{32}P have been proposed and are undergoing experimental or early clinical testing. The other approach is based on the placement, at the injured site, of a radioactive stent that provides continuous low dose-rate therapy. For this application, the most popular isotope is ^{32}P , which is ion-implanted on the stent surface (2).

Restenosis results from a complex process, which involves to different degrees, thrombosis, neointima formation and geometric factors. For years, it was assumed that restenosis was mainly due to medial smooth muscle cell (SMC) activation and proliferation followed by intimal migration. Overall, these cells undergo a few cell divisions before resuming a quiescent state (3). More recent animal data suggest that adventitial cell proliferation and secretion of extracellular matrix could contribute significantly to the negative vessel remodeling and the restenosis process (4, 5).

Despite impressive early results, radiation therapy has also shown side effects such as fibrosis or aneurysm formation (6, 7). It is therefore important to better define the cells to target and the critical volume. Moreover, as the animal models are usually devoid of atherosclerotic plaque, dosimetric data obtained in animals are not easily transferred to the clinical situation. In this article, we present histo-morphometric coronary artery data obtained from patients who died after balloon angioplasty and presented histological evidence of restenosis. These data are used to present the relative areas occupied by the different vessel layers and the associated cell densities. Simple calculations based on these values and previously described pathophysiologic consequences of balloon angioplasty or stent implantation allow us to hypothesize target volume and cells to be exposed to ionizing radiation in order to prevent restenosis.

Materials and Methods

Pathology

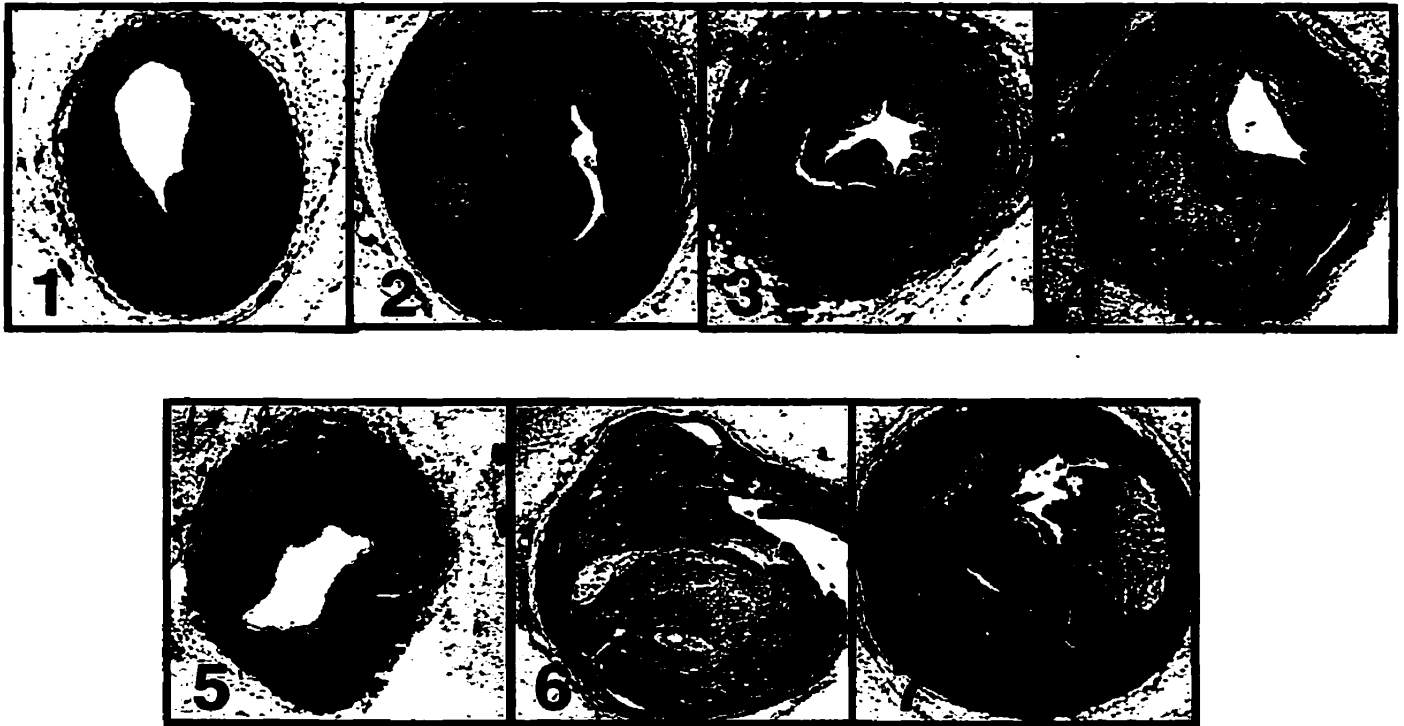
Coronary specimens embedded in paraffin blocs from 7 patients who died after balloon angioplasty and presented histologic evidence of restenosis were retrieved from the tissue data bank of the Montreal Heart Institute. This covered a period of about 17 years and more than 14,000 coronary angioplasties. The entire restenosed segment had to be embedded and hematoxylin-eosin-safran and movat pentachrome stainings were performed to clearly identify the different vascular layers. Using immediately adjacent slices (each 5 μm), 3 successive slices were stained only with hematoxylin to identify cell nuclei. Areas, layer thickness and distances were evaluated using movat pentachrome staining whereas hematoxylin stained slides were used to count cell nuclei. Each coronary segment involving the restenotic region was sectioned in 3-4 segments.

Image and morphometric analysis

Coronary specimens were analyzed at different magnifications using an inverted microscope. Color images of vessel segments were captured and digitized with either a 2.5 x or 25 x objective with a DXC-970MD video camera (Sony), a RasterOps 24XLTV videocard, and NIH image grabber software on a Macintosh PowerPC computer. Regions of interest were carefully selected and digitized images were stored on CD-Rom for further analysis.

Using a dedicated image analysis software (Sigma Pro, Jandel Scientific, Corte Madera, CA) we analyzed the following parameters: Total vessel area was delineated by the external limits of adventitia, which were recognized as the loose connective tissue or adipose tissue or myocardium surrounding the coronary artery. The region between the external elastic lamina (EEL) and the internal elastic lamina (IEL) delineated the media. We also encircled the atherosclerotic plaque area and the neointima area, which started from plaque rupture borders and

Figure 1: Representative Specimens of the 7 Coronary Arteries Analyzed.



covered the inner part of the vessel lumen. In addition, the centroids of the lumen and of the vessel were determined and the distance between each other was measured. Finally, we also measured the maximal and minimal distances between the lumen center and the vessel limits.

To evaluate cell densities present in each vessel layer, images were analyzed using the following protocol: high magnification fields were captured in Adobe Photoshop software and by adjusting filters, coloration and threshold, a binary image was obtained where nuclei appeared black and the rest of the image was white. Manual corrections were made as necessary by comparing initial to processed images by superposition. The binary images were then transferred into SigmaScan Pro and the number of nuclei was automatically calculated in the region of interest. Densities were obtained by correcting the nuclei number by the manually traced surface. Neointima densities were obtained by averaging measures at 6 different locations whereas media, adventitia and plaque densities were obtained by averaging 4 separate measures.

Data analysis

Values are presented as percentages or absolute values \pm SD. When necessary, comparisons were made using analysis of variance (ANOVA) followed by Bonferroni post-hoc analysis and a p value < 0.05 was considered significant.

Results

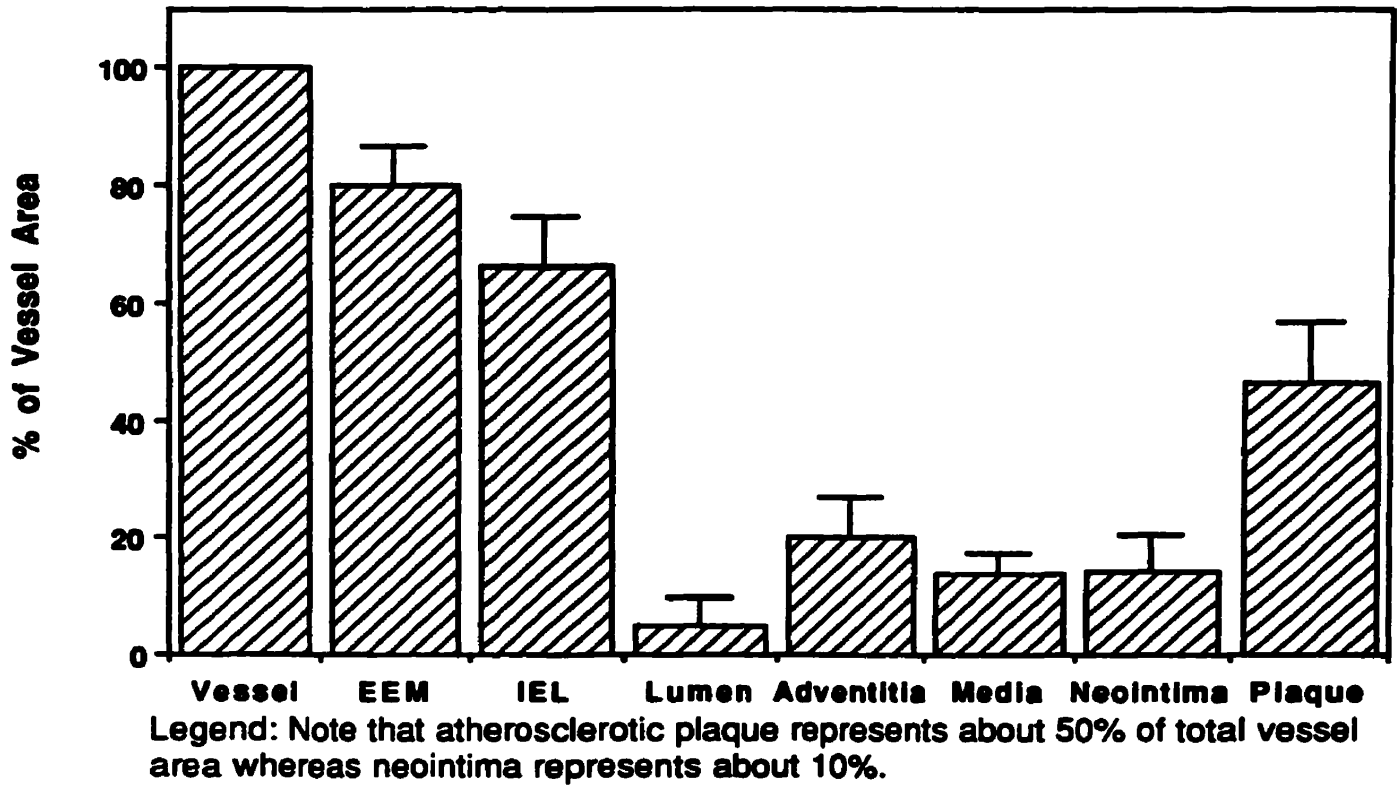
The clinical characteristics of the 7 patients are indicated in Table I. A total of 23 arterial sections were obtained and 322 digitized images analyzed. All patients but one, were males, 54 ± 7 years of age. All the dilated arteries originated from the native circulation with 3 left anterior descending arteries, 2 right coronary arteries, 1 circumflex and 1 diagonal branch. Time intervals after balloon angioplasty were highly variable with an average value of 8 ± 10 months. All patients died from cardiovascular causes.

Table 1: Clinical Characteristics

Patient	Age (years)	Artery	Time to restenosis
1	65	LAD	3 months
2	52	LAD	7 months
3	56	RCA	3 months
4	47	LAD	26 months
5	54	RCA	26 months
6	47	CX	35 months
7	51	DIAG	1 month

LAD: Left Anterior Descending artery, RCA: Right Coronary Artery, CX: Circumflex artery. DIAG: Diagonal branch.

Figure 2: Relative Vessel Layer Areas



Absolute and relative values for vessel layer areas are presented in Table II and Figure 2 respectively. Total vessel area averaged $12.56 \pm 2.49 \text{ mm}^2$. The External Elastic Lamina (EEL) which separates adventitia and media layers encircled an area of $10.06 \pm 2.05 \text{ mm}^2$. The residual lumen area of these restenosed vessels was rather small at $0.67 \pm 0.63 \text{ mm}^2$. It was clearly apparent that atherosclerotic plaque area occupied a large portion of these coronary vessels with an average value of $5.86 \pm 1.60 \text{ mm}^2$. In terms of relative value, this represented about 50% of the vessel area. In contrast, media and adventitia layers, which are likely target zones, represented about 33% of the total vessel area. For dosimetry purposes, targeting the EEL would mean that about 80 % of the total vessel area would be covered.

The adventitia and media were thin at $0.26 \pm 0.14 \text{ mm}$ and $0.15 \pm 0.06 \text{ mm}$ respectively (Table III, Figure 3). In contrast, the plaque and neointima were thicker at $0.80 \pm 0.50 \text{ mm}$ and $0.46 \pm 0.32 \text{ mm}$ ($P < 0.001$ vs adventitia and media) respectively. Of note, atherosclerotic plaques were most of the time eccentric (15/23) whereas neointima formation was more concentric. The distance between the lumen center to the outer vessel limit averaged $1.99 \pm 0.56 \text{ mm}$. It should also be noted that the lumen was most often eccentric as the lumen and vessel centroids were distant from $0.56 \pm 0.21 \text{ mm}$.

The cell densities differed also between the vessel layers (Table IV). The atherosclerotic plaque and adventitia were less cellular, $765 \pm 391 \text{ cells/mm}^2$ and $940 \pm 428 \text{ cells/mm}^2$ respectively ($P < 0.001$ vs media and neointima). The media layer was the most cellular with $2,018 \pm 719 \text{ cells/mm}^2$ ($P < 0.001$) followed by the neointima with $1,444 \pm 598 \text{ cells/mm}^2$. The vessel cell density corresponds to adventitial (cell density x area)/vessel area + medial (cell density x area)/vessel area + atherosclerotic (plaque cell density x area)/vessel area. In case of restenotic vessel, one has to add the relative neointima cell density. Using our specimens, the total vessel density might therefore be estimated at 817 cells/mm^2 and in case of restenotic vessel at 1034 cells/mm^2 .

Table II: Relative Vessel Layer Areas

Patient	Vessel area	EEL area	IEL area	Neointima area	Lumen area	Plaque area	Media area	Adventitia area
#1	13.6 ± 1.5	10.7 ± 0.7	8.5 ± 1.1	2.4 ± 0.9	1.5 ± 0.8	4.7 ± 1.2	2.3 ± 0.4	2.9 ± 0.8
#2	13.3 ± 0.2	10.1 ± 0.6	9.4 ± 0.4	2.1 ± 0.5	1.1 ± 0.5	6.1 ± 0.5	1.6 ± 0.1	2.3 ± 0.3
#3	12.9 ± 1.8	10.7 ± 1.5	9.0 ± 1.4	2.4 ± 0.6	0.2 ± 0.1	6.5 ± 1.2	1.7 ± 0.3	2.2 ± 0.4
#4	12.1 ± 0.5	10.7 ± 0.2	9.5 ± 0.3	2.1 ± 1.1	0.4 ± 0.3	7.1 ± 0.5	1.2 ± 0.3	1.4 ± 0.3
#5	12.4 ± 1.9	10.1 ± 1.0	8.4 ± 1.3	1.3 ± 1.0	0.6 ± 0.5	6.5 ± 0.2	1.7 ± 0.3	2.3 ± 0.9
#6	12.1 ± 5.8	8.3 ± 4.6	6.4 ± 4.1	1.2 ± 0.3	0.5 ± 0.5	4.8 ± 3.3	2.3 ± 0.4	3.7 ± 1.2
#7	11.2 ± 3.5	8.7 ± 2.5	7.1 ± 1.6	1.0 ± 0.6	0.4 ± 0.4	5.7 ± 1.8	1.6 ± 0.9	2.5 ± 1.0
Mean	12.6 ± 2.5	10.1 ± 2.0	8.3 ± 1.9	1.8 ± 0.8	0.7 ± 0.6	5.9 ± 1.6	1.7 ± 0.1	2.5 ± 0.9

EEL : External Elastic Lamina, IEL : Internal Elastic Lamina. All values in mm².

Table III: Vessel Layer Densities

Patient	Neointima density	Media density	Adventitia density	Plaque density
#1	884 ± 297	1584 ± 562	714 ± 240	851 ± 393
#2	1678 ± 582	2889 ± 743	961 ± 528	260 ± 143
#3	1442 ± 371	2493 ± 797	999 ± 592	755 ± 402
#4	1022 ± 323	1740 ± 409	618 ± 213	742 ± 320
#5	1868 ± 758	1667 ± 275	1110 ± 300	733 ± 319
#6	1679 ± 535	2060 ± 306	1204 ± 484	1192 ± 234
#7	1703 ± 434	1683 ± 616	1029 ± 166	808 ± 289
Mean	1445 ± 599	2019 ± 718	939 ± 428	765 ± 392

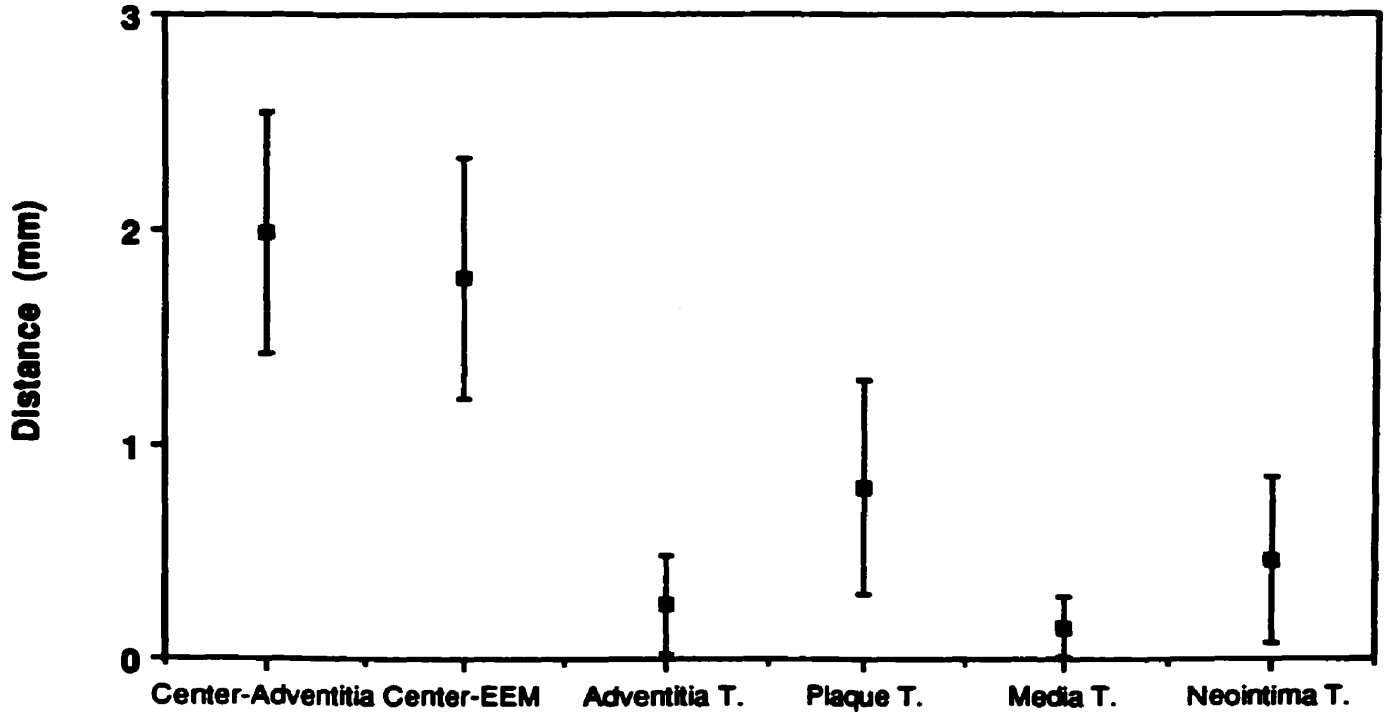
All values in mm².

Table IV: Vessel Layer Thickness and Relative Distances

Patient	Neointima thickness	Plaque thickness	Media thickness	Adventitia thickness	Center-Adventitia distance	Center-EEL distance	Centroids inter-distance
#1	0.61 ± 0.31	0.64 ± 0.37	0.18 ± 0.07	0.29 ± 0.20	2.07 ± 0.45	1.77 ± 0.46	0.50 ± 0.27
#2	0.43 ± 0.33	0.71 ± 0.47	0.16 ± 0.07	0.21 ± 0.08	2.08 ± 0.40	1.84 ± 0.37	0.32 ± 0.01
#3	0.65 ± 0.38	0.81 ± 0.48	0.16 ± 0.04	0.21 ± 0.08	2.04 ± 0.54	1.80 ± 0.52	0.62 ± 0.06
#4	0.51 ± 0.33	0.87 ± 0.52	0.10 ± 0.04	0.20 ± 0.07	2.00 ± 0.63	1.84 ± 0.64	0.74 ± 0.11
#5	0.33 ± 0.20	0.94 ± 0.57	0.14 ± 0.06	0.25 ± 0.12	2.04 ± 0.57	1.80 ± 0.56	0.73 ± 0.04
#6	0.30 ± 0.12	0.62 ± 0.39	0.20 ± 0.07	0.45 ± 0.18	2.05 ± 0.65	1.59 ± 0.50	0.36 ± 0.30
#7	0.26 ± 0.23	1.03 ± 0.63	0.15 ± 0.06	0.24 ± 0.07	1.87 ± 0.59	1.63 ± 0.59	0.61 ± 0.09
Mean	0.46 ± 0.32	0.80 ± 0.50	0.15 ± 0.07	0.26 ± 0.15	1.99 ± 0.56	1.78 ± 0.56	0.56 ± 0.21

All values in mm.

Figure 3: Vessel Layer Thickness and Target Distances



Legend: Center-adventitia: Distance from lumen center to outer limit of adventitia,
Center-EEM: Distance from lumen center to external elastic lamina, T: Thickness

Figure 4: Representative Specimen of a Human Coronary Lesion Obtained a Few Hours after Balloon Angioplasty



Legend: Representative specimen of a human coronary lesion obtained a few hours after balloon angioplasty. Plaque compression and limited intimal dissection are easily recognizable. Observe that the atherosclerotic plaque is concentrically distributed in this case. Vessel layers as obtained for histomorphometry are illustrated. Note that neointima is absent at the time of the procedure.

Discussion

Since the introduction of percutaneous coronary interventions in 1977, restenosis has permanently challenged investigators and led to several inconclusive pharmacological trials and development of new devices. Very recently radiation therapy has become investigated as a new tool to reduce restenosis after vessel injury (1). Despite extensive experimental work and initial clinical experience, there is little information concerning important data such as target volume or the exposed cells. Using pathologic specimens, we have attempted to review the basic cellular mechanisms of restenosis, which lead to speculate on possible critical volumes and target cells for either catheter-based brachytherapy or radioactive stent implantation.

Mechanisms of Percutaneous Transluminal Coronary Angioplasty (PTCA): Balloon angioplasty has been shown to create vessel wall breaks, splits or dissections, atherosclerotic plaque compression and vessel stretching to various extent (Figure 4) (8-11). In case of concentric lesion, the splits are usually limited to the atherosclerotic plaque whereas in case of eccentric lesion, they occur at the junctions between the atherosclerotic plaque and the normal vessel wall. Stents scaffold the vessel and tackle intimal flaps or dissections, creating a enlarged lumen compared with that seen with balloon angioplasty alone (12). Most of our lesions were eccentric with some portion of the vessel wall normal or mildly diseased. This is reflected by the distance between the true vessel center and the lumen center which were separated from each other by about 500 μm . Therefore, even a catheter centered in the vessel lumen after balloon angioplasty would not be necessarily in the center of the vessel. Previous reports have suggested that 75% of atherosclerotic coronary lesions are eccentric (13).

Mechanisms of restenosis: For years it has been assumed that restenosis resulted almost exclusively from neointima formation, which invaded the gaps and tears created by the vessel dilatation (10). In a manner similar to an exuberant healing tissue, this neointima could lead to further coronary obstruction. Neointima is formed by smooth muscle cells and myo-fibroblasts embedded in a loose connective tissue. Our pathologic specimens showed in all cases intimal

Figure 5: Mechanisms of Restenosis after Catheter-based Intervention and Stent Implantation

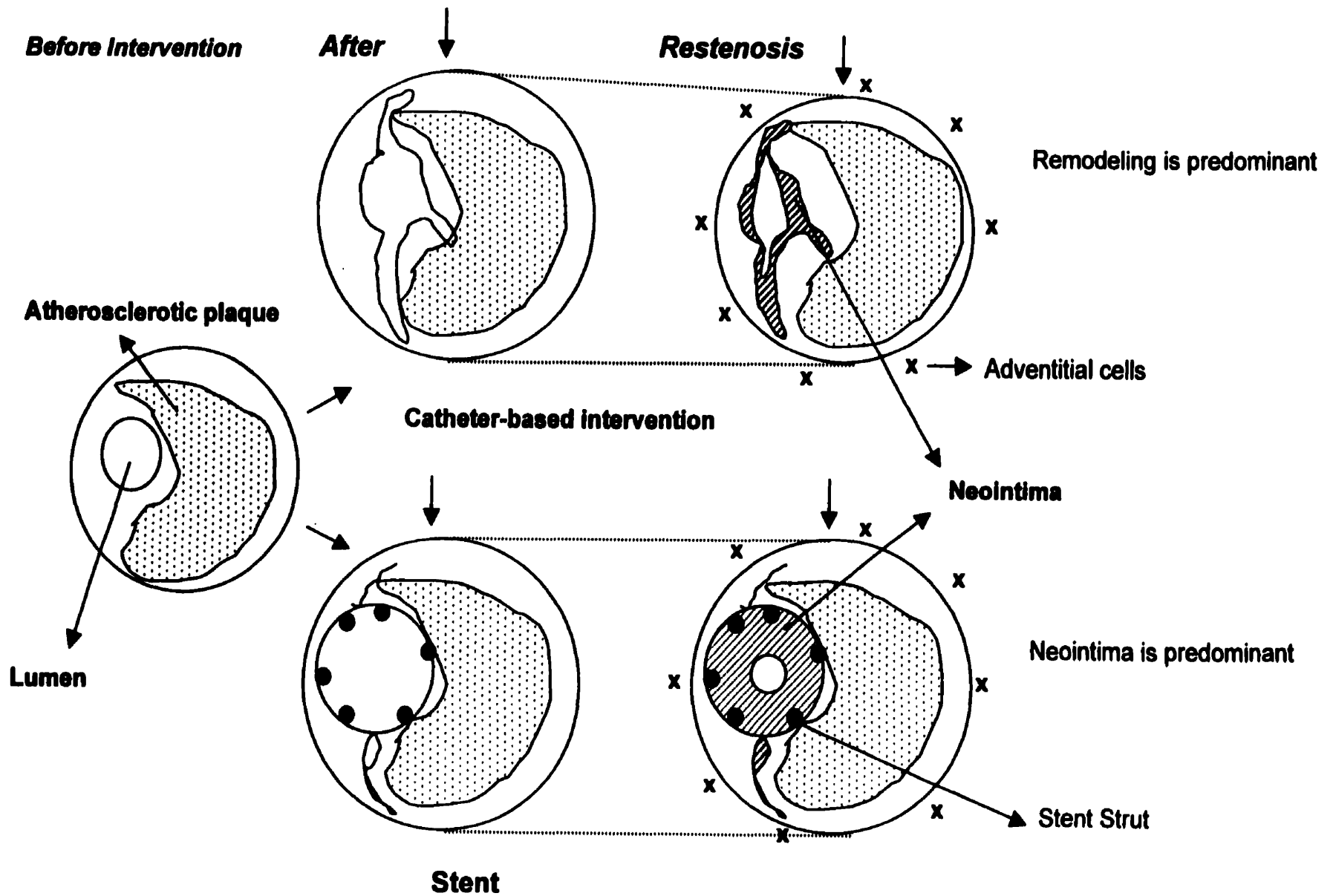
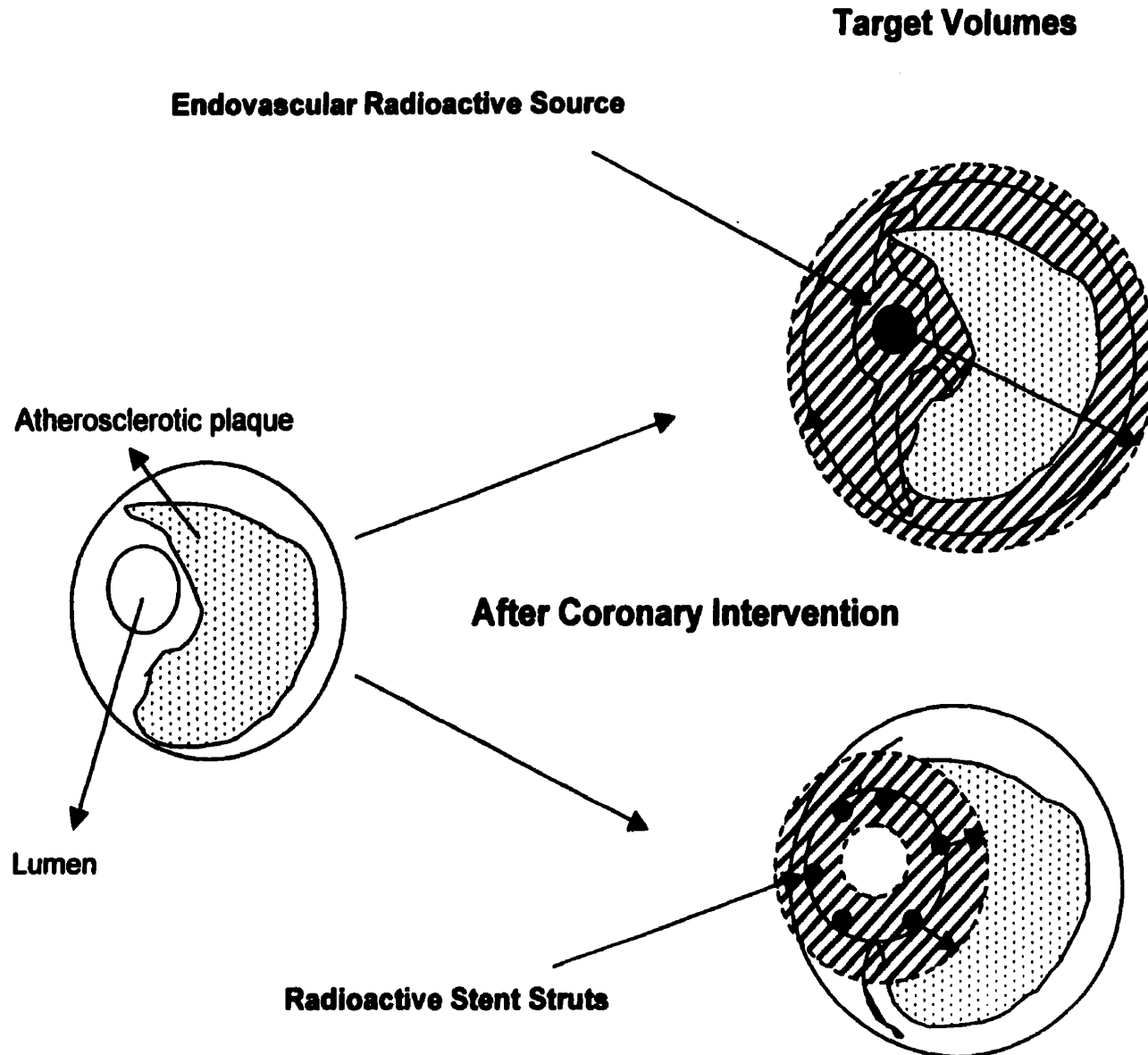


Figure 6: Hypothetical Target Volumes for Catheter-based Brachytherapy and Radioactive Stent



Legend: Hypothetical target volumes for endovascular catheter-based brachytherapy and radioactive stent. To prevent negative remodeling and neointima formation, catheter-based brachytherapy needs to target the outer vessel limits. Since remodeling is prevented by the scaffolding effect of the stent, the target volumes for radioactive stent does not include the outer vessel limits.

Figure 7: Neointimal Cell Densities as a Function of Time post-PTCA

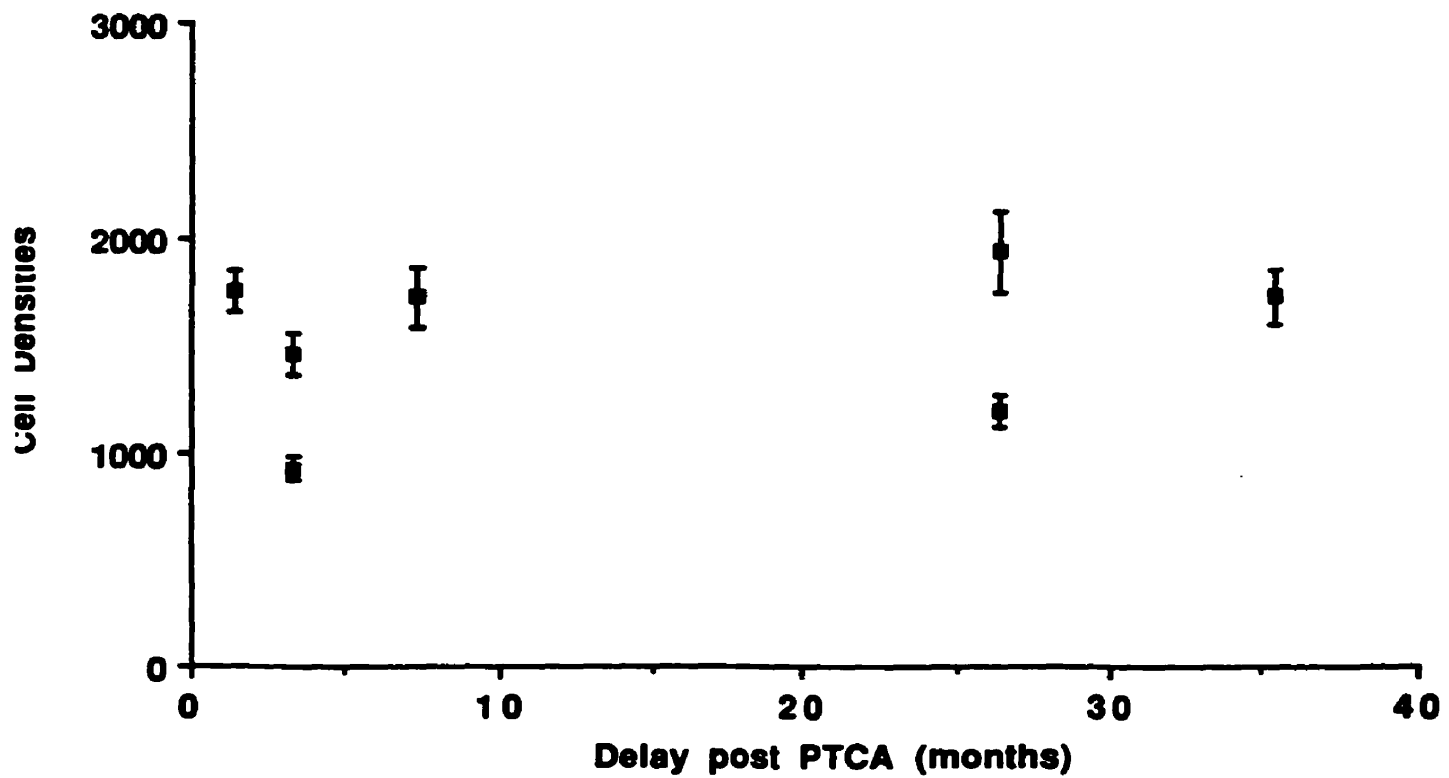


Table V: Calculated Target Volumes

Author (ref)	Methods	Surface (mm²)	Length	Volume
Teirstein et al. (36)	IVUS, post-stenting	(EEL) V_x < 3mm : 14.66 (EEL) V_x > 3mm : 16.69	19 mm or 35 mm	< 3mm: 278- 513 mm³ > 3 mm: 317- 584 mm³
Meerkin et al. (21)	IVUS, post-PTCA	(EEL) 14.49	30 mm	435 mm³
Carlier et al. (32)	IVUS, post-PTCA	(EEL) 17.00	30 mm	510 mm³
This study	Pathology, no PTCA	(EEL)10.06 (Adv.)12.26	20-30-35 mm 20-30-35 mm	201-302- 352 mm³ 245-368-429 mm³

IVUS: Intravascular Ultrasound Imaging, PTCA: Percutaneous Transluminal Coronary Angioplasty, EEL: External Elastic Lamina, Adv.: Adventitia.

proliferation originating from plaque tears or plaque-media borders. In one case, organized thrombus could also be recognized. In these restenotic vessels, neointima area represented about 10% of the total vessel area. However, early pathologic studies and more recently intravascular ultrasound (IVUS) studies suggested that intimal proliferation could not explain all restenoses after balloon angioplasty (14-16). These reports suggested the importance of vessel shrinkage in the development of delayed vessel obstruction.

Recent animal studies have indicated that adventitial myofibroblastic proliferation occurs early after vessel injury and could play a role in negative vessel remodeling by creating adventitial fibrosis leading to a stricture phenomenon (4, 17-19). Very recent data have shown that the adventitia layer, which contains small vessels (vasa vasorum), exhibits intense and transient neovascularization after vessel dilatation (20, 21). Furthermore, it has been postulated that some of these adventitial cells could also migrate into the intima and participate in the neointima build-up (5). In fact, intravascular ultrasound studies have demonstrated that negative vessel remodeling could account for more than 60% of restenosis pathophysiology after balloon angioplasty (15). There is therefore convincing evidence that catheter-based brachytherapy should target the medial and adventitial layers. In animal models and in early clinical testing, catheter-based brachytherapy reduced neointima formation and also prevented negative vessel remodeling (22, 23).

The pathophysiology of in-stent restenosis seems distinct from that of restenosis after catheter-based coronary interventions. It is now well established that the radial force of stents counteracts negative vessel remodeling (24, 25). Restenosis is then exclusively the consequence of concentric neointima formation, which may progressively occupy the stent lumen (26) (Figure 5). On the other hand, neointima formation is increased around the stent struts by the more severe trauma associated with stent implantation compared with balloon angioplasty (12, 27, 28). There is no difference in morphological aspects of neointima after stenting or balloon angioplasty (27). Previous reports have shown that neointima cell density after percutaneous vessel interventions

could vary between 688 ± 257 cells/mm² and 3260 ± 851 cells/mm² (27, 29). These variations are most probably due to differences between the tissues used (atherectomy fragments vs pathology specimens) and the techniques used to count nuclei.

Target volumes: Although the adventitia and the media were thin (< 300 μm) the atherosclerotic plaques were thicker (about 800 μm) and could significantly affect transmission of radiation for β -emitters from the lumen to the outer vessel layers. Moreover, atherosclerotic plaques may include calcifications, which may further alter homogeneity of dose distribution (30). This indicates a serious limitation to the usefulness of current animal models lacking an atherosclerotic plaque. To target the outer vessel limits from an endovascular source, it seems that a minimum distance of 1.99 mm is necessary. The American Association of Physicists in Medicine (AAPM) task group 60 has recommended prescribing doses for endovascular brachytherapy at a distance of 2 mm depth (31). There is presently much discussion to decide whether doses should be prescribed at a fixed distance or tailored to the patient. Our data suggest that there are large differences in vessel morphology among patients.

Assuming the coronary arteries as cylindrical, we can estimate, using the EEL as an anatomical landmark, a volume between 201 and 352 mm³ depending of the length of the treated segment. Using the adventitia limits, the volume would be slightly larger with values from 245 mm³ to 429 mm³. These values are in the same range than those reported by other investigators, which used intravascular ultrasound imaging (IVUS) to measure the distances from the IVUS catheter to the EEL separating the media and adventitia layers (Table V). In the SCRIPPS trial, the targeted volumes after coronary stenting might be estimated between 278 and 584 mm³ (32) whereas in the BERT feasibility study, estimates of targeted volumes after balloon angioplasty are between 435 and 510 mm³ (22, 33).

Given the large uncertainties concerning the minimum effective dose and the large differences in morphological characteristics of the treated vessels, IVUS could certainly help

investigators to better define the dosimetry related to catheter-based brachytherapy (34). Because the struts of radioactive stents are directly apposed against the vessel wall or the atherosclerotic plaque in which they produce small indentations less penetrating emitters would be required in this case (Figure 6). Furthermore, since neointima formation is directly related to the trauma to the vessel wall by stent struts, a therapeutic dose needs probably to be delivered to the directly surrounding tissue (27, 28, 35). If the circumferential adventitial tissue could be spared, this would reduce the target volume. In any case, the volumes treated by endovascular high dose-rate brachytherapy or low dose-rate radioactive stent remains below 1 cm³ for lesions up to 35 mm. This is reassuring in view of the small but not trivial risk of carcinogenesis associated with ionizing radiation.

Critical targets at the cellular level: Little is known concerning the number of cells, which must be sterilized in order to limit restenosis. Using PCNA staining, it has been evaluated that between 1 and 20% of cells proliferate for a limited period of time after balloon angioplasty or stent implantation. It is worth emphasizing that restenosis is associated with limited cell proliferation as the total number of cells stabilizes after a few weeks following vessel injury. Our data also showed that neointima cell density remains constant at the different time intervals studied (Figure 7).

Using in vitro experiments, we have previously shown that single doses above 8 Gy would sterilize about 99 % of fibroblasts or SMC, which are the likely target cells (36). If one considers a typical lesion length of 20 mm, our data allow estimating the number of cells that will be exposed. Considering the respective cell densities and layers areas, plaque cell density (765 cells/mm²) x area (5.86 mm²) + media cell density (2,018 cells/mm²) x area (1.71 mm²) + adventitia cell density (940 cells/mm²) x area (2.50 mm²) x length of the treated segment/slide thickness (= 5 μm); this gives a total of 4.11 x 10⁷ cells for a segment of 20 mm length. We can also estimate a mean number of neointimal cells given neointima cell density (1,444 cells/mm²) x area (1.82) x same length/slide thickness (= 5 μm) = 1 x 10⁷ cells. This means that neointima

represents a maximum of 25% of the total number of the exposed segment. This supports the notion that few cell divisions are required for neointima formation.

If one considers that 5 % of the vessel total cell number are clonogenic and contribute to restenosis, about 2×10^6 cells (5 % of 4.1×10^7) proliferate to ultimately give 1×10^7 cells (the total number of cells). Of course, this is somewhat simplified because all proliferative cells detected after balloon angioplasty do not necessarily contribute to neointima formation. This, however, further illustrates that restenosis is associated with a limited number of cell divisions. It is therefore difficult to extrapolate which level of irradiation will completely prevent restenosis formation. As already discussed doses around 8 Gy will create 99% of sterilization whereas doses around 12 Gy will create 99.9 % of sterilization. Indeed, only 2×10^3 cells (surviving fraction of 10^{-3}) would remain clonogenic after a single dose of 12 Gy. Restenosis is a temporary growth process where normal cells are transiently activated to proliferate by the acute release of growth factors associated with the vessel injury and the inflammatory response. Once these stimuli vanish, proliferating cells resume a quiescent state. This suggests that if radiation reduces the number of clonogenic cells, these surviving cells will divide during the few weeks after vessel injury and then resume a quiescent state. Therefore, radiation therapy would definitely impair the restenosis process if the total number of cells after radiation remains inferior to the total number of cells when there is no radiation. On the other hand, ionizing radiation may also have a stimulatory effect which can complicate the prediction of a successful dose and produce only a delay in the restenosis process (37).

Initial pilot studies using a $^{90}\text{Sr}/\text{Y}$ source and prescribed doses of 12-16 Gy at 2 mm depth have shown promising early results (22, 38). In contrast, Condado et al. delivering doses of 20-25 Gy at 1.5 to 2 mm depth (with some areas receiving doses up to 92 Gy) with an ^{192}Ir source observed the occurrence of 4 coronary aneurysms after 3 years follow-up (7). It should be mentioned that Condado et al. did not use IVUS and dose prescription was solely based on visual estimates obtained from angiographic images. In the SCRIPPS trial with a ^{192}Ir source, Teirstein et al. used IVUS to prescribe a minimum dose of 8 Gy to the EEL while keeping the maximum dose

below 30 Gy (32). Dosimetric analysis seems to indicate a better efficacy when the minimum dose was effectively delivered to the EEL (34).

Two year follow-up of this trial does not reveal loss of the early clinical benefit although these vessels were stented, which may have prevented late shrinkage due to delayed fibrosis (39). In contrast, Carlier et al. used dose-volume histograms to analyze the dosimetric aspects of the BERT trial using a non-centered $^{90}\text{Sr-Y}$ source. They reported that only about 35% of the adventitial volume received the prescribed dose (33). Meerkin et al. in the same study evaluated that adventitia received an average dose of 9.81 Gy with a minimum dose of 2.32 Gy and a maximum dose of 23.38 Gy (22). It appears therefore that IVUS imaging remains essential in the clinical evaluation of endovascular brachytherapy to better relate dosimetry with the vessel morphological structures. It is ultimately possible that IVUS would be necessary in order to tailor dose delivery for each patient, especially with β sources.

Several limitations might be applied to our study. First, we analyzed only a limited number of pathologic specimens covering large time intervals after balloon angioplasty. Our results were however in agreement with other similar reports describing morphological data after coronary interventions. Although each arterial segment was serially sectioned, the exact distance between slides was not known precluding exact three-dimensional reconstruction. Therefore, our calculations to extrapolate total cell number in each vessel layer were only approximations. Since vessel densities in the different layers have not been reported previously, this study is a first attempt to determine the number of exposed cells. Despite expected shrinkage associated with tissue fixation, our calculated target volumes were in agreement with those obtained in vivo by IVUS.

In conclusion, our results show that target volumes for endovascular brachytherapy, assuming adventitia and media as target zones would remain small. We also showed the importance of atherosclerotic plaque and vessel inhomogeneities in determining dose distribution

to the outer vessel wall i.e. media and adventitia. Given the large variations in vessel morphology, intravascular imaging should remain part of our armamentarium to better define the therapeutic dose window as well as the potential side effects of endovascular radiation therapy on coronary vessel walls.

References

1. Bertrand O, Mongrain R, Lehnert S, et al. Intravascular radiation therapy in atherosclerotic disease: promises and premises. *Eur Heart J* 1997;18:1385-95.
2. Carter A, Fischell TA. Current status of radioactive stents for the prevention of in-stent restenosis. *Int J Radiat Oncol Bio Phys* 1998;41:127-33.
3. Clowes AW, Reidy MA, Clowes MM. Kinetics of cellular proliferation after arterial injury: smooth muscle growth in the absence of endothelium. *Lab Invest* 1983;49:327-33.
4. Scott NA, Cipolla GD, Ross CE, et al. Identification of a potential role for the adventitia in vascular lesion formation after balloon overstretch injury of porcine coronary arteries. *Circulation* 1996;93:2178-87.
5. Shi Y, O'Brien JE, Fard A, Mannion J, Wang D, Zalewski A. Adventitial myofibroblasts contribute to neointimal formation in injured porcine coronary arteries. *Circulation* 1996;94:1655-64.
6. Weinberger J, Amols H, Ennis R, Schwartz A, Wiedermann J, Marboe C. Intracoronary irradiation: Dose response for the prevention of restenosis in swine. *Int J Radiat Oncol Bio Phys* 1996;36:767-75.
7. Condado JA, Waksman R, Gurdiel O, et al. Long-term angiographic and clinical outcome after percutaneous transluminal coronary angioplasty and intracoronary radiation therapy in humans. *Circulation* 1997;96:727-32.
8. Essed CE, Van den Brand M, Becker AE. Transluminal coronary angioplasty and early restenosis. Fibrocellular occlusion after wall laceration. *Br Heart J* 1983;49:393-6.
9. Ueda M, Becker AE, Fujimoto T, Tsukada T. The early phenomena of restenosis following percutaneous transluminal coronary angioplasty. *Eur Heart J* 1991;12:937-45.
10. Austin GE, Ratliff MB, Hollman J, Tabei S, Phillips DF. Intimal proliferation of smooth muscle cells as an explanation for recurrent coronary artery stenosis after percutaneous transluminal coronary angioplasty. *J Am Coll Cardiol* 1985;6:369-75.

11. Garrat KN, Edwards WD, Vliestra RE, Kaufman UP, Holmes DR. Coronary morphology after percutaneous directional coronary atherectomy in humans: autopsy analysis of three patients. *J Am Coll Cardiol* 1990;16:1432-6.
12. Anderson PG, Bajaj RK, Baxley WA, Roubin GS. Vascular pathology of balloon-expandable flexible coil stents in humans. *J Am Coll Cardiol* 1992;19:372-81.
13. Brown BG, Bolson EL, Dodge HT. Dynamic mechanisms in human coronary stenosis. *Circulation* 1984;70:917-22.
14. Waller BF, Gorfinkel HJ, Rogers FJ, Kent KM, Roberts WC. Early and late morphologic changes in major epicardial coronary arteries after percutaneous transluminal coronary angioplasty. *Am J Cardiol* 1984;53:42C-7C.
15. Mintz GS, Popma JJ, Pichard AD, Kent KM, Satler L, Leon MB. Arterial remodeling after coronary angioplasty: a serial intravascular ultrasound study. *Circulation* 1996;94:35-43.
16. Cote G, Tardif JC, Lesperance J, et al. Effects of probucol on vascular remodeling after coronary angioplasty. *Circulation* 1999;99:30-5.
17. Geary RL, Nikkari ST, Wagner WD, Williams JK, Adams MR, Dean RH. Wound healing: a paradigm for lumen narrowing after arterial reconstruction. *J Vasc Surg* 1998;27:96-106 (-8).
18. Post MJ, Borst C, Kuntz RE. The relative importance of arterial remodeling compared with intimal hyperplasia in lumen renarrowing after balloon angioplasty. A study in the normal rabbit and the hypercholesterolemic Yucatan micropig. *Circulation* 1994;89:2816-21.
19. Shi Y, O'Brien JE, Ala-Kokko L, Chung W, Mannion JD, Zalewski A. Origin of extracellular matrix synthesis during coronary repair. *Circulation* 1997;95:997-1006.
20. Kwon MK, Sangiorgi G, Ritman EL, et al. Adventitial vasa vasorum in balloon-injured coronary arteries. Visualization and quantitation by a microscopic three-dimensional computed tomography technique. *J Am Coll Cardiol* 1998;32:2072-9.
21. Pels K, Labinaz M, Hoffert C, O'Brien ER. Adventitial angiogenesis early after coronary angioplasty. Correlation with arterial remodeling. *Arterioscler Thromb Vasc Biol* 1999;19:229-38.

22. Meerkin D, Tardif JC, Joyal M, et al. Post-angioplasty intracoronary radiation therapy (ICRT) induced morphological change: An IVUS study. *Circulation* 1999;99:1660-65..
23. Waksman R, Rodriguez JC, Robinson KA, et al. Effect of intravascular irradiation on cell proliferation, apoptosis, and vascular remodeling after balloon overstretch injury of porcine coronary arteries. *Circulation* 1997;96:1944-52.
24. Hehrlein C, Zimmermann M, Pill J, Metz J, Kübler W, von Hodenberg E. The role of elastic recoil after balloon angioplasty of rabbit arteries and its prevention by stent implantation. *Eur Heart J* 1994;15:277-80.
25. Hoffman R, Mintz GS, Dussailant GR, et al. Patterns and mechanisms of in-stent restenosis. A serial intravascular ultrasound study. *Circulation* 1996;94:1247-54.
26. Kjelsberg MA, Seifert P, Edelman ER, Rogers C. Design-dependent variations in coronary stent stenosis measured as precisely by angiography. *J Inv Cardiol* 1998;10:142-50.
27. Farb A, Sangiorgi G, Carter AJ, et al. Pathology of acute and chronic coronary stenting in humans. *Circulation* 1999;1:44-52.
28. Komatsu R, Ueda M, Naruko T, Kojima A, Becker AE. Neointima tissue response at sites of coronary stenting in humans. Macroscopic, histological, and immunohistochemical analyses. *Circulation* 1998;98:224-33.
29. Pickering J, Weir L, Jakanowski L, Kearney M, Isner J. Proliferative activity in peripheral and coronary atherosclerotic plaque among patients undergoing percutaneous revascularization. *J Clin Invest* 1993;91:1469-72.
30. Crilly R, Roberts W, Spears R. The effect of calcification in atherosclerotic lesions on the dose distribution of axially delivered β and γ radiation (Abstract). In: Waksman R, Leon MB, eds. *Advances in Cardiovascular Radiation Therapy*. Washington, 1997:12.
31. Nath R, Amols H, Coffey C, et al. Intravascular brachytherapy physics: Report of the AAPM radiation therapy Committee task group No. 60. *Med Phys* 1999;26:119-152.
32. Teirstein P, Massulo V, Jani S, et al. Catheter-based radiotherapy to inhibit restenosis after coronary stenting. *N Engl J Med* 1997;336:1697-703.

33. Carlier S, Marijnissen JPA, Coen VLMA, et al. Guidance of intracoronary radiation therapy based on dose-volume histograms derived from quantitative intravascular ultrasound. *IEEE Trans Med Imag* 1998;17:772-8.
34. Teirstein PS, Massulo V, Jani S, et al. A subgroup analysis of the Scripps coronary radiation to inhibit proliferation poststenting trial. *Int J Rad Biol Oncol Phys* 1998;42:1097-104.
35. Foster MT, Atkinson JB, Yeah TK, Fischell TA. Histopathology of restenosis after stenting of narrowed coronary arteries after cardiac transplantation during the teenage years. *Am J Cardiol* 1997;80:389-93.
36. Bertrand OF, Mongrain R, Thorin E, Chow D, Lehnert S. Radiosensitivity of human coronary smooth muscle cells exposed to high dose-rate γ irradiation (Abstract). *J Am Coll Cardiol* 1997;31:277A-8A.
37. Brenner D, Miller R, Hall E. The radiobiology of intravascular irradiation. *Int J Radiat Oncol Bio Phys* 1996;36:805-10.
38. King SB, Williams DO, Chougoule L, et al. Endovascular beta-radiation to reduce restenosis after coronary balloon angioplasty: results of the Beta Energy Restenosis Trial (BERT). *Circulation* 1998;97:2025-30.
39. Teirstein PS, Massulo V, Jani S, Russo RJ, Cloutier DA. Two-year follow-up after catheter-based radiotherapy to inhibit coronary restenosis. *Circulation* 1999;99:243-7.

**CHAPTER VI: In Vitro Response of Human and Porcine Vascular Cells
Exposed to High Dose-rate γ Irradiation**

Abstract

Radiation biology of vascular cells is an important issue of the use of ionizing radiation for the prevention of restenosis after vessel injury. Controversy remains whether there are differences in intrinsic radiosensitivities between vascular cells. The objective of this study was to compare the *in vitro* response of human and pig endothelial cells, smooth muscle cells and fibroblasts exposed to conventional high dose-rate γ irradiation.

Clonogenic survival curves and growth responses were obtained after irradiation of plateau-phase cells with a ^{60}Co source at a dose-rate of 1.5 Gy/min. DNA single strand breaks were evaluated using alkaline filter elution technique.

Overall, the pig cell lines had a similar response than human cell lines to conventional high dose-rate irradiation. Using clonogenic assays, the human aortic smooth muscle cell line was more sensitive than the fibroblast and endothelial cell lines whereas the pig endothelial cell line was more sensitive than smooth muscle cells and fibroblasts. Early after irradiation (10 days) there was a temporary growth inhibition effect similar between endothelial, smooth muscle cells and fibroblasts with doses above 4 Gy. There was also a non-linear dose dependent growth delay up to 4 weeks after irradiation. This effect was also consistent between the different cell lines. Using alkaline filter elution, there was no significant difference in relative elution between endothelial cells, smooth muscle cells and fibroblasts.

In vitro response of human and pig endothelial cells, smooth muscle cells and fibroblasts exposed to high dose-rate irradiation appeared similar. The pig model seems well suited to evaluate the short and long term effects of ionizing radiation in the prevention of restenosis after vessel injury.

Introduction

The use of ionizing radiation has recently received much interest in cardiology as a new tool to reduce restenosis after vessel injury (1). Since the introduction of balloon angioplasty to relieve obstructions in atherosclerotic coronary arteries in 1977, interventional cardiologists have been frustrated by the fact that a significant number of patients (about 30 %) present with a recurrence of their symptoms, usually in the first 6 months after the procedure. The process of restenosis which bears similarities with a healing process is due to a complex interplay between thrombus formation and organization, neointima formation due to cell proliferation and vessel shrinkage, commonly referred as negative remodeling (2-6). Neointima is formed by smooth muscle cells and myo-fibroblasts which migrate from the media and probably from the adventitia into the intima and proliferate for a few cell cycles before resuming a quiescent state (3, 5, 6). These cells generate also a significant amount of extra-cellular matrix which contributes to the neointima build-up. Several clinical studies which sought to prevent restenosis using pharmacological approaches and targeting specific cell signals or growth-factors have been so far unsuccessful (7).

Due to its capability to kill proliferating cells, ionizing radiation has recently been proposed as a possible new approach. However, many questions remain unanswered such as the precise target volume, the target cells, the optimal dose and timing and the long term effects on the vascular system. There are convincing experimental data showing a clear radiation-induced limitation of neointima formation after short term follow-up (usually 2-4 weeks); however, fibrosis, a well known consequence of irradiation, has also been shown in the different layers of the vessel wall after irradiation (8-10). In addition, a few preliminary clinical studies have reported the occurrence of vessel aneurysms after administration of large single doses of irradiation (11, 12). It is therefore necessary to establish in detail the radiobiology of the vascular cells exposed to radiation after vessel injury. Indeed, despite several reports studying the radiation response of vascular cells, it remains unclear whether there are significant differences in intrinsic radiosensitivity between endothelial cells, smooth muscle cells (SMC) and fibroblasts.

The purpose of this paper is first, to report the initial characterization of human vascular cells exposed to conventional high dose rate (1-2 Gy/min) γ irradiation using clonogenic assays. Second, as the pig model is commonly used to study the restenosis process, we have compared the radiation response of vascular cells isolated from pig aortas. Third, we have compared the growth of these vascular cell populations at early (10 days) and late (4 weeks) times after irradiation. Finally, we have used the alkaline filter elution technique to compare DNA single strand break formation between human and pig cell lines.

Materials and Methods

Cell lines

Human dermal fibroblasts (donor age = 25 years), coronary smooth muscle cells (donor age = 3 years) and aortic endothelial cells (donor age = 27 years) were obtained from Clonetics Inc. (San Diego). Cells between passage 4 to 9 were used for experiments. Pig aortic fibroblasts and smooth muscle cells were isolated from adult slaughtered animals. Aortic endothelial cells were isolated from pig aortas using collagenase. Immunostaining was used to characterize the cells as fibroblasts (α actin negative), smooth muscle cells (α actin positive) and endothelial cells (factor VIII/Vw positive). Cells between passage 3 to 10 were used for experiments. All cells were grown as monolayers in plastic flasks (T25, Nunc Corporation) at 37° C with humidified environment containing 5% CO₂. Culture medium for pig vascular cells, human fibroblasts and smooth muscle cells consisted of Dulbecco's Minimal Essential Medium (Gibco) supplemented with 20% fetal bovine serum, L-Glutamine 1% and gentamycin (0.6 μ g/ml). Human endothelial cells required Clonetics endothelial basal medium-2 supplemented with fetal bovine serum 5%, hydrocortisone, human fibroblast growth factor, vascular endothelial growth factor, insulin-like growth factor, ascorbic acid, human epidermal growth factor and gentamycin. Confluent cells were used for all experiments and proliferative activity of cells in plateau phase was verified by flow cytometry.

Radiation procedure

Cells were irradiated 48 hrs post confluence using a ^{60}Co source (Theratron, Atomic Energy of Canada Ltd.) at a dose rate of about 1.5 Gy/min, at room temperature. Immediately after irradiation, cells were returned to the incubator overnight (min 12 hours) to allow full repair of potentially lethal damage. After trypsinization, cells were plated in T25 flasks at increasing densities (200 cells at 0 Gy to 8000 cells at 12 Gy) with a feeder of heavily irradiated cells (1×10^4 cells irradiated at 30 Gy). For each experiment, cells were plated in duplicate or triplicate flasks and each experiment was reproduced a minimum of three times.

Survival

The culture medium was changed 2-3 times and cells were fixed with formaldehyde and stained with crystal violet after 10-14 days. Colonies containing more than 50 cells were counted. The surviving fractions were calculated as the ratio of plating efficiencies of irradiated to unirradiated control cells. Clonogenic survivals were analyzed according to the single hit multitarget model and the D_0 and the extrapolation number, n were calculated by linear regression. Survival curves were fitted to the linear-quadratic model (L-Q) where surviving fractions = $\exp(-\alpha D - \beta D^2)$ with D = dose. The parameters α and β were determined by non linear regression. Surviving fractions at 2 Gy (SF2) were extrapolated from the raw data. The mean inactivation dose (\bar{D}) is the integral of curves fitted by the linear quadratic model and plotted on linear coordinates (13).

Growth inhibition and delay

Two different protocols were followed. Cell monolayers were trypsinized after irradiation and 1×10^4 cells from each dose were plated into 12 well-flasks without feeder. To measure kinetics of growth, cells were grown up until confluence was noted in the well containing the unirradiated cells. At that time, all cells were trypsinized and counted with a haemocytometer. In other experiments to measure the population growth delay effect of radiation, we evaluated the

time to obtain confluence in each well. Cells were considered confluent when > 95% of the cells covered the well surface when examined with an inverted contrast phase microscope and a magnification x 40.

Alkaline filter elution

Radioactive labeling and elution procedure have been described in detail elsewhere (14). Briefly, cells in exponential growth were incubated for 48 hrs with radioactive thymidine (3H). Following removal of radioactive thymidine, cells were cultured for 24 hrs in medium containing non radioactive thymidine. For alkaline elution, we used the technique described by Kohn et al. with slight modification (14, 15). Before irradiation, cells were trypsinized at 4°C degree and suspended in 10 cc of cold PBS at a density around 4×10^5 cells/tube. Cells were irradiated on ice with a Theratron 780 (Energy Atomic of Canada Ltd.) to deliver doses between 1-4 Gy at a dose-rate of about 1.5 Gy/min.

After irradiation, control and irradiated cells were rapidly layered onto 25 mm (2 μ m pore size) polycarbonate filter (Nucleopore), washed twice with cold PBS and lyzed on the filter for maximum 30 min at room temperature in the dark, with 2 % SDS, 0.02 M EDTA at pH 10.0 with 0.05 mg/ml proteinase K (Merck, Germany). DNA was eluted with tetrapropylammoniumhydroxide, 0.02 M EDTA, pH 12.1 at a flow rate of 0.035 ml/min in the dark. Fractions were collected at 90 min intervals for 15 hrs. The radioactivity remaining on the filter and that in the eluate were determined by liquid scintillation counting. The first 2 collected fractions were discarded and correction for differences in flow rate was made on the basis of the eluted volume of each vial which were separately weighed. The percentage of activity retained on the filter after elution for unirradiated cells were compared. Relative elution (RE) was calculated according to the formula: $RE \text{ activity} = \log I/C$ where I represents the activity of the eluted fraction of irradiated cells and C, the activity of the eluted fraction of unirradiated cells.

Statistical analysis

Values are presented as mean \pm SEM and Confidence Intervals unless otherwise stated. Data were analyzed by Student's t test or one-way analysis of variance (ANOVA). A P value $<$ 0.05 was considered significant.

Results

Clonogenic survival

Flow cytometric analysis showed that 87 ± 4 % of human cells and 86 ± 4 % of pig cells were in G_0/G_1 at the time of irradiation. Figures 1 and 2 show survival curve for each cell line. Among human cells, the SMC strain appeared more radiosensitive than the fibroblastic and endothelial cell strains. This was essentially reflected by the absence of shoulder and survival was an exponential function of the dose. In terms of radiation response parameters, the α value for the L-Q model and the D bar and the SF2 for the SMC line were significantly smaller than the corresponding values for the endothelial cells and fibroblasts (Table 1). It should also be noted that the shoulder effect as reflected by the n value, was particularly pronounced for the endothelial cell line. Among the pig vascular cell lines, SMC and fibroblasts which were isolated from the same animal showed close survival curves with a distinct shoulder effect. In contrast, the endothelial cell strain showed no shoulder. In fact, the pig endothelial cell line and the human SMC line behaved similarly with β values not significantly different from zero.

Growth inhibition and growth delay

For all human cells, unirradiated cells initially plated at a density of 1×10^4 cell/well grew rapidly and reached confluence in about 10 days. At this early time, few irradiated surviving cells with doses above (4 Gy) have divided as the total number of cells was not significantly increased compared with initial plating. The number of cells irradiated with more than 4 Gy was also significantly lower than control. This effect appeared similar between fibroblasts, SMC and

Figure 1: Human Cell Survival Curves

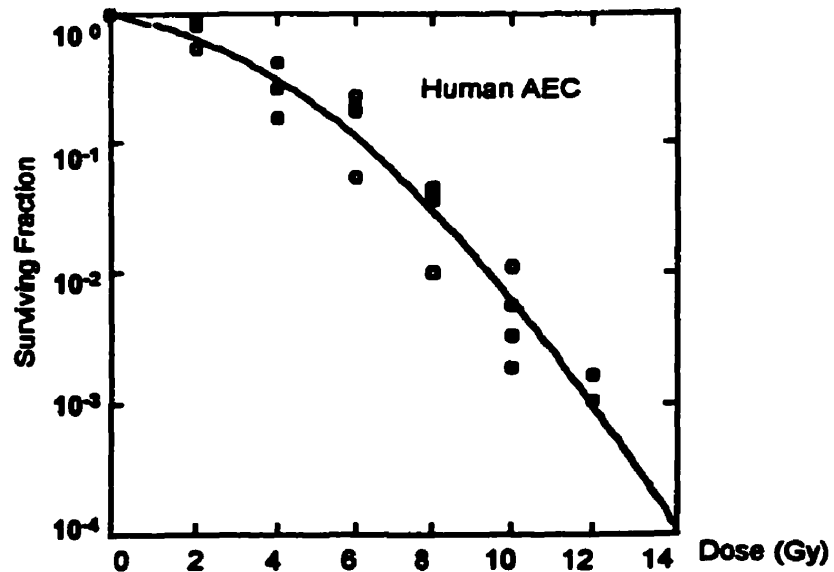
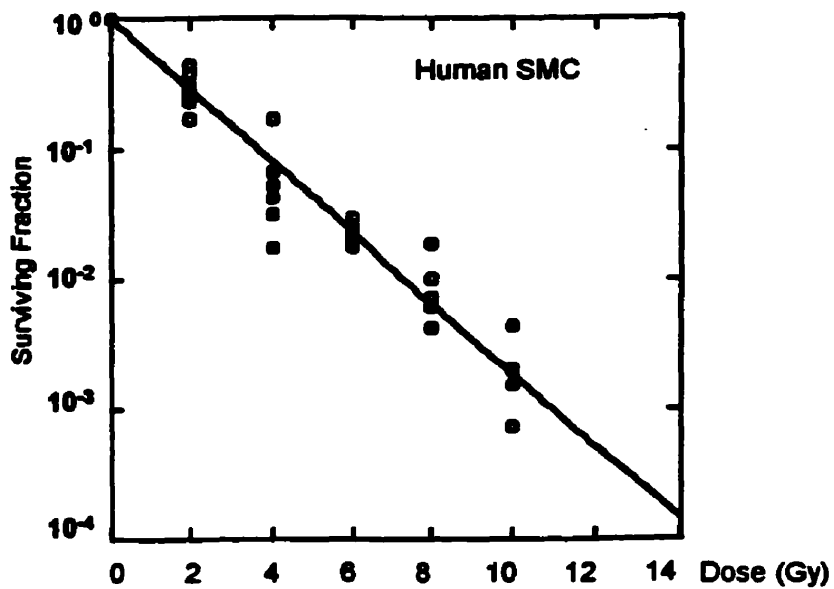
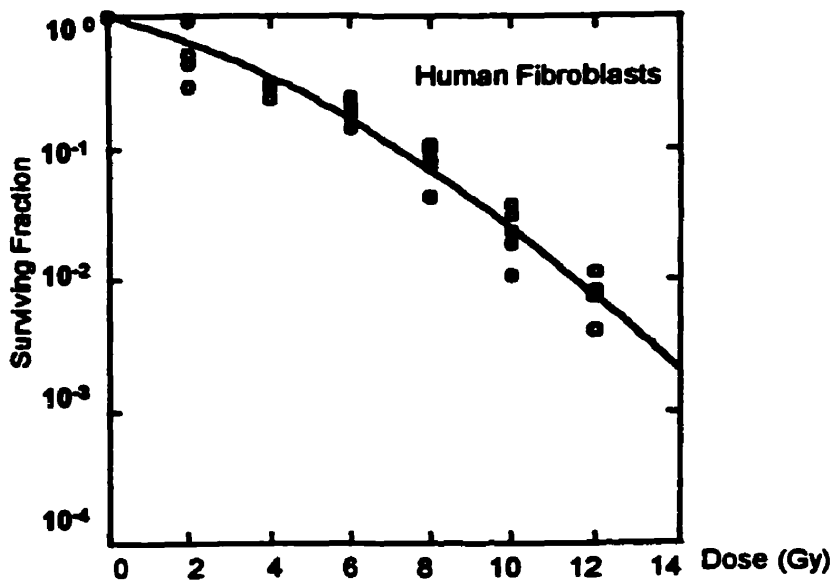


Figure 2: Pig Cell Survival Curves

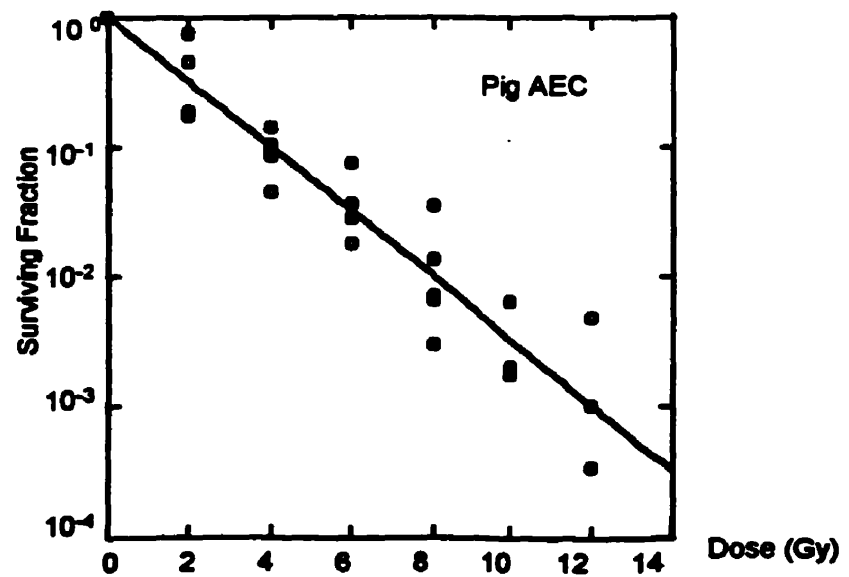
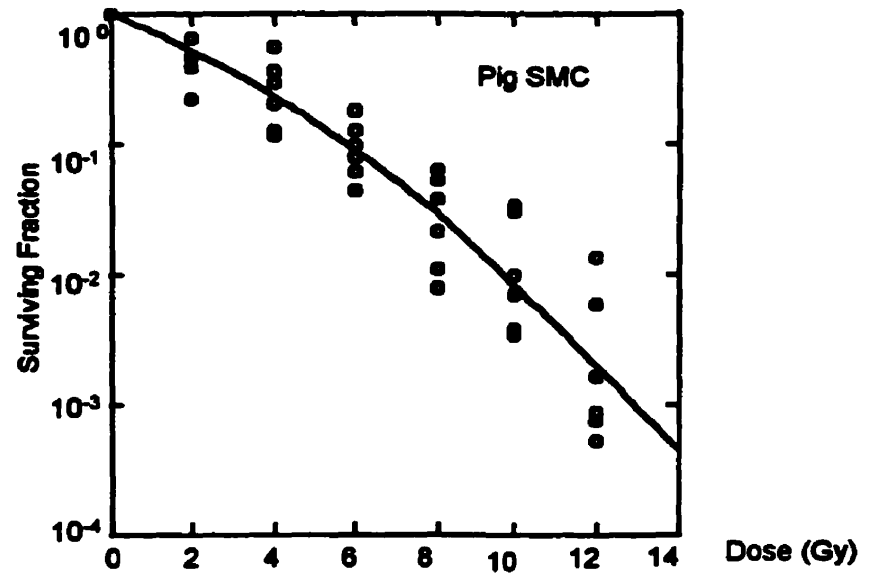
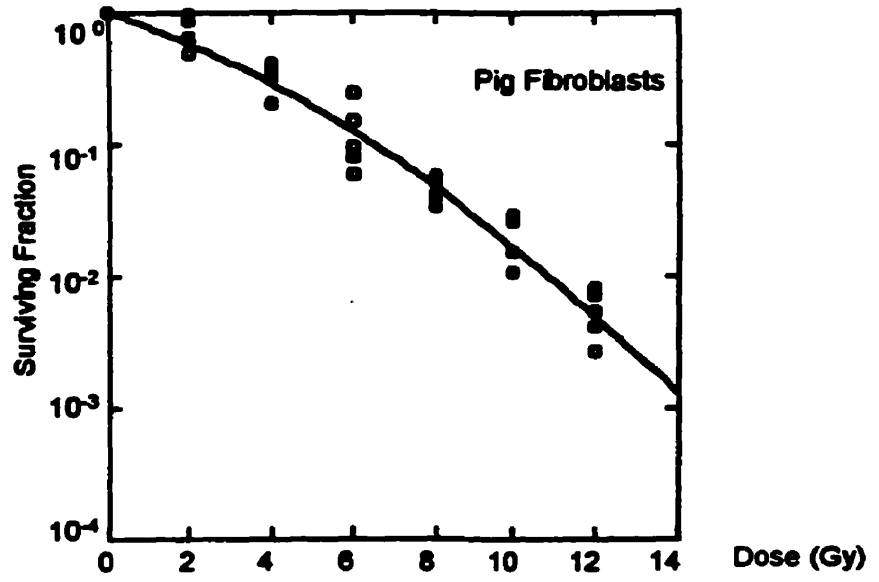
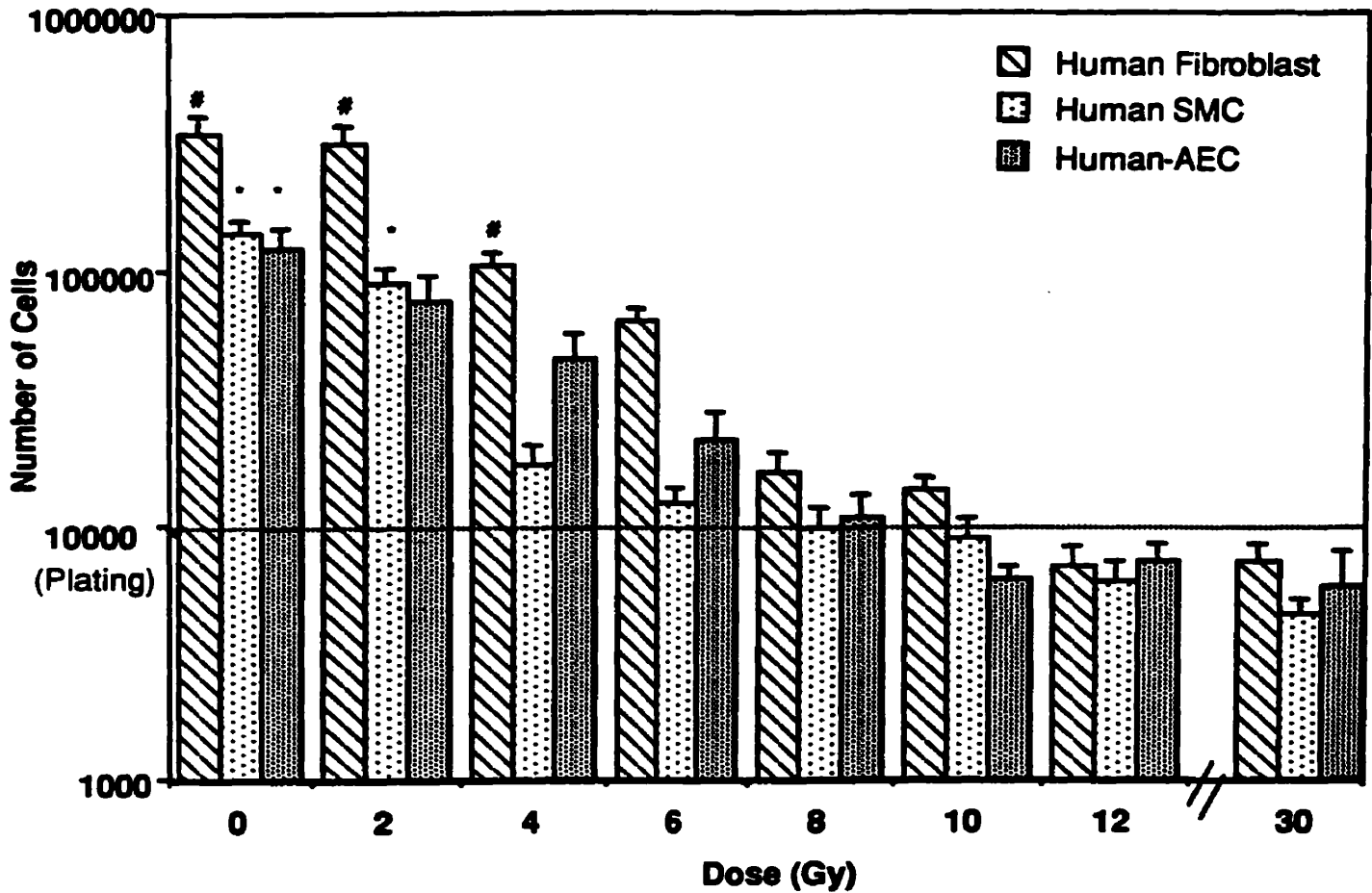


Table 1: Comparison of Radiation Response Parameters

Author (ref)	Conditions	Cells	D ₀	n	α	β	SF2	D bar
Burnet et al. (27)	plateau, ip feeder	H FIB.	1.32	-	0.748	0.0068	0.22	1.31
			1.46	-	0.648	0.0262	0.25	1.40
			1.48	-	0.625	0.0347	0.25	1.40
			1.09	-	0.898	0.0204	0.15	1.06
Badic et al. (28)	plateau, dp feeder	H FIB.	-	-	0.24	0.03	0.55	2.72
			-	-	0.28	0.02	0.52	2.61
			-	-	0.45	0.01	0.39	2.05
Russel et al. (29)	plateau, ip	H FIB	-	-	-	-	0.25 (0.031-0.723)	-
Hei et al. (30)	exp, no feeder	HUVEC	1.65	2.20	0.39 ± 0.06	0.011 ± 0.005	-	-
Marchese et al. (31)	plateau, dp, no feeder	HUVEC	-	-	0.48 - 0.54	0.00024 - 0.00029	-	-
Verheij et al. (32)	exp, no feeder	HUVEC	1.35	-	0.260 ± 0.03	0.050 ± 0.004	-	-
This Study	plateau, dp, feeder	H FIB.	2.13 ± 0.15 (CI 1.76 - 2.50)	2.20 ± 0.53 (CI 0.9 - 3.49)	0.232 ± 0.040 ^a (CI 0.137 - 0.327)	0.0146 ± 0.004 (CI 0.0062 - 0.030)	0.55 ± 0.14 ^a	3.25 ± 0.31 ^a
H SMC		1.68 ± 0.23 (CI 1.12 - 2.24)	0.95 ± 0.24 (CI 0.42 - 2.2)	0.615 ± 0.122 ^a (CI 0.318 - 0.912)	-0.0014 ± 0.015 (CI -0.0388 - 0.030)	0.30 ± 0.03 ^a	1.91 ± 0.10 ^a	
H AEC		1.43 ± 0.09 (CI 1.20 - 1.66)	5.90 ± 2.70 (CI 1.27 - 5.51)	0.136 ± 0.035 ^a (CI 0.050 - 0.222)	0.0430 ± 0.0060 (CI 0.0179 - 0.0523)	0.78 ± 0.08 ^a	3.51 ± 0.31 ^a	
P FIB.		1.91 ± 0.29 (CI 1.91 - 2.62)	3.8 ± 1.10 (CI 2.3 - 7.1)	0.228 ± 0.073 (CI 0.051 - 0.405)	0.0178 ± 0.0076 (CI - 0.0008 - 0.0364)	0.71 ± 0.08	3.36 ± 0.22	
P SMC		1.42 ± 0.14 (CI 1.10 - 1.76)	5.20 ± 3.63 (CI <1 - 14.08)	0.197 ± 0.117 (CI -0.089 - 0.483)	0.0316 ± 0.0110 (CI 0.0047 - 0.0585)	0.56 ± 0.12	2.98 ± 0.38	
P AEC		1.61 ± 0.32 (CI 0.82 - 2.39)	1.24 ± 0.97 (CI <1 - 3.61)	0.577 ± 0.137 (CI 0.242 - 0.912)	0.0003 ± 0.0190 (CI - 0.0462 - 0.0467)	0.46 ± 0.12	2.22 ± 0.30	

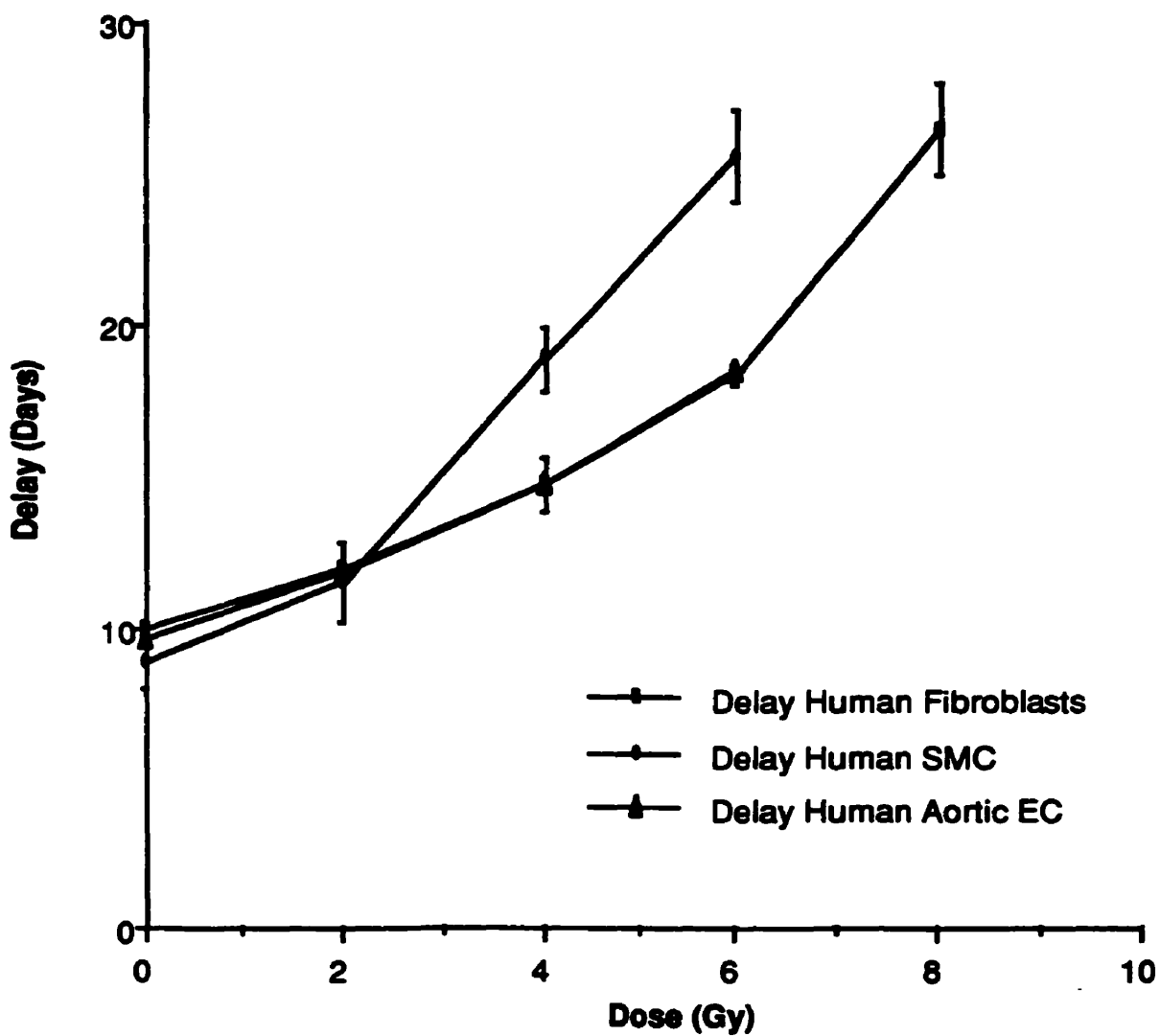
H Fib: Human fibroblasts, HUVEC: Human umbilical vein endothelial cells, H SMC: Human smooth muscle cells, HAEC: Human aortic endothelial cells, P: Pig, exp: Exponentially growing, dp: Delayed plating, ip: Immediate plating. * p<0.005, ^ap<0.0005, ^bp<0.0001.

Figure 3: Early Effects of Radiation on Cell growth



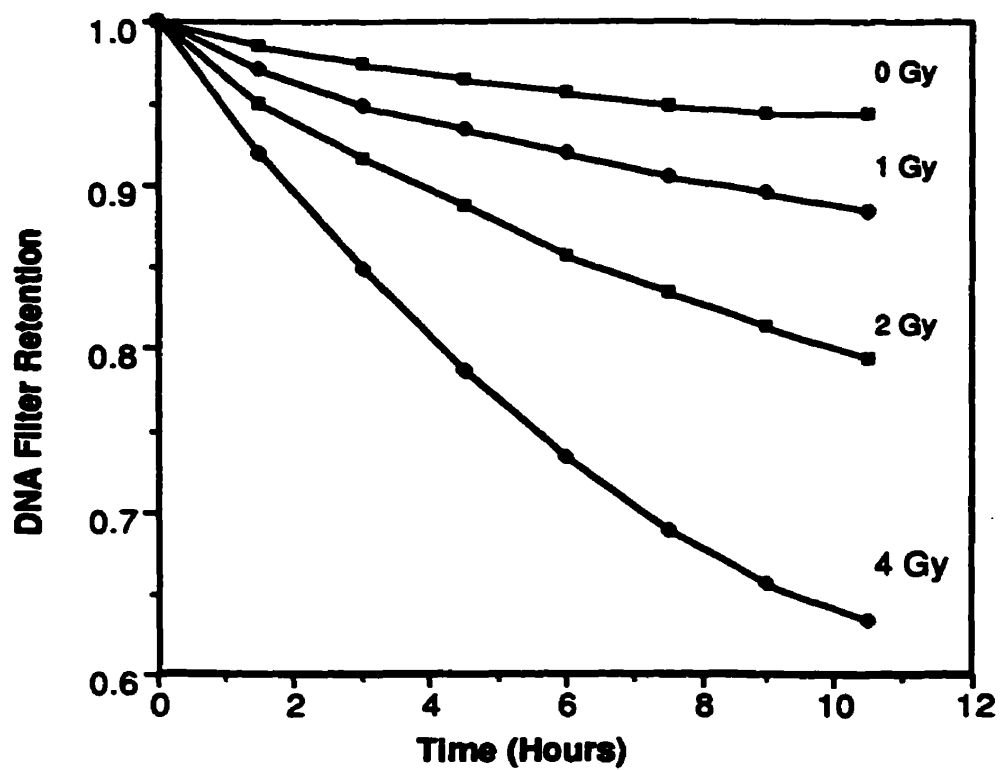
Legend: Growth arrest effect of radiation on human cell populations. At the time of confluence of unirradiated cell (about 10 days), the total number of cells which have been irradiated with doses above 4 Gy is not different than at initial plating. * P < 0.01, # P < 0.001 vs initial plating.

Figure 4: Growth Delay of Human Cells after HDR Irradiation



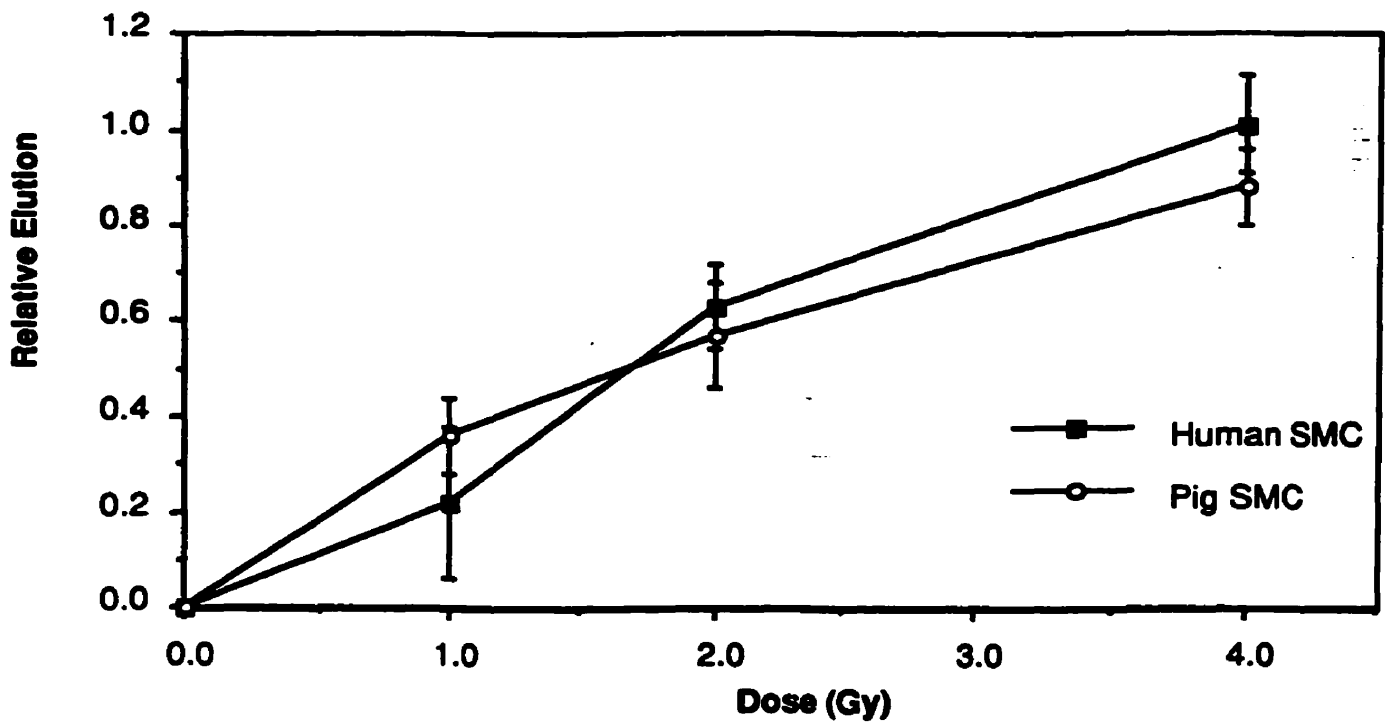
Legend: Growth delay after irradiation of human cells. Please note that unirradiated cells reached confluence in about 10 days. Irradiation lead to a growth delay which was a non-linear function of the dose.

Figure 5: Elution of Human Fibroblasts



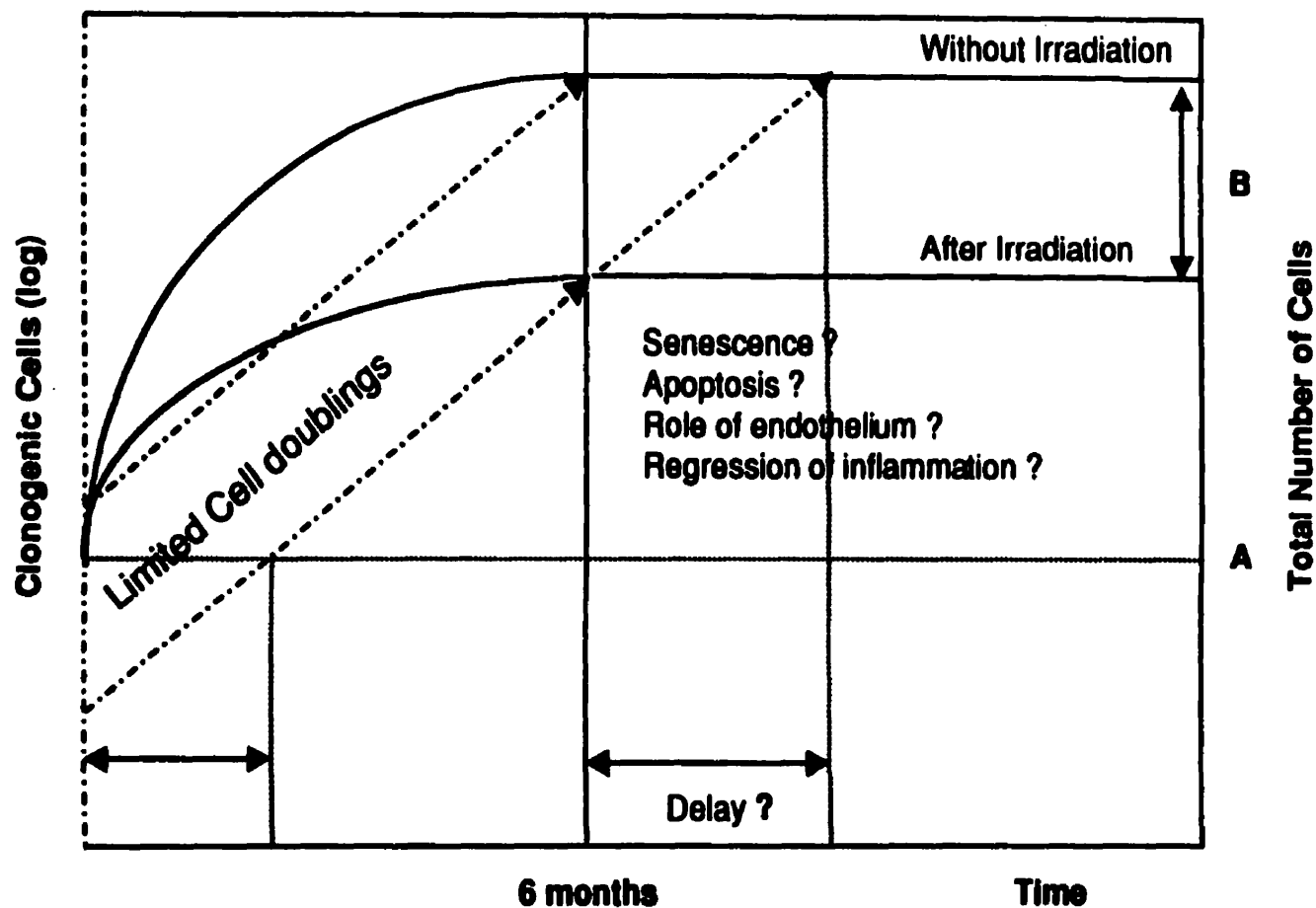
Legend: Representative experiment with alkaline filter elution of human fibroblasts. There was a dose-dependent decrease in filter retention activity up to 4 Gy.

Figure 6: Comparison between Relative Elution of Human and Pig SMC



Legend: Graph showing similar relative elution between human smooth muscle cells (SMC) and pig SMC.

Figure 7: Hypothetical Effects of Radiation for Restenosis Prevention



A: No change in absolute number of cells at early time

B: Lower total number of cells after irradiation

Legend: Hypothetical pathways of growth and restenosis formation without and after irradiation. Restenosis is formed after a number- and time-limited cell proliferation and is usually completed during the first 6 months after the procedure. After irradiation, surviving clonogenic cells may proliferate for a limited number of times before resuming a quiescent state.

endothelial cells (Fig 3). The same effect has been noted after irradiation of pig cells (data not shown). By extending the period of observation to 4 weeks, we observed definite recovery and replication in flasks with cells irradiated up to 8 Gy. However, confluence was never obtained above 8 Gy in human cell lines and 10 Gy in pig cells after 4 weeks. As shown in Fig 4, there was a non-linear dose dependent delay for cells to reach confluence after irradiation.

DNA single strand breaks

The fraction of unirradiated DNA retained on filter after 15 h elution was higher for human fibroblasts ($94 \pm 1 \%$) and for smooth muscle cells ($96 \pm 1 \%$) than for endothelial cells ($79 \pm 3 \%$) ($P < 0.01$). Elution at pH 12.1 has been shown to be proportional to the number of DNA single strand breaks (14). Because human endothelial cells required different culture medium, this technique gave us additional information on the radiation response of the different human cell lines when exposed to ionizing radiation in the same experimental conditions. As shown in Figure 5, there was a dose dependent increase in the elution rate with doses up to 4 Gy. Conversely, there was no significant difference between relative elution (RE) among human cell lines with RE at 4 Gy calculated at 0.85 ± 0.07 for fibroblasts, 1.01 ± 0.11 for SMC and 0.64 ± 0.07 for endothelial cells. RE appeared also similar between human and pig SMC (Fig 6).

Discussion

These results are part of an ongoing program devoted to characterizing the radiobiology of human vascular cells exposed to high and low dose-rate irradiation in the context of restenosis prevention. There are currently two approaches for endovascular radiation. One is based on high activity γ or β sources, such as ribbons, seeds, or liquid, to deliver a single dose locally through a catheter for a limited time exposure (1, 16-18). The other approach uses radioactive stents for prolonged exposure and continuous low dose-rate treatment (1).

Despite impressive short term results several adverse effects such as increased neointima formation, vascular fibrosis and aneurysm development have been described in animal models and subsequently in early clinical experience (8-12). Some investigators have also reported good long term results with endovascular brachytherapy of stented human femoral arteries (19). It is therefore important to better establish the radiation biology of the vascular system. Although the radiation response of the atherosclerotic vessel wall is probably highly complex and involves several autocrine and paracrine pathways, this study is the first to systematically evaluate the biophysical aspects of radiation response of the different components of normal vessel wall in human and pig cells, exposed to conventional high dose-rate γ irradiation.

It has been debated for a long time whether there is difference in radiosensitivity between vascular cell lines (20-26). Using clonogenic assays, these cells showed a broad range of radiosensitivities. The differences between human cell lines were largely attributable to the relative radiosensitivity of the SMC strain. Compared with other published values (Table 1), it appeared that the human fibroblast strain was quite radioresistant with a mean D_0 of 2.13 Gy and a D bar of 3.25 Gy. Several reports have already shown that human fibroblastic and endothelial radiosensitivities are broadly distributed (27-32). Overall, the pig cell lines had similar radiosensitivities than human cell lines. In the pig cells, however, the endothelial cells were relatively more radiosensitive than the two other strains. It is interesting to note that clonogenic assays with human endothelial cells required culture medium supplemented with specific growth-factors such as bFGF and VEGF, known to influence survival after irradiation (33, 34). With these culture conditions, the endothelial cell strain presented the largest n value. These results agree with those obtained by Hall et al. which showed little variations in survival curves between human endothelial cells and fibroblasts exposed to similar dose-rate (26). It is noteworthy that human relative elutions showed a similar trend than clonogenic results with slightly higher elution for human SMC compared with the other 2 cell lines.

Several authors using growth assays have suggested that endothelial cells are more radiosensitive than fibroblasts or SMC (20-24). We designed similar experiments using confluence as an end-point to evaluate the early (10 days) and late (4 weeks) effect of radiation on population growth. These experiments were conducted in parallel with clonogenic assays. At 10 days after irradiation, few surviving cells irradiated with doses ≥ 6 Gy have divided, as the total number of cells is not increased compared with the number of cells initially plated. Furthermore, the number of cells irradiated with doses between 6 and 30 Gy plateaued. Using human fibroblasts, Little et al. showed that doses up to 10 Gy provoked temporary growth arrest that may last for several days (35). Our results suggest that this effect may also operate with SMC and endothelial cells. Contrary to published results, we were unable to see significant differences in early growth between human cell lines (20, 21). Similarly, up to 4 weeks, there was a dose dependent delay for cells to reach confluence. This effect was also similar among the 3 cell lines. A similar effect has been noted by Brenner et al. where human aortic SMC were unable to completely fill a gap of 3 mm created in Petri Dish after single doses of 6 Gy (36).

Interpreting these in vitro results, it appears that impressive short term beneficial results of brachytherapy in animal models of restenosis, resulted from a combination of the killing effect of radiation and a temporary growth arrest effect. This may explain why the number of proliferating cells after balloon injury were lower early after irradiation compared with control unirradiated segments (37, 38). It may also explain why the total number of cells in different vascular layers was not different early (2 weeks) after irradiation (14 Gy-28 Gy) compared with unirradiated segments (38).

In contrast to tumor growth, restenosis is a proliferation- and time-limited phenomenon (Figure 7). In human restenotic vessels, proliferation rates between 1% and 20 % have been reported (39, 40). The total number of cells has been shown to increase for a limited period of time and the total cell doublings has been estimated between 3 and 10 (3, 41). In addition, clinical experience has shown that restenosis beyond 6 months after coronary intervention is rare (42).

Therefore, even if enough clonogenic cells have survived the initial radiation injury, other mechanisms such as apoptosis, inhibitory effect of endothelial cell lining or regression of the inflammatory response may prevent late restenosis by terminating clonogenic cell expansion. Conversely, delayed restenosis noticed at low doses might have been produced by delayed proliferation (37, 43).

Our results do not suggest very large difference in radiosensitivity between smooth muscle cells and endothelial cells. The issue of re-endothelialization is important to consider. With catheter-based radiotherapy the risk of altered re-endothelialization is probably limited as the endothelial cells lining the inner vessel wall is already largely damaged by the action of the balloon catheter (usually inflated between 6-8 atm). It has been shown that re-endothelialization after vessel injury proceeds by colonization of unaffected cells migrating from the 2 edges of the dilated site and from the ostia of collaterals (44). However, it remains possible that, for long irradiated segments, endothelial cells will not retain the possibility to completely repopulate the denuded region especially if some endothelial cells from the borders have also been irradiated. This could also lead to negative results as the normal endothelium is also known to prevent cell replication in the arterial wall (45). Recent evidence though, suggest that endothelial cells progenitors could be transported by blood flow to reach damaged vascular site and initiate re-endothelialization (46). Delayed or lack of endothelial recovery could be more problematic in case of radioactive stent implantation and longer exposure (37). Additional information is also clearly required on the cytokine and growth factor production and effects after endovascular radiation of the vascular system in the context of restenosis prevention. Moreover, atherosclerosis has also been suggested to influence radiation response by lack of p53 radioinduction and therefore, radiation response of atherosclerotic cells will need to be evaluated (47, 48).

In conclusion, we have shown that normal human and pig cells lines present similar in vitro response when exposed to conventional high dose-rate irradiation. Using clonogenic assays intrinsic radiosensitivities appeared broadly distributed without specific differences. Our results also illustrate the importance of the timing to evaluate the effects of radiation exposure. This

further stresses the need to perform long term follow-up in animal models before applying this technology to a large number of patients. In this regard, the pig model seems well suited to assess the long term effects of single large doses of ionizing radiation for prevention of restenosis.

Acknowledgements: We gratefully acknowledge Danny Chow and Paul Kauler for technical help and Louise Gilbert for help with the flow cytometry analysis. We also thank Jean Laurier for helpful discussion.

References

1. Bertrand OF, Mongrain R, Lehnert S, et al. Intravascular radiation therapy in atherosclerotic disease: promises and premises. *Eur Heart J* 1997;18:1385-95.
2. Fuster V, Falk E, Fallon JT, Badimon L, Chesebro J, Badimon JJ. The three processes leading to post PTCA restenosis: Dependence on the lesion substrate. *Thromb Haemost* 1995;74(1):552-9.
3. Liu MW, Roubin GS, King SB. Restenosis after coronary angioplasty. Potential biologic determinants and role of intimal hyperplasia. *Circulation* 1989;79(6):1374-1387.
4. Schwartz RS, Holmes DR, Topol EJ. The restenosis paradigm revisited: an alternative proposal for cellular mechanisms. *J Am Coll Cardiol* 1992;20:1284-93.
5. Shi Y, O'Brien JE, Fard A, Mannion J, Wang D, Zalewski A. Adventitial myofibroblasts contribute to neointimal formation in injured porcine coronary arteries. *Circulation* 1996;94:1655-64.
6. Scott NA, Cipolla GD, Ross CE, et al. Identification of a potential role for the adventitia in vascular lesion formation after balloon overstretch injury of porcine coronary arteries. *Circulation* 1996;93:2178-87.
7. Franklin SM, Faxon DP. Pharmacological prevention of restenosis after coronary angioplasty: review of randomized clinical trials. *Coronary Artery Dis* 1993;4:232-242.
8. Schwartz RS, Koval TM, Edwards WD. Effect of external beam irradiation on neointimal hyperplasia after experimental coronary artery injury. *J Am Coll Cardiol* 1992;19:1106-1113.
9. Weinberger J, Amols H, Ennis R, Schwartz A, Wiedermann J, Marboe C. Intracoronary irradiation: dose response for the prevention of restenosis in swine. *Int J Radiat Oncol Bio Phys* 1996;36(4):767-775.
10. Mazur W, Ali M, Khan M, et al. High dose rate intracoronary radiation for inhibition of neointimal formation in the stented and balloon-injured porcine models of restenosis: Angiographic, morphometric, and histopathologic analyses. *Int J Radiat Oncol Bio Phys* 1996;36(4):777-88.

11. Condado JA, Waksman R, Gurdziel O, et al. Long-term angiographic and clinical outcome after percutaneous transluminal coronary angioplasty and intracoronary radiation therapy in humans. *Circulation* 1997;96:727-32.
12. Waksman R, Crocker IR, Lumsden AB, MacDonald J, Kikeri D, Martin LG. Long-term results of endovascular radiation therapy for prevention of restenosis in the peripheral system (Abstract). *Circulation* 1996;94:I-300.
13. Fertil B, Dertinger H, Courdi A, Malaise EP. Mean inactivation dose: a useful concept for intercomparison of human cell survival curves. *Rad Res* 1984;99:73-84.
14. Alaoui M, Batist G, Lehnert S. Radiation-induced damage to DNA in drug- and radiation-resistant sublines of a human breast cancer cell line. *Radiat Res* 1992;129:37-42.
15. Kohn KW, Ewig RAG, Erickson C, Zwelling LA. Measurements of strand breaks and cross-links by alkaline elution. In: Friedberg EC, Hanawalt PC, ed. *DNA repair: A laboratory manual of research procedures*. New York: Marcel Dekker Inc., 1981: 319-401 (vol 1).
16. Teirstein P, Massulo V, Jani S, et al. Catheter-based radiotherapy to inhibit restenosis after coronary stenting. *N Engl J Med* 1997;336(24):1697-703.
17. Verin V, Urban P, Popowski Y, et al. Feasibility of intracoronary β -irradiation to reduce restenosis after balloon angioplasty. A clinical pilot study. *Circulation* 1997;95:1138-44.
18. Waksman R, Robinson KA, Croker IR, Gravanis MB, Cipolla GD, King SB. Endovascular low-dose irradiation inhibits neointima formation after coronary artery balloon injury in swine. *Circulation* 1995;91:1533-39.
19. Schopohl B, Liermann D, Pohlitz L, et al. ^{192}Ir endovascular brachytherapy for avoidance of intimal hyperplasia after percutaneous transluminal angioplasty and stent implantation in peripheral vessels: 6 years of experience. *Int J Radiat Oncol Bio Phys* 1996;36(4):835-40.
20. DeGowin RL, Lewis IJ, Mason RE, Borke MK, Hoak JC. Radiation-induced inhibition of human endothelial cells replicating in culture. *Radiat Res*.1976;68:244-250.
21. Johnson L, Longenecker JP, Fajardo LF. Differential radiation response of cultured endothelial cells and smooth myocytes. *Anal Quant Cytol* 1982;4:188.

22. Dimitrievich GS, Fischer-Dzoga K, Griem M. Radiosensitivity of vascular tissue. I. Differential radiosensitivity of capillaries: A quantitative in vivo study. *Radiat Res* 1984;99:511-35.
23. Fajardo LF, Berthrong M. Vascular lesions following radiation. *Path Ann* 1988;23:297-330.
24. Fischer-Dzoga K, Dimitrievich GS, Griem ML. Radiosensitivity of vascular tissue. II. Differential radiosensitivity of aortic cells in vitro. *Radiat Res* 1984;99:536-546.
25. Rubin DB, ed. *The radiation biology of the vascular endothelium*. Boca Raton, Boston, London, New York, Washington DC: CRC Press, 1998:254.
26. Hall E, Marchese M, Hei TK, Zaider M. Radiation response characteristics of human cells in Vitro. *Radiat Res* 1988;114:415-424.
27. Burnet NG, Wurm R, Peacock JH. Low-dose rate fibroblast radiosensitivity and the prediction of patient response to radiotherapy. *Int J Radiat Oncol Bio Phys* 1996;70(3):289-300.
28. Badie C, Aslbeih G, Reydellet I, Arlett C, Fertil B, Malaise EP. Dose-rate effects on the survival of irradiated hypersensitive and normal human fibroblasts. *Int J Radiat Biol* 1996;70:563-70.
29. Russel NS, Grummels A, Hart AAM, et al. Low predictive value of intrinsic fibroblast radiosensitivity for fibrosis development following radiotherapy for breast cancer. *Int J Rad Biol* 1998;73:661-670.
30. Hei TK, Marchese MJ, Hall EJ. Radiosensitivity and sublethal damage repair in human umbilical cord vein endothelial cells. *Int J Radiat Oncol Bio Phys* 1987;13:879-884.
31. Marchese MJ, Hei TK, Kushner S. Radiation repair in human endothelial cells. *Int J Radiat Oncol Bio Phys* 1987;13:1857-60.
32. Verheij M, Koomen GCM, van Mourik JA, Dewit L. Radiation reduces cyclooxygenase activity in cultured human endothelial cells at low doses. *Prostaglandins* 1994;48:351-366.
33. Fuks Z, Persaud RS, Alfieri A, et al. Basic fibroblast growth factor protects endothelial cells against radiation-induced programmed cell death in vitro and in vivo. *Cancer Res* 1994;54:2582-2590.

34. Katoh O, Tauchi H, Kawaishi K, Kimura A, Satow Y. Expression of the vascular endothelial growth factor (VEGF) receptor gene, KDR, in hematopoietic cells and inhibitory effect of VEGF on apoptotic cell death caused by ionizing radiation. *Cancer Res* 1995;55:5687-5692.
35. Little JB. Changing views of cellular radiosensitivity. *Rad Res* 1994;140:299-311.
36. Brenner D, Miller R, Hall E. The radiobiology of intravascular irradiation. *Int J Radiat Oncol Bio Phys* 1996;36(4):805-810.
37. Herlein C, Gollan C, Dönges K, et al. Low-dose radioactive endovascular stents prevent smooth muscle cell proliferation and neointimal hyperplasia in rabbits. *Circulation* 1995;92:1570-75.
38. Waksman R, Rodriguez JC, Robinson KA, et al. Effect of intravascular irradiation on cell proliferation, apoptosis, and vascular remodeling after balloon overstretch injury of porcine coronary arteries. *Circulation* 1997;96:1944-52.
39. O'Brien ER, Alpers CE, Stewart DK, et al. Proliferation in primary and restenotic coronary atherectomy tissue: implications for antiproliferative therapy. *Cir Res* 1993;73:223-31.
40. Pickering J, Weir L, Jakanowski J, Kearney M, Isner J. Proliferative activity in peripheral and coronary atherosclerotic plaque among patients undergoing percutaneous revascularization. *J Clin Invest* 1993;91:1469-80.
41. Schwartz RS, Chu A, Edwards WD, et al. A proliferation analysis of arterial neointimal hyperplasia: lessons for antiproliferative restenosis therapies. *In J Card* 1996;53:71-80.
42. Serruys PW, Luijten HE, Beatt KJ, et al. Incidence of restenosis after successful coronary angioplasty: a time related phenomenon: a quantitative angiographic follow-up study of 342 patients at 1, 2, 3 and 4 months. *Circulation* 1988;77:361-371.
43. Verin V, Popowski Y, Urban P, et al. Intra-arterial beta irradiation prevents neointimal hyperplasia in a hypercholesterolemic rabbit restenosis model. *Circulation* 1995;92:2284-90.
44. Van Belle E, Bauters C, Asahara T, Isner J. Endothelial regrowth after arterial injury: From vascular repair to therapeutics. *Cardiovasc Res* 1997;38:54-68.
45. Clowes AW, Reidy MA, Clowes MM. Kinetics of cellular proliferation after arterial injury: smooth muscle growth in the absence of endothelium. *Lab Invest* 1983;49:327-333.

46. Asahara T, Krasinski K, Chen D, et al. Circulating endothelial progenitor cells in peripheral blood incorporate into re-endothelialization after vascular injury (Abstract). *Circulation* 1997;96:I-725.
47. Hannan M, Khougeer F, Halees Z, Sanei AM, Khan BA. Increased radiosensitivity and radioresistant DNA synthesis in cultured fibroblasts from patients with coronary atherosclerosis. *Arterioscl Thromb Vasc Biol* 1994;14:1761-66.
48. Nasrin N, Mimish L, Manogaran P, et al. Cellular radiosensitivity, radioresistant DNA synthesis, and defect in radioinduction of p53 in fibroblasts from atherosclerosis patients. *Arterioscler Thromb Vasc Biol* 1997;17(5):947-53.

**CHAPTER VII: Dosimetric Considerations to Study *in Vitro* the Effects
of Low Energy β Emitters on Vascular Cells**

Abstract

Radiation therapy is being evaluated as a new treatment option for the prevention of restenosis after atherosclerotic vessel dilation. As part of a project to develop a radioactive stent, we have developed an experimental set-up to study the radiobiology of vascular cells exposed to low energetic β -isotopes. The purpose of this technical report is to compare the dosimetric aspects using the Medical Internal Radiation Dose (MIRD) calculations with dosimetric measurements using GR200F thermoluminescent dosimeters.

We carried on irradiation by mixing in petri dishes a chelated complex of ^{45}Ca -DTPA with a physiologic solution. Experiments were performed at high and low dose-rates and TLDs were fixed at the bottom and at the upper cover lid of the petri dishes during irradiation. Using MIRD, the estimated dose-rates were $1.64 \times 10^{-3} \times \text{activity } (\mu\text{Ci}/\text{cm}^3)$ and $2.73 \times 10^{-5} \times \text{activity } (\mu\text{Ci}/\text{cm}^3)$ for LDR (Gy/h) and HDR (Gy/min) respectively. Measurements at LDR showed for bottom TLDs, a dose-rate (Gy/h) of $1.7 \times 10^{-3} \times \text{activity} + 0.0002$ and for top TLDs, a dose-rate of $1.3 \times 10^{-3} \times \text{activity} - 0.0001$. Measurements at HDR showed for bottom TLDs, a dose-rate (Gy/min) of $3.06 \times 10^{-5} \times \text{activity } (\mu\text{Ci}/\text{cm}^3) + 0.0021$ and for top TLDs, a dose-rate of $4.61 \times 10^{-5} \times \text{activity } (\mu\text{Ci}/\text{cm}^3) - 0.0002$.

Human fibroblasts were exposed to ^{45}Ca -DTPA with large excess of free DTPA and liquid scintillation analysis of cell pellets confirmed that DTPA limited very effectively intracellular penetration of ^{45}Ca .

In conclusion, our results showed that bottom TLDs readings were closer to MIRD calculations than top readings at both HDR and LDR. It seems that doses administered to cell layers at the bottom of petri dishes would be better evaluated by the MIRD dose than half the MIRD dose as previously suggested.

Introduction

Radiation therapy is a new treatment tool in atherosclerotic cardiovascular diseases (1). Since the introduction of balloon angioplasty to relieve coronary obstructions, cardiologists have remained frustrated by a significant number of patients presenting with a recurrence of their symptoms in the 6 months following the procedure. This is usually caused by a restenosis formation at the previously dilated site. Restenosis is a complex phenomenon which results from thrombosis formation and organization, neointima formation secondary to cell proliferation and vessel shrinkage commonly referred as negative vessel remodeling. There is some evidence to suggest that this negative remodeling is also associated with fibroblast proliferation in the outer portion of the vessel which secondarily squeeze the vessel provoking reduction in the lumen dimensions. Therefore, radiation therapy holds the promises by killing proliferating cells to limit neointima formation and negative vessel remodeling.

There are currently two approaches to administer radiation therapy: The first uses catheter-based systems with high activity sources (ribbon, seeds, liquid) to deliver locally single doses at high dose-rate in a limited period of time. The other approach uses small endoprotheses called stents which scaffold the vessel lumen after dilatation and are rendered radioactive for continuous low-dose rate therapy. Both systems have shown impressive results after short-term follow-up in several animal models and have prompted the investigators to initiate early clinical experience (2, 3). However, some investigators have also noticed several side-effects such as fibrosis and vessel aneurysms and long term consequences of these effects are still unknown. So far, high energetic β isotopes such as $^{90}\text{Sr}/\text{Y}$, ^{188}Re , ^{90}Y or γ emitters such as ^{192}Ir have been used with catheter-based systems and ^{32}P has been ion-implanted on stent surface. Consequently, a large number of vascular cells included in the vessel segment receive a significant dose. It is therefore necessary to better evaluate the radiation biology of the vascular cells. As part of a program to design a radioactive stent with a low energy β emitter, we have designed a specific experimental set-up to expose vascular cells in culture at high and low dose-rates. The purpose of

this paper is to report the design of the experimental set-up and the results concerning the dosimetric aspects.

Material and Methods

Prototype

Petri dishes are placed up to nine at a time in appropriately shielded alcoves. The alcoves are built in Plexiglas with a thickness of 2 mm. This thickness has been calculated to stop the highest energy electrons from ^{45}Ca (E mean: 77 KeV, E max: 255 KeV) the penetration of which in water has been estimated around 400 μm by Monte-Carlo simulations. In addition to limit bremsstrahlung crosstalk between the petri-dishes, a lead sheet of 2 mm was inserted between the Plexiglas walls. This thickness stops 99.99% of the mean energy photons and about 85% of the maximum energy photons.

Radiation protocol

To ensure homogeneous dose distribution to the cells, we mixed the isotope with the culture medium. In order to limit isotope absorption into the cells, a ^{45}Ca -DTPA complex was developed by Draximage Inc. (Montreal, Canada). To further ensure that the complex will not cross the cell membrane, a large amount of free DTPA (2000%) was added in excess in the solution.

Cells

To evaluate the efficacy of the chelator, we used human dermal fibroblasts which were grown in Dulbecco's MEM (Gibco Inc.) supplemented with 1 % glutamine and gentamycin 0.1%. Cells were grown up to confluence and were incubated with the radioactive solution for 48 hrs. After exposure, cells were washed three times before liquid scintillation analysis.

Figure 1: Prototype of β -irradiation Chambers Used for Experiments

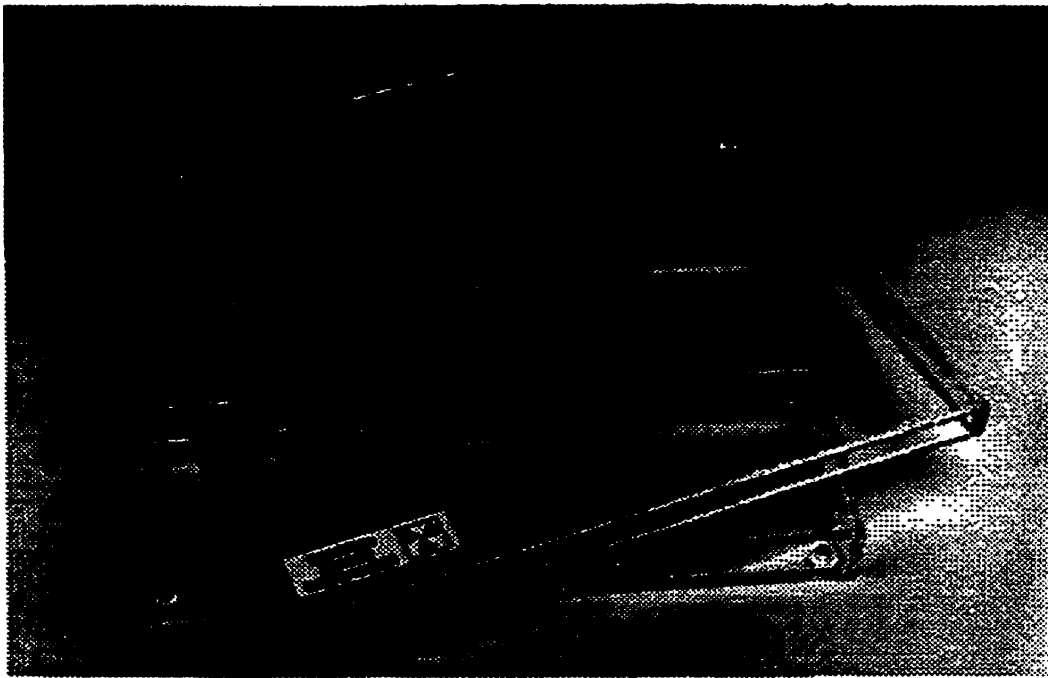
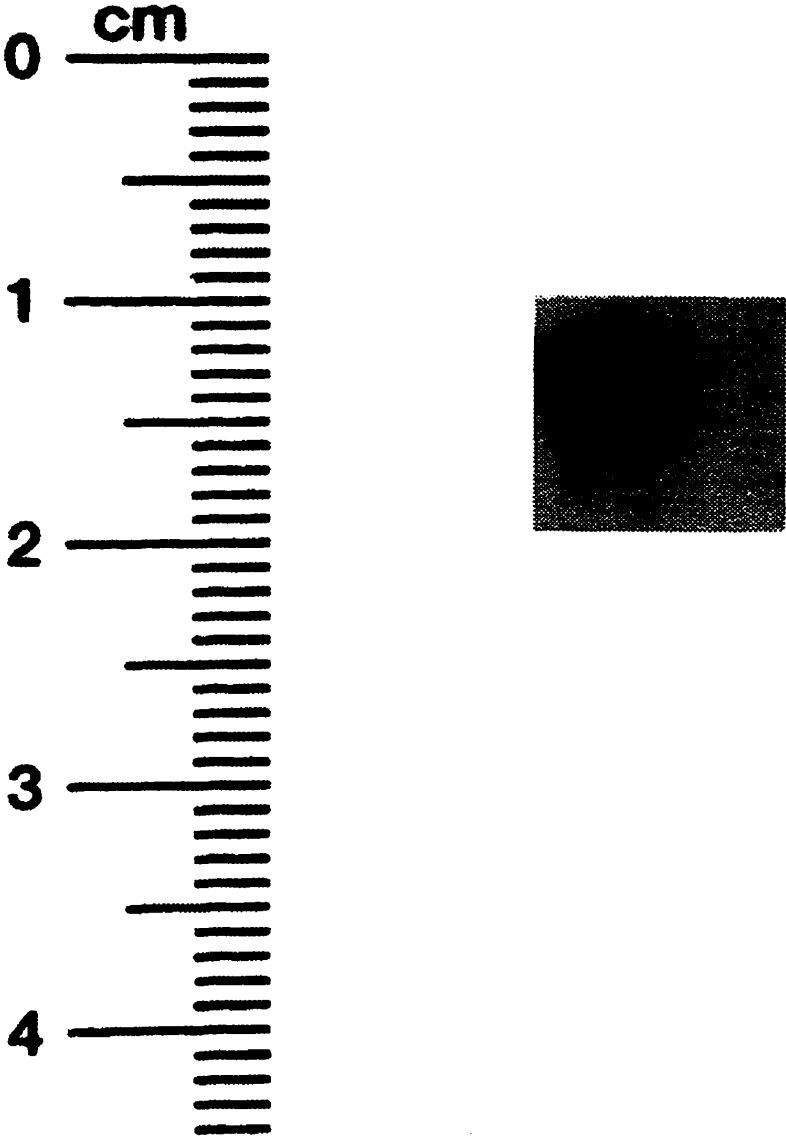


Figure 2: Example of a GR200F TLD Embedded in a Plastic Pouch



Dosimetry calculations

To calculate the doses received by the cell monolayers lying at the bottom of petri dish, we applied dosimetric calculations as well as measurements. The Medical Internal Radiation Dose (MIRD) was calculated as previously described (4). The mean absorbed dose was calculated according to the following formulae:

The instantaneous dose-rate is given by :

$$\dot{D} = C_0 e^{-\lambda t} \sum \delta_i \varepsilon_i \quad (1)$$

where C_0 is the initial specific activity in $\mu\text{Ci}\cdot\text{g}^{-1}$, δ_i is the equilibrium dose constant in $\text{g}\cdot\text{rad}\cdot\mu\text{Ci}^{-1}\cdot\text{s}^{-1}$ for the i^{th} radiation emitted. ε_i is the fraction of radiation i which is absorbed (= 1 for non penetrating β particles). λ is the decay constant for ^{45}Ca ($1.78 \times 10^{-4} \text{ h}^{-1}$) and t_0 is the duration of cell exposure in hours. For an initial ^{45}Ca activity, and $i = 1$ (only one beta emission per disintegration), the average dose-rate was calculated as following:

$$\bar{D} = C_0 \delta \int_0^{t_0} e^{-\lambda t} dt / (t_0) \quad (2)$$

Upon integration, we obtained for the mean dose:

$$\bar{D} = \frac{C_0 \delta}{\lambda} (1 - e^{-\lambda t_0}) \quad (3)$$

In the previous relation, δ is the equilibrium dose constant (which corresponds to the dose rate in an infinitely large homogeneous mass containing a uniformly distributed radioisotope) (5). This constant can be calculated with $\delta = k_1 k_2 E_{av}$, with k_1 being a constant equal to $1.6 \times 10^{-8} \text{ g rad/MeV/decay}$ and k_2 being equal to $3.7 \times 10^4 \text{ decays}\cdot\text{s}^{-1}\cdot\mu\text{Ci}^{-1}$ and E_{av} is the average energy of

the radioisotope (in the case of ^{45}Ca , $E_{av}=0.077$ MeV) (4). We then find that $\delta = 4.558 \times 10^{-5}$ $\text{g}\cdot\text{rad}\cdot\mu\text{Ci}^{-1}\cdot\text{s}^{-1}$. Since for ^{45}Ca , $\lambda=1.78 \times 10^{-4}$ h^{-1} , and that the duration of the experiments lasted between 30 minutes and 13 hours, the decay factors were respectively equal to 0.9999 and 0.9977, and we can consider these factors as being constant. Consequently, the dose rate was calculated with :

$$\dot{D} = C_0 4.558 \times 10^{-5} \text{ g} \cdot \text{rad} \cdot \mu\text{Ci}^{-1} \cdot \text{s}^{-1} \quad (4)$$

and if the activity is given in $\mu\text{Ci}/\text{cm}^3$ (assuming a density of 1 g/cm^3), we have :

$$\dot{D} = C_0 (\mu\text{Ci}/\text{cm}^3) \cdot 0.00164 \frac{\text{Gy}/\text{h}}{\mu\text{Ci}/\text{cm}^3} \quad (5)$$

Dosimetry measurements

Dose measurements were performed by fixing a GR200F thermoluminescent dosimeter (Figure 2) at the bottom and on the cover lid of petri dishes. These TLDs, manufactured in China, have been characterized by Atomic Energy of Canada Limited and are made of 5 mg cm^{-2} layer of LiF:Mg, Cu, P powder on a 1 cm^2 Kapton base. The dose readings are linear up to 10 Gy (6). The TLDS were read on a Teledyne 7300B extremity dosimeter reader by planchet heating at AECL facilities (Chalk River, Ontario). To prevent inadvertent exposure by liquid drops containing ^{45}Ca , each TLD was inserted in a very thin sealed plastic pouch and the attenuation by the thin layer of plastic was measured to be about 40%.

Results

Dose-rate calculations

For the LDR experiment, the activities per volume used for the calibration were 23.2 μCi , 46.4 μCi , 92.8 μCi , 185.6 μCi . The corresponding estimated dose rate using equation 5 was \dot{D} (Gy/h) = 0.00164 x Activity ($\mu\text{Ci/cm}^3$). For the HDR, we used the following activities 0.63 mCi, 1.25 mCi, 1.88 mCi, 2.50 mCi, 3.13 mCi for which the corresponding estimated dose rate was \dot{D} (Gy/min) = 2.7333×10^{-5} x activity ($\mu\text{Ci/cm}^3$).

Dose-rate measurements

Different experimental conditions for high and low dose-rate exposure were applied. For low dose-rate exposure, 6 cm diameter petri dishes were chosen. Initial activity of $^{45}\text{Ca-DTPA}$ was verified by liquid scintillation counting. Four different activities of $^{45}\text{Ca-DTPA}$ were mixed with phosphate buffered saline to maintain a total volume of 20 ml/petri dish. The petri dishes remained in the alcove chambers at room temperature during 13 hours. At that time, the radioactive solution was quickly removed and the TLDs placed at the bottom of the petri dishes rinsed 3 times. The TLDs were carefully removed from the plastic pouchs to avoid any contamination, placed in an envelope and shipped to AECL for readings. It should be noted that we used a courier delivery service which guaranteed that the TLDs would not be exposed to any radioactive sources during transportation (CANPAR).

The results of the measurements are shown in Figure 3. There was a linear increase in the dose with the activity for bottom and top TLDs. Using a least mean square fit to our experimental points, we obtained the following equations : For bottom TLDs, $\dot{D} = 1.7 \times 10^{-3} \times A + 0.0002$ where \dot{D} is dose-rate (Gy/h) and A is activity in $\mu\text{Ci/cm}^3$. The correlation coefficient for this

Figure 3: Low Dose-Rate Calibration

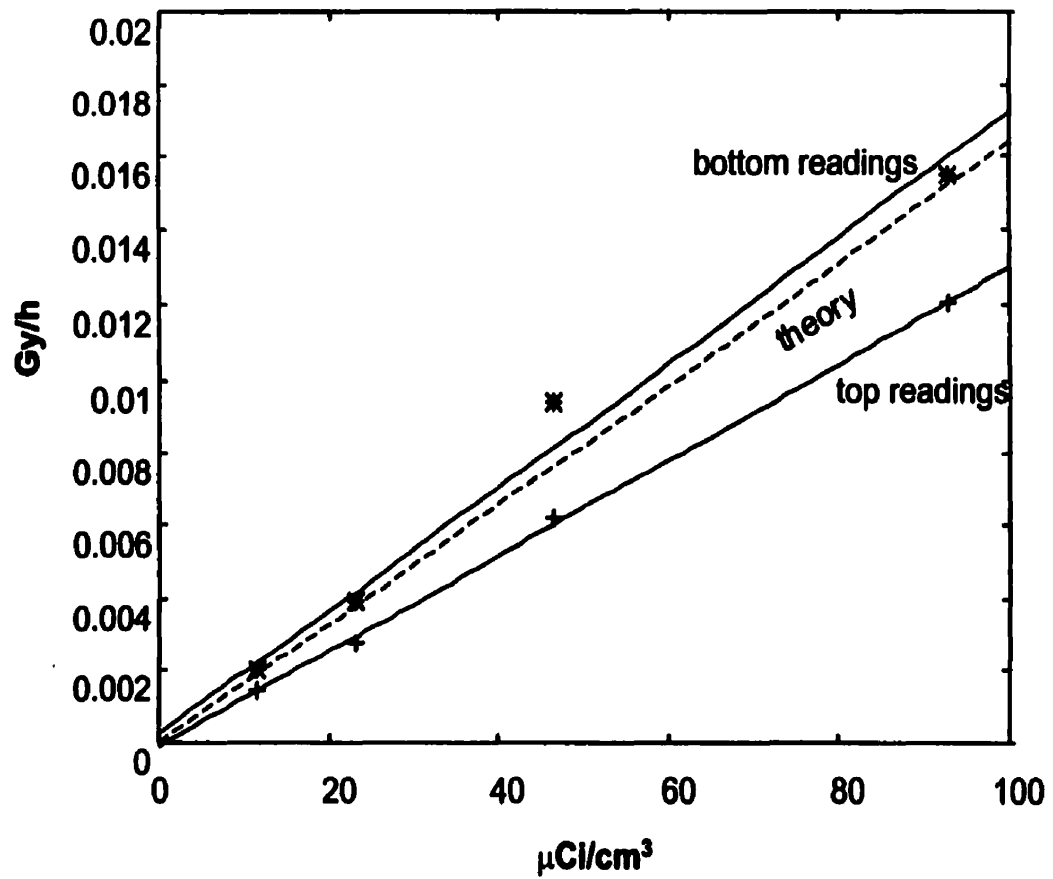
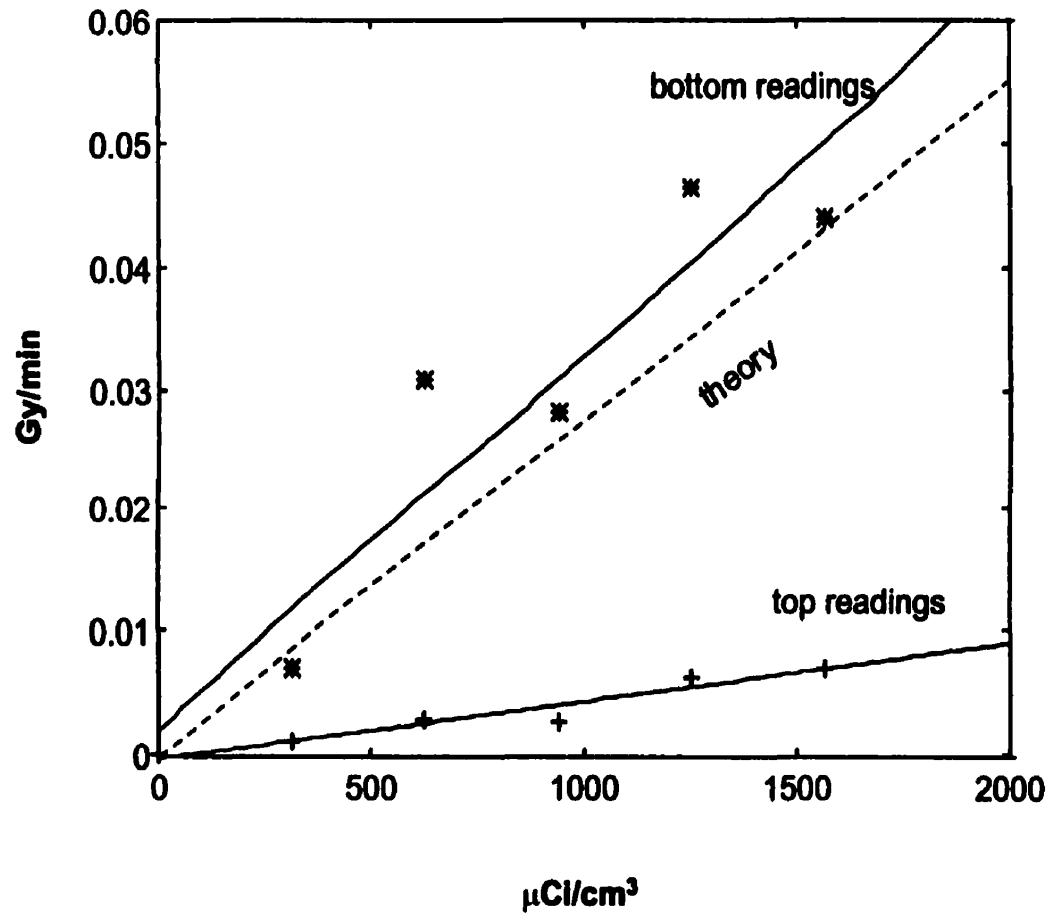


Figure 4: High Dose-Rate Calibration



relationship (r) was 0.99. For top TLDs, $\dot{D} = 1.3 \times 10^{-3} \times A - 0.0001$. The correlation coefficient was 0.99. The ratio of dose read by bottom TLDs to the dose read by top TLDs was 1.4.

For the high dose-rate exposure (Figure 4), we used 3 cm diameter petri dishes to achieve higher specific activities. The total volume was 2 cc. For these experiments, a total of 5 different activities were tested. The exposure lasted for 20 min before removal and washing of the TLDs. Similarly, the TLDs were removed from plastic pouches and sent to AECL for readings using the same mail delivery provider. Using a least mean square fit to our experimental points, we obtained the following equations. For bottom TLDs, \dot{D} (Gy/min) = $3.06 \times 10^{-5} \times A + 0.0021$. The correlation coefficient was 0.94. For top TLDs, \dot{D} (Gy/min) = $4.61 \times 10^{-5} \times A - 0.0002$. The correlation coefficient was 0.96.

Effects of chelation

To limit ^{45}Ca intracellular absorption, we used a ^{45}Ca -DTPA complex with large excess (> 2000%) of free DTPA. Cells remained incubated with the radioactive medium for 48 hrs. After 3 successive washes with phosphate buffer saline (PBS), cells were centrifuged for 5 minutes at 2000 rpm and the medium was carefully suctioned off and cell pellet placed in a scintillation vial. By liquid scintillation counting, the cell residual activity was measured to be 0.0056 % of the initial activity placed in the petri dish (5 mCi).

Discussion

In order to study the radiation biology of vascular cells in relation with restenosis prevention, we have designed an experimental set-up specifically adapted for high and low dose-rate exposure using low energy β -emitters such as ^{45}Ca . ^{45}Ca was chelated with large amount of DTPA which has been shown to limit intracellular isotope penetration. DTPA does not modify radiation response of exposed cells (7). Using this complex, the residual activity on cell

membranes or inside the cells was kept extremely low. This finding is important as ^{45}Ca -DTPA will be slowly released from a polymer matrix covering the stent struts.

Radioactive stents which delivered the dose at very low dose-rates used β -emitters such as ^{32}P or ^{48}V a (8) (9). Short term efficacy of ^{32}P coated stent has been demonstrated at very low and high activities, but produced negative results at intermediate activity (10). Investigators have also studied in vitro response of vascular cells exposed to a radioactive (^{32}P) stent wire but no dose was reported (11). This suggests that precise dosimetry to evaluate the radiation biology of vascular cells is mandatory. Some bio-assays have been developed to study the in vitro radiation responses of several cell types exposed to β emitters but there is no previous report which measured the administered doses of dissolved β emitters into the culture medium (12, 13). We were interested to develop an experimental set-up which allowed precise dosimetry. First, the GR200 F TLDs provided by AECL allowed us to verify the exactness of dose assumptions based on algorithms extrapolated from clinical experience (MIRD approach). Second, we investigated the possibility to fix a TLD at the upper cover lid in order to monitor the dose during cell experiments.

For low dose-rates exposure, there was an excellent correlation between the calculated doses and the doses read by the TLDs at the bottom of the petri dishes. There was also a good relationship with the readings of the TLDs placed at the top compared with theoretical dose, although the doses read by these TLDs were 40% lower than the doses read by the bottom placed TLDs. The situation was more complex for high dose-rate exposure. We also noticed a linear relationship between the activities and the TLDs dose readings. However, the ratio between doses read at the bottom versus doses read at the top was higher than 2.5. The reasons for these discrepancies remain unclear. It is noteworthy that data associated with bottom readings were much scattered than those associated with top readings. This may suggest that the TLDs were still being irradiated during rapid washings and removal from the plastic pouches (about 2 minutes). We initially speculated that by limiting the gap between the medium surface and the upper cover

lid TLDs, we would nearly create a mirror situation of what would be read by the TLD at the bottom of the petri dish. It appears that the doses read by the bottom TLDs are closer to predicted doses than doses read by top TLDs. It remains possible that the closed atmosphere once the cover lid is placed on the petri dish created a confined environment with condensation that altered the readings by the TLDs attached at the upper cover lid. We also observed that small air bubbles were present in some TLDs pouches and this may also have affected the TLDs exposure, especially for high dose-rate experiments. Indeed, total exposure was limited to 20 minutes compared with 13 hrs for low dose-rate exposures. It should also be noted that doses calculated according to MIRD slightly underestimated the measured doses by bottom TLDs in both low dose-rate and high dose-rate experiments. This most likely would indicate that bottom TLDs were irradiated from more than one side (180°). As this situation would be similar with cells lying at the bottom of petri dishes, doses calculated by MIRD should not be divided by half.

In summary, we designed an experimental set-up which allowed homogeneous cell exposure to low energy β -emitters. For low dose-rate exposure of cells lying at the bottom of the petri dish, doses might be extrapolated from the initial activity using either calculations or verified by special TLDs placed at the upper cover lid. This last solution implies, however, significant corrections. For high dose-rate exposure lasting a few minutes, it is probably simpler and better to calculate delivered doses using MIRD. Our experimental results suggest, however, that doses should not be divided by 2.

References

1. Bertrand OF, Mongrain R, Lehnert S, et al. Intravascular radiation therapy in atherosclerotic disease: promises and premises. *Eur Heart J* 1997;18:1385-95.
2. Schopohl B, Liermann D, Pohlit L, et al. ^{192}Ir endovascular brachytherapy for avoidance of intimal hyperplasia after percutaneous transluminal angioplasty and stent implantation in peripheral vessels: 6 years of experience. *Int J Radiat Oncol Bio Phys* 1996;36:835-40.
3. Teirstein P, Massulo V, Jani S, et al. Catheter-based radiotherapy to inhibit restenosis after coronary stenting. *N Engl J Med* 1997;336:1697-703.
4. Berger MJ. Distribution of absorbed dose around point sources of electrons and beta particles in water and other media. *J Nucl Med* 1971;5-23.
5. Cember H. Introduction to health physics. 2d edition ed. New York: Pergamon Press, 1983.
6. Yuen PS, Richler WF, Aikens MS. Study of GR200F LiF:Mg,Cu,P detectors for extremity dosimetry. *Rad Prot Dosimetry* 1993;47:341-6.
7. Jostes RF, Hui TE, James AC. In vitro exposure of mammalian cells to radon: dosimetric considerations. *Rad Res* 1991;127:211-9.
8. Hehrlein C, Stintz M, Kinscherf R, et al. Pure β -particle-emitting stents inhibits neointima formation in rabbits. *Circulation* 1996;93:641-5.
9. Li AN, Eigler NL, Litvak F, Whiting JS. Characterization of a positron emitting V48 nitinol stent for intracoronary brachytherapy. *Med Phys* 1998;25:20-8.
10. Carter A, Laird J, Bailey L, et al. Effects of endovascular radiation from a β -particle - emitting stent in a porcine coronary restenosis model. A dose-response study. *Circulation* 1996;94:2364-68.
11. Fischell TA, Khanna BK, Fischell DR, et al. Low-dose β -particle emission from "stent" wire results in complete, localized inhibition of smooth muscle cell proliferation. *Circulation* 1994;90:2956-63.

12. Speidel MT, Holmquist B, Kassis AI, et al. Morphological, biochemical, and molecular changes in endothelial cells after alpha-particle irradiation. *Radiat Res* 1993;136:373-81.
13. Häfeli UO, Sweeney SM, Beresford BA, et al. Effective targeting of magnetic radioactive ⁹⁰Y-microspheres to tumor cells by an externally applied magnetic field. Preliminary in vitro and in vivo results. *Nucl Med Biol* 1995;22:147-55.

**CHAPTER VIII: Effects of Low Dose-Rate β -Irradiation on Smooth
Muscle Cells: Comparison with High Dose-Rate Exposure**

Abstract

Radiation therapy is undergoing extensive pre-clinical and clinical testing as a new tool to reduce restenosis after vessel injury. Catheter-based radiotherapy delivers single doses at high dose-rate whereas radioactive stents use a continuous low-dose rate approach. Single doses in excess of 10 Gy have clearly shown a reduction in neointima formation and negative vessel remodeling in several animal models. To date, however, no definite dose threshold has been identified after radioactive stent implantation. Since dose-rate is an important parameter modulating the overall biological response to ionizing radiation, we have compared the in vitro response of pig aortic smooth muscle cells at conventional high dose-rate (1.5 Gy/min) and at low dose-rate (0.675 Gy/h). Smooth muscle cells showed significant repair of sub-lethal DNA damage and about twice the dose was necessary at low dose-rate to produce the same effect as that seen at high dose-rate. This has important implications for the design of a radioactive stent.

Introduction

Ionizing radiation has recently been investigated as a means of prevention to reduce restenosis incidence after vessel injury (1). External and endovascular routes have been proposed to deliver the dose to the target site. Catheter-based radiotherapy deliver single doses at high dose-rate (HDR) whereas radioactive stents use a continuous low dose-rate (LDR) approach. Single doses in excess of 10 Gy have been shown effective to reduce neointima formation and negative vessel remodeling in numerous animal models (1). Using radioactive stents, investigators have also shown short term benefit, although a dose threshold has not been clearly identified (2).

We have initiated an ongoing program to better define the radiobiology of vascular cells exposed to high and low dose-rate. We have already reported that human and pig vascular cells exhibit a similar radiation response at high dose-rate exposure (3). In this study, we have compared the in vitro response of pig smooth muscle cells to conventional high dose-rate irradiation with the response to continuous low dose-rate which could result from exposure to a radioactive stent.

Materials and Methods

Cell lines

Pig aortic smooth muscle cells were isolated from adult slaughtered animals using explant technique. Immunostaining with α -actin was used to characterize the cells as SMC. Cells between passage 3 to 10 were used for experiments. Cells were grown as monolayers either in plastic flasks (HDR) (T25, Nunc Corporation) or 60 mm petri dishes (LDR) at 37° C with humidified environment containing 5% CO₂. Culture medium consisted of Dulbecco's Minimal Essential Medium (Gibco) supplemented with 20% fetal bovine serum, L-Glutamine 1% and gentamycin (0.6 μ g/ml). Confluent cells were used for all experiments and low proliferative activity of cells in plateau phase was verified by flow cytometry.

Radiation Procedure for HDR

Cells were irradiated 48 hrs post confluence using a ^{60}Co source (Theratron, Atomic Energy of Canada Ltd.) at a dose rate of about 1.5 Gy/min, at room temperature. Immediately after irradiation, cells were returned to the incubator overnight to allow full repair of potentially lethal damage. After trypsinization, cells were plated in T₂₅ flasks at increasing densities (200 cells at 0 Gy to 8000 cells at 12 Gy) with a feeder of heavily irradiated cells (1×10^4 cells irradiated at 30 Gy). For each experiment, cells were plated in triplicate flasks and each experiment was reproduced a minimum of three times.

Radiation Procedure for LDR

To ensure homogeneous dose distribution, we mixed the β -isotope with the culture medium and, to limit isotope absorption into the cells, a chelated complex of ^{45}Ca -DTPA developed by Draximage Inc. was used. To calculate the doses received by the cell monolayers attached to the bottom of the petri dish, we used the Medical Internal Radiation Dose (MIRD) method. We have previously validated this technique using special TLD dosimeters (4, 5). At the end of irradiation exposure, radioactive medium was collected and cells were washed three times using PBS. After trypsinization, cells were plated in T25 flasks at increasing densities (2000 cells at 0 Gy to 40,000 cells at 30 Gy) without feeder. For this series, two separate experiments were conducted and cells were incubated in 4 different flasks.

Survival

The culture medium was changed 2-3 times and cells were fixed with formaldehyde and stained with crystal violet after 10-14 days. Colonies containing more than 50 cells were counted. The surviving fractions were calculated as the ratio of plating efficiencies of irradiated to unirradiated control cells. Clonogenic survivals were analyzed according to the single hit multitarget model and the D_0 dose (dose to reduce survival by $1/e$ on the exponential part of the

curve) and the extrapolation number, n were calculated. Survival curves were fitted to the linear-quadratic model where surviving fractions = $\exp(-\alpha D - \beta D^2)$ with D = dose. The parameters α and β were determined by non-linear regression analysis. The mean inactivation dose was calculated using the technique proposed by Fertil et al (6). The dose-rate effect was calculated as the ratio of the dose to produce 1% survival at LDR over the dose to produce 1 % survival at HDR and $D_0 \text{ LDR} / D_0 \text{ HDR}$.

Growth delay

Cell monolayers were trypsinized a minimum of 12 hrs after HDR or immediately after LDR irradiation and 1×10^4 cells from each dose were plated into 12 well-flasks without feeder. We evaluated the time to obtain confluence in each well. Cells were considered confluent when > 95% of the cells covered the well surface when examined with a contrast phase inverted microscope at a magnification of x40 .

Data analysis

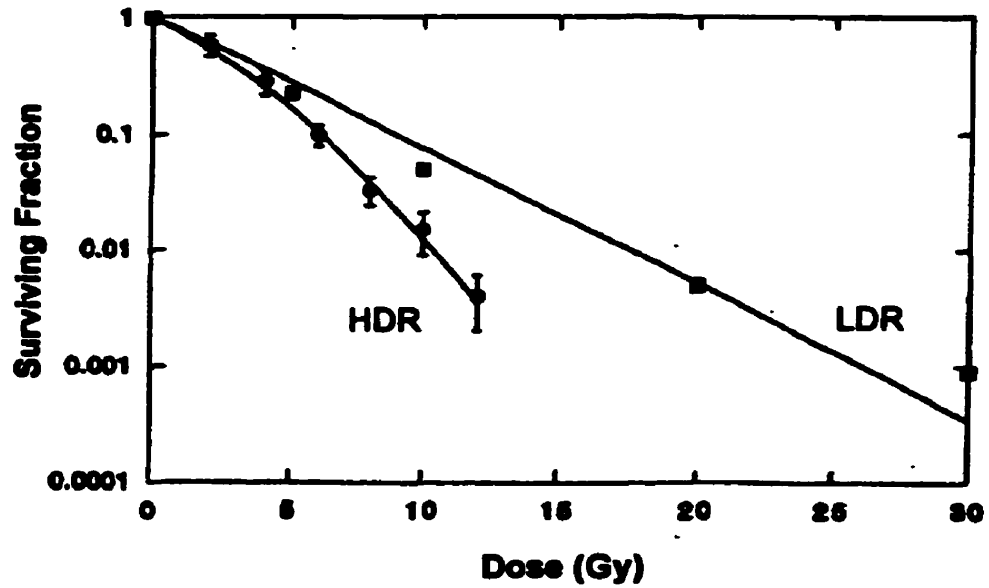
Values are presented as mean \pm SEM. When necessary, data were analyzed by Student's t test and a p value < 0.05 was considered significant.

Results

Clonogenic survival

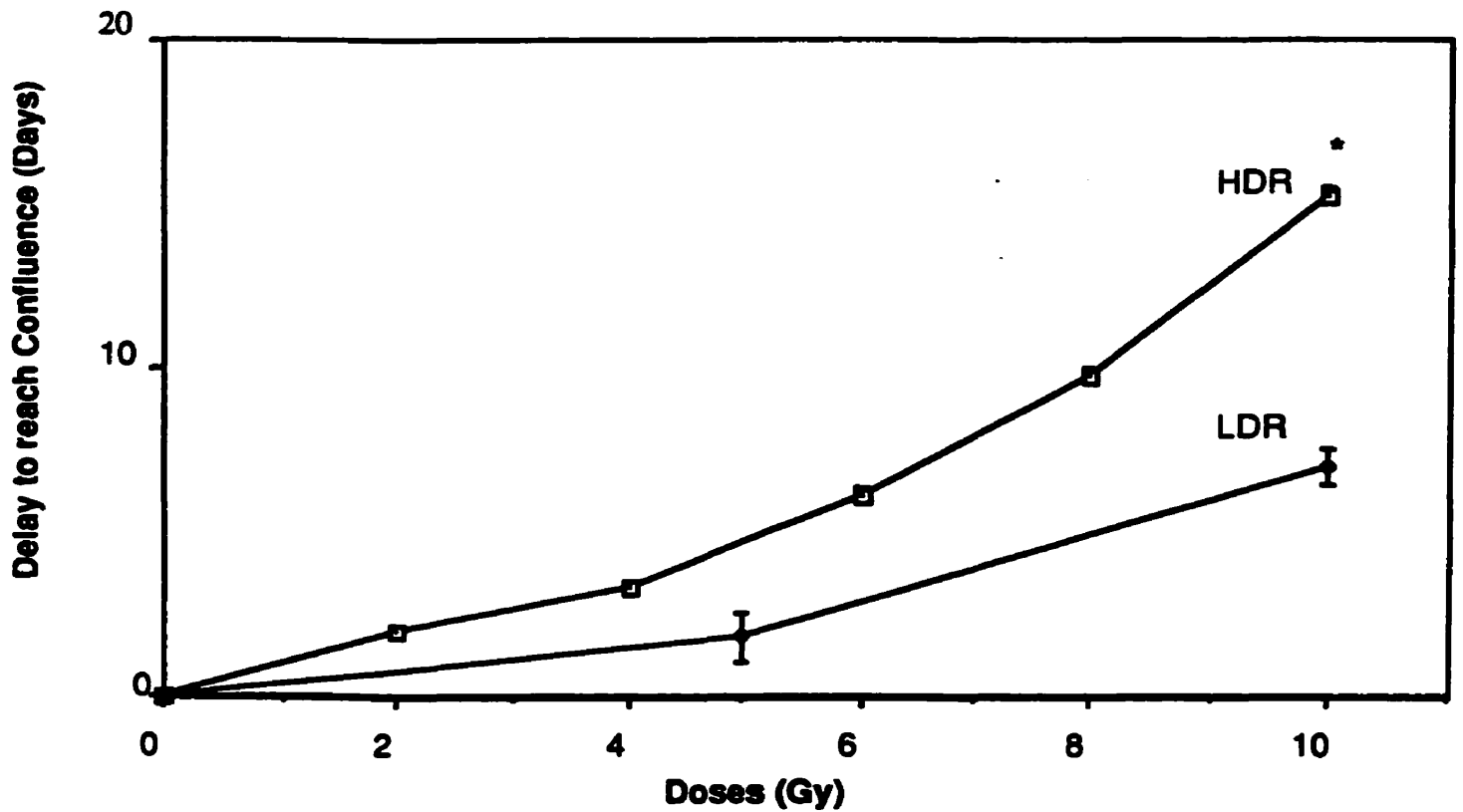
At HDR, SMC exhibited a characteristic dose-response survival curve, with a significant shoulder effect similar to other normal cells. Using the linear quadratic formalism, an α value of 0.289 ± 0.059 and a β value of 0.0150 ± 0.0007 have been calculated. The D_0 dose was 1.94 ± 0.18 Gy and n was 2.18 ± 0.72 . Using the model-free technique originally proposed by Fertil et al. a mean inactivation dose of 3.01 Gy was calculated.

Figure 1: Clonogenic Survival of Pig SMC at HDR and LDR



Legend: Clonogenic survival of pig smooth muscle cells (SMC) at high dose-rate (HDR) and low dose-rate (LDR). Note that at LDR, the shoulder disappeared and surviving fraction became a linear function of dose.

Figure 2: Growth Delay after HDR and LDR



Legend: Growth delay of pig smooth muscle cells after high dose-rate (HDR) and low dose-rate (LDR) exposure. Unirradiated cells became confluent in about 10 days. In accordance with cell survival, growth delay is less marked after LDR irradiation. * $P < 0.001$

At LDR, SMC appeared to significantly repair sub-lethal DNA damage as the survival curve was clearly less steep. At this low-dose rate, the β component disappeared and the survival curve was well fitted by linear regression analysis, that is survival was an exponential function of the dose⁻¹ and α value was 0.25 Gy⁻¹. The D_0 and the mean inactivation dose were equivalent as there was no shoulder at 3.40 ± 0.07 Gy. It was clearly apparent from Figure 1 that there was an important difference between response at HDR and LDR. The dose-rate modifying factor (D_0 LDR/ D_0 HDR) was calculated at 1.75 and $\text{Survival}_{0.01}\text{LDR}/ \text{Survival}_{0.01}\text{HDR}$ was 1.82.

Growth delay

Unirradiated cells initially plated at a density of 1×10^4 cell/well grew rapidly and reached confluence in about 6-10 days. After HDR and LDR, there was a non-linear dose-dependent delay to reach confluence.

Discussion

These results are part of an ongoing program devoted to characterizing the radiobiology of vascular cells exposed to high and low dose-rate irradiation. There are currently two approaches for endovascular radiation. One is based on high activity γ or β sources, such as ribbons, seeds, or liquid, to deliver a single dose locally through a catheter for a limited time exposure. The other approach uses radioactive stents for prolonged exposure and continuous low dose-rate treatment.

Several research groups have shown a dose-dependent decrease in neointima formation in various animal models after single dose administration in excess of 10 Gy (1, 7). Similar biological effects have been noted after use of γ (¹⁹²Ir) and β (⁹⁰Sr/Y, ⁹⁰Y, ³²P) sources (8). Using γ sources, some investigators have subsequently reported persistence of the initial benefit at 6 months (8, 9). More recently, a clinical study reported that a single dose of about 8 Gy using a ¹⁹²Ir source was able to significantly reduce the incidence of in-stent restenosis at 6 months and

these effects were maintained at 3 years (P.W. Serruys, presented at European Society of Cardiology, Vienna, Austria, 22-26 August, 1998) (10). All these catheter-based studies delivered the dose at dose-rates between 0.66 Gy/min and > 3 Gy/min (1).

Other investigators have explored the use of radioactive stents (2, 11, 12). The first series were radioactivated by exposure to bombardment with heavy particles and generated a series of γ and β isotopes and X-rays (11). More recently, pure β -emitting stents have been designed using ion-implantation of ^{32}P (2, 12, 13). With these radioactive stents, no dose threshold has been identified yet (2). Extremely low doses have shown an early benefit whereas intermediate doses have been associated with exaggerated neointima formation (2, 11-13). According to the dose calculations performed by the American Association of Physicists in Medicine (AAPM Task Group 60), the dose-rates (dose delivered in 28 days at 1mm from stent struts) can be roughly estimated, varying from 2.2×10^{-3} Gy/h to 0,33 Gy/h (14).

The dose-rate is an important parameter in brachytherapy determining the overall response of the exposed tissue (15, 16). For most cells, the lethal effect of ionizing radiation is lessened as the dose-rate is decreased (16). This is the consequence of repair of sub-lethal damage that occurs as the dose is delivered over a longer period of time (16). Our results showed that SMC have significant sub-lethal damage repair capabilities. In fact, at 0,675 Gy/h SMC repaired almost completely sub-lethal DNA damage as the β component of the linear-quadratic relationship disappeared. A dose about twice at 0.675 Gy/h was necessary to produce the same killing effect as at conventional HDR. The extent of this effect could explain some of the negative results noted after radioactive stent implantation. In a recent feasibility study using ^{32}P stents which delivered a dose of about 20 Gy at 1 mm depth in 1 month failed to produce a reduction in restenosis rate (17).

The dose-rate effect is significant between 0.1 Gy/h and several Gy/min (16). As the half-times for repair of normal cells are in the order of 30-90 min, delivering the dose within that

interval of time will produce a similar biological effect (18, 19). If, however, the dose is administered over a few hours or days, the overall effect will be dominated by repair. If the dose-rate is below a certain level, cell proliferation will occur during irradiation exposure and compensate for cell killing. Based on previous clinical experience and on in vitro results, we have chosen a dose-rate which it was assumed would allow maximal sub-lethal damage repair (20, 21). At this level of continuous low dose-rate administration, a good therapeutic ratio has been demonstrated between control of actively dividing cells and dose-limiting normal tissue toxicities such as fibrosis (20). It is therefore possible that radioactive stents delivering an effective total dose at a dose-rate of around 0.5 Gy/h will control neointima formation while limiting side-effects such as fibrosis. Using such a dose-rate, our in vitro results suggest that a dose 1.5-2.0 times greater than used for HDR could be contemplated for a given effect. It is interesting to note that initial experiments using radioactive stents with multiple isotopes showed maximal benefit when more than 50% (about 10 Gy) of the dose was delivered during the first day (11). In contrast, a dose about 4 times higher had to be used to produce the same effect when a pure ^{32}P stent with a much lower dose-rate was employed (12).

Our results also shed some light on delayed restenosis observed after both HDR and LDR delivery. For both modes of administration, there was a dose-dependent delay for the cells to reach confluence. This effect was non-linear as no confluence was reached for cells irradiated up to 10 Gy after HDR or LDR. This may reflect in both situations that not enough cells have survived irradiation to proliferate until confluence was reached. Some authors have suggested that irradiation will induce a dose-dependent delay in restenosis provided that surviving SMC do not reach senescence (18). Restenosis, however, is clearly a time-limited phenomenon where SMC and myofibroblast proliferation is transiently activated by the vessel injury and the inflammatory response leading to localized growth factor release (22). Therefore, as for the experimental conditions described, if the stimulus for growth disappears, no late proliferation will occur and the total number of cells forming neointima should remain less than for unirradiated vessels. This has been shown by Hehrlein et al. who showed less SMC in the neointima after 1 year follow-up after radioactive stent implantation compared with non-radioactive stents (11).

Limitations: Comparison of high dose-rate and low dose-rate experiments were made using two radioactive sources of different qualities. It is generally assumed, however, that high energy electrons induce similar biological effects than γ sources. Nevertheless, it remains possible that low energy β emitters such as ^{45}Ca have a different relative biological effectiveness compared with γ sources. These are in vitro results and direct extrapolation to the in vivo situation should be made with caution. In particular, the role of cytokines and growth-factors in the overall response of the vascular system cannot be reproduced in vitro and are likely to influence the response.

In summary, we have shown that in vitro SMC exhibit a significant dose-rate effect. This indicates that radioactive stents could deliver the dose at a sufficiently high dose-rate to compensate for cell proliferation while at the same time the total dose should be increased to account for sub-lethal damage repair. Further investigations are clearly required to establish whether continuous low dose-rate administration may improve the therapeutic ratio.

References

1. Bertrand OF, Mongrain R, Lehnert S, et al. Intravascular radiation therapy in atherosclerotic disease: promises and premises. *Eur Heart J* 1997;18:1385-95.
2. Carter A, Laird J, Bailey L, et al. Effects of endovascular radiation from a β -particle - emitting stent in a porcine coronary restenosis model. A dose-response study. *Circulation* 1996;94:2364-68.
3. Bertrand OF, Mongrain R, Thorin E, Lehnert S. Radiation responses of human and porcine vascular cells exposed to high dose-rate γ irradiation (abstract). *Eur Heart J* 1998;19:633.
4. Mongrain R, Bertrand OF, Thorin E, Lehnert S. A tissue culture model to study the effects of low energy β emitters on vascular cells: dosimetric considerations (abstract). *Cardiovasc Rad Med* 1999;1:85.
5. Bertrand OF, Mongrain R, Yuen PS, Lehnert S. Dosimetric considerations to study in vitro the effects of low energy β emitters on vascular cells. *Cardiovasc Rad Med* 1999 (submitted).
6. Fertil B, Dertinger H, Courdi A, Malaise EP. Mean inactivation dose: a useful concept for intracomparison of human cell survival curves. *Rad Res* 1984;99:73-84.
7. Weinberger J, Amols H, Ennis R, Schwartz A, Wiedermann J, Marboe C. Intracoronary irradiation: Dose response for the prevention of restenosis in swine. *Int. J. Radiat. Oncol. Bio. Phys.* 1996;36(4):767-775.
8. Waksman R, Robinson KA, Croker IR, Gravanis MB, Cipolla GD, King SB. Endovascular low-dose irradiation inhibits neointima formation after coronary artery balloon injury in swine. *Circulation* 1995;91:1533-39.
9. Wiedermann, JG, Marboe C, Amols A, Weinberger J. Intracoronary irradiation markedly reduces neointimal proliferation after balloon angioplasty in swine: Persistent benefit at 6-month follow-up. *J Am Coll Cardiol* 1995;25:1451-1456.
10. Teirstein P, Massulo V, Jani S, et al. Catheter-based radiotherapy to inhibit restenosis after coronary stenting. *N Engl J Med* 1997;336(24):1697-703.

11. Hehrlein C, Gollan C, Dönges K, et al. Low-dose radioactive endovascular stents prevent smooth muscle cell proliferation and neointimal hyperplasia in rabbits. *Circulation* 1995;92:1570-75.
12. Hehrlein C, Stintz M, Kinscherf R, et al. Pure β -particle-emitting stents inhibits neointima formation in rabbits. *Circulation* 1996;93:641-5.
13. Laird JR, Carter A, Kufs WM, et al. Inhibition of neointimal proliferation with low-dose irradiation from a β -particle-emitting stent. *Circulation* 1996;93:529-36.
14. Nath R, Amols H, Coffey C, et al. Intravascular brachytherapy physics: report of the AAPM radiation therapy committee task group n° 60. *Med Phys* 1999;26:119-52.
15. Barendsen GW. Dose fractionisation, dose rate and iso-effect relationships for normal tissue responses. *Int J Radiat Oncol Bio Phys* 1982;8:1981-1997.
16. Hall EJ, Brenner DJ. The dose-rate effect revisited: Radiobiological considerations of importance in radiotherapy. *Int J Radiat Oncol Bio Phys* 1991;21:1403-1414.
17. Carter A, Fischell TA. Current status of radioactive stents for the prevention of in-stent restenosis. *Int J Radiat Oncol Bio Phys* 1998;41(1):127-133.
18. Brenner D, Miller R, Hall E. The radiobiology of intravascular irradiation. *Int J Radiat Oncol Bio Phys* 1996;36(4):805-810.
19. Hall EJ, Marchese MJ, Astor MB, Morse T. Response of cells of human origin, normal and malignant, to acute and low dose rate irradiation. *Int J Radiat Oncol Bio Phys* 1986;12:655-9.
20. Mazon JJ, Simon JM, Le Péchoux C, et al. Effect of dose-rate on local control and complications in definitive irradiation of T1-2 squamous cell carcinomas of mobile tongue and floor of mouth with interstitial iridium-192. *Radiother Oncol* 1991;21:39-47.
21. Hall EJ. *Radiobiology for the radiologist*. (4 ed.) Philadelphia: J.B. Lippincott Company, 1994.
22. Carter A, Laird JR, Farb A, Kufs W, Wortham DC, Virmani R. Morphologic characteristics of lesion formation and time course of smooth muscle cell proliferation in a porcine proliferative restenosis model. *J Am Coll Cardiol* 1994;24:1398-405.

General Conclusion

These studies were designed to better evaluate the radiobiology of vascular cells in the context of the use of radiation therapy to prevent restenosis after vessel injury. They are also part of an ongoing project to design a novel radioactive stent. The use of ionizing radiation is well established as an effective treatment in various malignant and benign diseases. Efficacy is primarily based on the relative higher radiosensitivity of proliferative cells compared to quiescent cells. Restenosis involves a transient and limited cell proliferation component, which indicates the rationale of using ionizing radiation. However, besides the killing effect, radiation has also multiple biological effects, which complicate the prediction of an optimal dose. Consequently, serious side effects such as fibrosis, delayed obstructions and aneurysms might ultimately develop after irradiation of coronary vessels.

Scrupulous attention to the radiobiology and dosimetric aspects are absolutely mandatory to better define a possible therapeutic ratio. In this work, we showed that the target volumes for endovascular brachytherapy remain limited. It was further suggested that radioactive stent could target smaller volumes than catheter-based brachytherapy. It seems that the necessary target distances for a radioactive stent allows to contemplate the use of a ^{45}Ca -DTPA polymer coated stent. It is however clear that the design of the stent and the maximum inter-strut distances will need to be carefully selected before embarking on *in vivo* testing. Given the doses actually used in clinical experience and based on our calculations, only a few thousands cells would remain clonogenic after radiation exposure. Depending on the stimulus growth, this would create a definitive impairment or a very significant delay in the recurrence of restenosis. *In vitro* responses of pig and human vascular cells to high dose-rate γ irradiation did not suggest large differences in intrinsic radiosensitivities between fibroblasts, smooth muscle cells and endothelial cells. Radioactive stent present radiobiological and radiation protection advantages. As illustrated by our *in vitro* results using an original low energy β isotopic complex, the existence of a significant

dose-rate effect for likely target cells i.e. smooth muscle cells suggests that a good therapeutic ratio is theoretically achievable with a permanent implant such as a radioactive stent.

The development of an isotope-release polymer-coated stent brings however formidable challenges that remain to be solved. It is my hope at the conclusion of this thesis that this project will continue to run and expand. Indeed, it is only by an integration of the different disciplines and expertise that we will progress in the knowledge of this fascinating new application for a rather old therapy. Ultimately, improved knowledge will undoubtedly lead to better care of our patients.

Contribution to Original Research

1. Using histo-morphometric analysis, we have described for the first time potential target volumes for endovascular radiation therapy and the relative importance of each vessel layer. In particular, the critical role of the atherosclerotic plaque has been underlined. With an original technique, we also calculated for the first time the respective vessel cell layer densities and extrapolated the number of cells to be exposed to irradiation.
2. We systematically studied the *in vitro* radiation response of fibroblasts, smooth muscle cells and endothelial cells exposed to high dose-rate γ irradiation. This was also a first attempt to directly compare human and porcine vascular cells using clonogenic assays, growth delays and alkaline filter elution.
3. An original experimental setup was designed for *in vitro* exposure of cell monolayers to low energy β -emitters. Using special dosimeters, we demonstrated that doses delivered are better calculated by the MIRD dose than using half the calculated dose as previously suggested in the literature. The efficacy of excess of free DTPA in limiting ^{45}Ca intracellular penetration has also been demonstrated.
4. Using an original complex of ^{45}Ca -DTPA we demonstrated for the first time a significant dose-rate effect for vascular smooth muscle cells, which represent likely target cells for the prevention of restenosis. Furthermore, at a dose-rate of 0.675 Gy/h, these cells expressed maximal sub-lethal damage repair.